

Aus dem Max von Pettenkofer-Institut für Hygiene und Medizinische Mikrobiologie
Lehrstuhl für Medizinische Mikrobiologie und Krankenhaushygiene
der Ludwig-Maximilians-Universität München
Leitung: Prof. Dr. Sebastian Suerbaum

**The role of human CEACAMs for the interaction
of *Helicobacter pylori* with neutrophils**

Dissertation
zum Erwerb des Doktorgrades der Naturwissenschaften
an der Medizinischen Fakultät der
Ludwig-Maximilians-Universität zu München

vorgelegt von

Ina-Kristin Behrens

aus
Hannover

2020

Mit Genehmigung der Medizinischen Fakultät
der Universität München

Betreuer: Prof. Dr. Rainer Haas

Zweitgutachter: Prof. Andreas Ladurner, PhD

Dekan: Prof. Dr. med. dent. Reinhard Hickel

Tag der mündlichen Prüfung: 03.08.2020

Eidesstattliche Versicherung

Ich, Ina-Kristin Behrens, erkläre hiermit an Eides statt, dass ich die vorliegende Dissertation mit dem Thema:

**The role of human CEACAMs for the interaction
of *Helicobacter pylori* with neutrophils**

selbstständig verfasst, mich außer der angegebenen keiner weiteren Hilfsmittel bedient und alle Erkenntnisse, die aus dem Schrifttum ganz oder annähernd übernommen sind, als solche kenntlich gemacht und nach ihrer Herkunft unter Bezeichnung der Fundstelle einzeln nachgewiesen habe.

Ich erkläre des Weiteren, dass die hier vorgelegte Dissertation nicht in gleicher oder ähnlicher Form bei einer anderen Stelle zur Erlangung eines akademischen Grades eingereicht wurde.

Wunstorf, 22.08.2020, Ina-Kristin Behrens

Teile dieser Arbeit wurden unter folgendem Titel veröffentlicht:

Behrens I-K, Busch B, Ishikawa-Ankerhold H, Palamides P, Shively JE, Stanners C, Chan C, Leung N, Gray-Owen S, Haas R. 2020. The HopQ-CEACAM interaction controls CagA translocation, phosphorylation, and phagocytosis of *Helicobacter pylori* in neutrophils. mBio 11:e03256-19. <https://doi.org/10.1128/mBio.03256-19>.

Weitere Publikationen im Promotionszeitraum, die nicht in dieser Arbeit enthalten sind:

- Zhang J, Wieser A, Lin H, Li H, Hu M, **Behrens I-K**, Schiergens T, Mayerle J, Gerbes A, Steib C. 2020. Kupffer cell activation by different microbial lysates: Toll-like receptor-2 plays pivotal role on thromboxane A₂ production in mice and humans. Eur J Immunol. doi: 10.1002/eji.201948507
- Jagau H, **Behrens I-K**, Steinert M, Bergmann S. 2019. Pneumococcus Infection of Primary Human Endothelial Cells in Constant Flow, J. Vis. Exp., e60323
doi:10.3791/60323

Contents

| | |
|---|-----------|
| ABSTRACT | 1 |
| ZUSAMMENFASSUNG | 2 |
| 1 Introduction | 4 |
| 1.1 Neutrophil Granulocytes | 4 |
| 1.1.1 Origin and development of neutrophils and other myeloid leukocytes | 5 |
| 1.1.2 Neutrophil recruitment and chemokine production | 6 |
| 1.1.3 Phagocytosis and production of reactive oxygen species | 7 |
| 1.2 The pathogen - <i>Helicobacter pylori</i> | 8 |
| 1.2.1 Clinical manifestation and treatment | 8 |
| 1.2.2 Colonization of the human stomach by <i>H. pylori</i> | 9 |
| 1.2.3 CagA - The oncoprotein of <i>H. pylori</i> | 9 |
| 1.3 Immune response to <i>H. pylori</i> | 12 |
| 1.3.1 Massive recruitment of neutrophils | 13 |
| 1.3.2 Manipulation of macrophages and DCs | 14 |
| 1.3.3 Downregulation of the adaptive immune response by T-cells | 15 |
| 1.4 CEACAMs | 15 |
| 1.4.1 Structure and function of CEACAMs | 16 |
| 1.4.2 Human CEACAM1 | 17 |
| 1.4.3 Human CEACAM3 | 18 |
| 1.4.4 Human CEACAM6 | 18 |
| 1.4.5 Murine CEACAM1 and 2 | 19 |
| 1.4.6 <i>H. pylori</i> - CEACAM interaction | 20 |
| 1.5 <i>H. pylori</i> infection model systems | 21 |
| 1.6 Aims of this work | 22 |
| 2 Material and methods | 23 |
| 2.1 Isolation and cultivation of cells | 23 |
| 2.1.1 Mouse lines | 23 |
| 2.1.2 Isolation of murine neutrophils | 24 |

| | | |
|-------|--|----|
| 2.1.3 | Isolation of human neutrophils | 24 |
| 2.1.4 | Isolation of murine DCs and M Φ | 24 |
| 2.1.5 | Isolation of human DCs and M Φ | 25 |
| 2.1.6 | Cell lines and their cultivation | 26 |
| 2.1.7 | Immortalization and differentiation of cells | 28 |
| 2.1.8 | Cryoconservation of cells | 28 |
| 2.1.9 | Generation of ER-Hoxb8 neutrophil cell lines | 28 |
| 2.2 | Microbiological methods | 29 |
| 2.2.1 | Bacterial strains | 29 |
| 2.2.2 | Cultivation of bacteria | 31 |
| 2.2.3 | Cryoconservation of bacteria | 31 |
| 2.3 | <i>In vitro</i> infection | 31 |
| 2.3.1 | Survival assay | 31 |
| 2.4 | Biochemical methods | 32 |
| 2.4.1 | Bacterial and cellular lysates | 32 |
| 2.4.2 | Sodium dodecyl sulfate polyacrylamide gel electrophoresis | 32 |
| 2.4.3 | Immunoblot | 33 |
| 2.4.4 | CagA phosphorylation | 35 |
| 2.4.5 | Antibodies - Immunoblots | 35 |
| 2.4.6 | <i>In vitro</i> phosphorylation | 36 |
| 2.4.7 | Src homology protein tyrosine phosphatase-1 inhibition | 37 |
| 2.5 | Flow cytometry | 37 |
| 2.5.1 | Antibodies - flow cytometry | 37 |
| 2.5.2 | Cell characterization | 38 |
| 2.5.3 | CEACAM expression | 38 |
| 2.5.4 | Interaction experiment | 38 |
| 2.5.5 | Binding assay | 38 |
| 2.5.6 | Phagocytosis assay | 39 |
| 2.5.7 | Detection of ROS | 39 |
| 2.5.8 | Quantification of CagA translocation | 39 |
| 2.5.9 | Chemokine measurement | 40 |
| 2.6 | Microscopy | 40 |
| 2.6.1 | Confocal microscopy of <i>H. pylori</i> - neutrophil interaction | 40 |
| 2.6.2 | Giemsa staining | 41 |
| 2.7 | CRISPR/Cas9 | 41 |
| 2.8 | 2D migration | 44 |
| 2.9 | Statistics | 44 |

| | | |
|----------|---|-----------|
| 3 | Results | 45 |
| 3.1 | The role of human CEACAMs for the interaction of <i>H. pylori</i> with neutrophils | 45 |
| 3.1.1 | CEACAM expression in neutrophils | 45 |
| 3.1.2 | Interaction of <i>H. pylori</i> with neutrophils | 47 |
| 3.1.3 | Binding versus phagocytosis of <i>H. pylori</i> | 50 |
| 3.1.4 | Survival of <i>H. pylori</i> after phagocytosis by PMNs | 51 |
| 3.1.5 | Production of reactive oxygen species | 53 |
| 3.1.6 | Confocal microscopy studies of the interaction of <i>H. pylori</i> and PMNs | 54 |
| 3.1.7 | The role of human CEACAMs on CagA translocation and phosphorylation | 56 |
| 3.1.8 | Influence of SHP-1 on CagA phosphorylation | 59 |
| 3.1.9 | 2D migration of murine and humanized PMNs | 60 |
| 3.2 | The role of human CEACAMs on the secretion of chemokines | 62 |
| 3.2.1 | Chemokine secretion of PMNs infected with <i>H. pylori</i> | 62 |
| 3.2.2 | Chemokine secretion of DCs and M Φ infected with <i>H. pylori</i> | 63 |
| 3.3 | Interaction of <i>H. pylori</i> with DCs and M Φ | 65 |
| 3.3.1 | CEACAM expression of DCs and M Φ | 65 |
| 3.3.2 | Interaction of <i>H. pylori</i> with DCs and M Φ | 67 |
| 3.3.3 | CagA translocation and phosphorylation | 67 |
| 3.4 | Impact of a chronic infection with <i>H. pylori</i> on the interaction with neutrophils | 69 |
| 3.4.1 | Effect on CagA translocation and phosphorylation | 69 |
| 3.4.2 | Effect on CEACAM expression | 72 |
| 4 | Discussion | 74 |
| 4.1 | <i>H. pylori</i> interacts with human CEACAMs to manipulate neutrophils | 75 |
| 4.1.1 | CEACAMs facilitate survival of phagocytosis | 76 |
| 4.1.2 | CEACAMs enable CagA phosphorylation in PMNs | 78 |
| 4.1.3 | <i>H. pylori</i> -CEACAM interactions change the chemokine secretion of neutrophils | 80 |
| 4.1.4 | The role of CEACAM3 in a <i>H. pylori</i> infection | 81 |
| 4.1.5 | CEACAMs play a major role on PMNs rather than on M Φ and DCs | 81 |
| 4.1.6 | Characterization of PMNs from naive versus <i>H. pylori</i> -infected hosts | 83 |
| 4.2 | Conclusion and outlook | 84 |
| | LIST OF ABBREVIATIONS | 85 |
| | LIST OF FIGURES | 89 |
| | LIST OF TABLES | 91 |

| | |
|------------------------|------------|
| LITERATURE | 92 |
| ACKNOWLEDGEMENT | 109 |

Abstract

Despite a strong immune response *H. pylori* persists for decades in the human stomach. The bacterium actively manipulates immune cells resulting in massive infiltration of neutrophil granulocytes (neutrophils) leading to tissue damage. *H. pylori* injects the cytotoxin-associated gene A (CagA), a bacterial oncoprotein, via its type IV secretion system into gastric epithelial cells, where it gets phosphorylated and activates intracellular signaling cascades. This procedure can promote various malignancies, such as gastric cancer and is the reason for the classification of *H. pylori* as a class I carcinogen by the world health organization (WHO). However, the infection of mice with *H. pylori*, which is only possible by a mouse adapted *H. pylori* strain, results in a mild pathology. Humans express several carcinoembryonic antigen-related cell adhesion molecules (CEACAMs) on the surface of different cells. These glycoproteins function as pathogen receptors for several human pathogens and influence signaling pathways. For *H. pylori* human CEACAMs are essential to translocate CagA into gastric epithelial cells, while murine CEACAMs do not function as receptors for the bacterium. The aim of this thesis was to analyze the role of human CEACAMs for the interaction of *H. pylori* with neutrophils. Thus, experiments with neutrophils and other myeloid cells isolated from mice expressing human CEACAM receptors (CEACAM-humanized mice) were performed.

It was found that *H. pylori* efficiently interacts with CEACAMs on neutrophils. Notably, human CEACAMs enable the CagA phosphorylation in murine neutrophils and increase the secretion of the proinflammatory chemokine MIP-1 α , which might lead to a stronger infiltration of immune cells into the mouse stomach. Furthermore, an increased oxidative burst and high survival rates of *H. pylori* were detected in humanized CEACAM3 and 6 neutrophils, providing a possible explanation for the inefficiency of neutrophils in bacterial clearance. In addition, *in vivo* data demonstrated a down-regulation of CEACAM expression in neutrophils from chronically infected mice.

In conclusion, these data provide new insights into the interaction of *H. pylori* with neutrophils extending our knowledge about bacterial manipulation of the immune response. Moreover, this work highlights the important function of CEACAMs on neutrophils in a *H. pylori* infection, which generally strengthens the role of CEACAMs for pathogens and recommends the humanized CEACAM mouse as a new model organism in *H. pylori* infection research.

Zusammenfassung

Trotz einer starken Immunantwort überdauert *H. pylori* für Jahrzehnte im menschlichen Magen. Das Bakterium manipuliert aktiv Immunzellen, was zu einer massiven Einwanderung von neutrophilen Granulozyten (Neutrophilen) führt, die das Gewebe schädigen. *H. pylori* injiziert das Zytotoxin-assoziierte Genprodukt A (CagA) mit seinem Typ IV Sekretionssystem in die Magenepithelzellen, wo dieses phosphoryliert wird und intrazelluläre Signalkaskaden aktiviert. Dies fördert die Entstehung von Entzündungen (Gastritis) sowie verschiedener Erkrankungen wie Magenkrebs und ist der Grund für die Einstufung von *H. pylori* durch die Weltgesundheitsorganisation als Klasse I krebserregendes Bakterium. In der Maus hingegen, die überhaupt nur mit an die Maus adaptierten *H. pylori* Stämmen infiziert werden kann, verursacht *H. pylori* nur eine milde Pathologie. Menschen exprimieren unterschiedliche Zelladhäsionsmoleküle der karzinoembryonalen Antigenfamilie (CEACAMs) auf der Oberfläche verschiedener Zellen. Diese Glykoproteine dienen verschiedenen humanen Pathogenen als Rezeptoren und beeinflussen zelluläre Signalwege. Für *H. pylori* sind humane CEACAMs essentiell für die Injektion von CagA in Magenepithelzellen, wohingegen murine CEACAMs für das Bakterium nicht als Rezeptor fungieren. Das Ziel dieser Arbeit war es, die Rolle von humanen CEACAMs für die Interaktion von *H. pylori* mit Neutrophilen zu analysieren. Dafür wurden Experimente mit Neutrophilen und anderen myeloiden Zellen von Mäusen, die humane CEACAM Rezeptoren exprimieren (humanisierte CEACAM Mäuse) durchgeführt.

Es konnte gezeigt werden, dass *H. pylori* effizient mit CEACAMs auf Neutrophilen interagiert. Bemerkenswerterweise ermöglichen humane CEACAMs die CagA Phosphorylierung in murinen Neutrophilen und erhöhen die Menge des proinflammatorischen Chemokines MIP-1 α , was wahrscheinlich zu einer stärkeren Einwanderung von Immunzellen in den Magen führt. Zudem wurde in humanisierten CEACAM3 und 6 Neutrophilen eine stärkere Produktion von reaktiven Sauerstoffen und eine erhöhte Überlebensrate von *H. pylori* festgestellt. Dies könnte eventuell erklären, warum die Neutrophilen das Bakterium nicht abtöten und eliminieren konnten. Zusätzlich zeigten *in vivo* Daten, dass in Neutrophilen von chronisch mit *H. pylori* infizierten Mäusen die Expression von CEACAMs herunter reguliert ist.

Zusammenfassend bietet diese Arbeit neue Einblicke in die Interaktion von *H. pylori* mit Neutrophilen und erweitert das Wissen, wie das Bakterium die Immunantwort ma-

nipuliert. Zudem verdeutlicht dieses Projekt die wichtige Funktion von CEACAMs auf Neutrophilen für eine *H. pylori* Infektion, wodurch generell die Rolle von CEACAMs für Pathogene unterstrichen und die humanisierte CEACAM-Maus als neuer Modelorganismus in der *H. pylori* Forschung ausgewiesen wird.

1. Introduction

1.1 Neutrophil Granulocytes

No mammal, including humans, can win a battle against pathogens without or with a significantly reduced number of neutrophil granulocytes (generally termed neutrophils in this thesis) [1]. These cells represent the first line of defense against invading pathogens. They are recruited as the first immune cells to the site of infection or inflammation. There, neutrophils release reactive oxygen species (ROS) and kill invading bacteria. However, at the same time, the surrounding tissue is damaged as well. Therefore, the degradation of neutrophils is as important as their presence. Apoptotic signals cause them to be killed by themselves or by monocytes, in order to prevent the destruction of tissue by their release of toxic chemicals. A further task of neutrophils is the secretion of proinflammatory chemokines, whereby further immune cells are recruited to the site of infection. For many years it has been claimed that neutrophils have a short lifespan and that their only function is the phagocytosis of invading pathogens in an acute infection. Recent studies showed that neutrophils are much more complex. Murine neutrophils have a lifetime of up to 12.5 h (hours) and human neutrophils survive up to 5.4 days [2]. Characteristic for differentiated neutrophils is their polymorph-segmented nucleus (see Fig. 1.1 showing a neutrophil stained with Giemsa). Therefore, these leukocytes were also called polymorphonuclear granulocytes (PMNs). Hypersegmentation occurs during differentiation. The nucleus of a PMN has a size about $10 \mu\text{m}$. Biochemically, PMNs can be identified by CD66abce (human) and Ly6G in combination with the cluster of differentiation (CD)11b (murine).

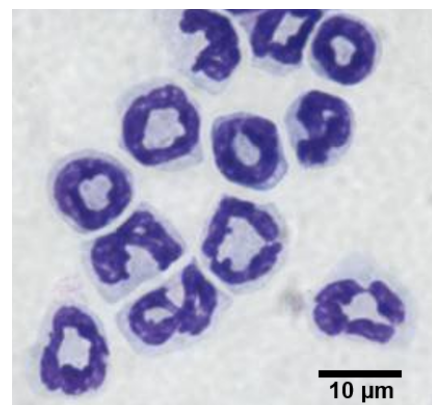


Fig. 1.1: Differentiated neutrophils stained with Giemsa solution

Staining of differentiated murine neutrophils with Giemsa shows the polymorph-segmented nuclei.

1.1.1 Origin and development of neutrophils and other myeloid leukocytes

With 50-70%, neutrophils represent the largest group of leukocytes, also known as white blood cells, in the human organism. In mice, however, neutrophils constitute only 10-25% of the leukocyte population [3]. Compared to other blood components such as blood platelets, leukocytes join their nuclei. Because of their structure, they are divided into granulocytes, monocytes and lymphocytes. Leukocytes originate from hematopoietic stem cells in the bone marrow. These stem cells can differentiate into a lymphoid or myeloid precursor cell. A lymphoid precursor cell develops into a lymphocyte. These include B-cells, T-cells and natural killer cells. With 75-90%, lymphocytes represent the most frequent cell type of leukocytes in mice [3].

Myeloid precursor cells develop, driven by granulocyte macrophage colony stimulating factor (GM-CSF) and granulocytes colony stimulating factor (G-CSF) into myeloblasts (see Fig. 1.2). Myeloblasts can transform into granulocytes or monocytes. Stem cell factor (SCF), GM-CSF, G-CSF, interleukin (IL)-3 and IL-6 influence the development into granulocytes, whereas SCF, GM-CSF, M-CSF, IL-3 and IL-6 result in development of monocytes. Monocytes generally develop, stimulated by M-CSF into macrophages (M Φ) or by GM-CSF into dendritic cells (DCs) (see Fig. 1.2) [4].

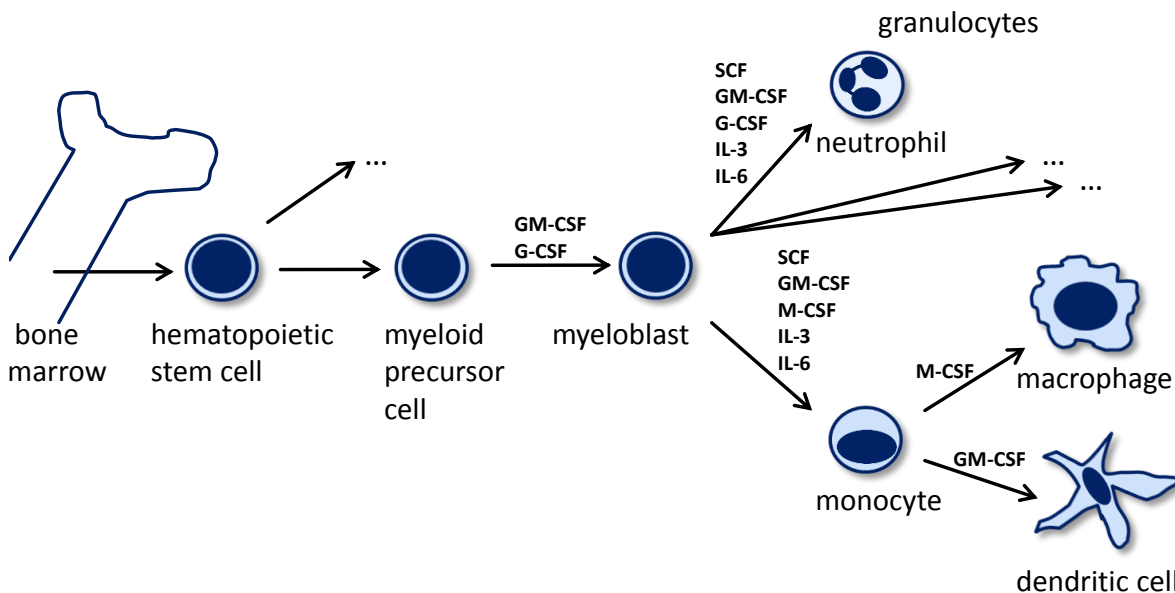


Fig. 1.2: Hematopoiesis of neutrophils, M Φ and DCs

Neutrophils originate from hematopoietic stem cells, which develop into a myeloid precursor cell and subsequently into myeloblasts. Myeloblasts can mature to granulocytes such as neutrophils or to monocyte. Monocytes develop into M Φ or DCs. Modified according to [4].

Granulocytes is the group name for neutrophils, eosinophils and basophils. According to their name they are characterized by their “granules” in the cytoplasm. Eosinophils and

basophils circulate in the blood to protect against parasites, while neutrophils circulate in the blood and transmigrate into the tissue to protect against bacteria and fungi.

1.1.2 Neutrophil recruitment and chemokine production

After their generation in the thymus and bone marrow, neutrophils circulate in the blood and lymphatic system and are in principal able to reach any location in the organism. Neutrophils find their way to the site of an infection along a gradient of increasing concentrations of chemical attractants. These can originate from bacteria, or be secreted by cells. An effective, rapidly produced chemoattractant for neutrophils is the proinflammatory lipid mediator leukotriene B4 (LTB4). LTB4 functions as an intracellular communication signal between neutrophils and triggers swarming of neutrophils [5].

Apart from proinflammatory lipid mediators, also special cytokines, called chemokines, are able to attract different cell populations. For that, their signals function through G-protein-coupled receptor interactions. In general, chemokines can be divided into two groups, CXC and CC chemokines, depending on their amino acid composition. The most important chemokine for the recruitment of neutrophils in humans is IL-8, also known as CXC motif chemokine 8 (CXCL8) (see Tab. 1.1) [6], [7], [8]. Rodents lack the human IL-8 gene [9]. In mice the keratinocyte chemoattractant (KC)/CXCL1 and the macrophage inflammatory protein 2 (MIP2)/CXCL2 are important chemokines for the recruitment of neutrophils [10], [8], [11], [12]. They are secreted by resident cells and invading leukocytes.

Tab. 1.1: Chemokines attracting neutrophils to the site of infection

| chemokine | organism | secreted by | to attract | reference |
|--------------|----------|--|-------------|-----------------|
| IL-8 (CXCL8) | human | residente cells and invading leukocytes | neutrophils | [6], [7], [8] |
| KC (CXCL1) | murine | residente cells and invading leukocytes | neutrophils | [10], [8] |
| MIP2 (CXCL2) | murine | residente cells invading leukocytes | neutrophils | [11], [12], [8] |

Murine neutrophils themselves secrete the macrophage inflammatory protein-1 (MIP-1 α)/CCL3, the macrophage inflammatory protein-1 beta (MIP-1 β)/CCL4, the monokine induced by gamma-interferon (MIG)/CXCL9 and the interferon-gamma induced protein 10 kDa (IP-10)/CXCL10 (see Tab. 1.2) [13], [14], [15]. For MIP1- α Charmoy *et al.* could show that the protein is important for the recruitment of DCs. Pharmacological and

genetic inhibition of MIP-1 α leads to a considerable reduction of the number of recruited DCs [14]. For MIP-1 α and β , Stebut *et al.* could demonstrate that neutrophils regulate M Φ recruitment by secretion of MIP1 α and β [15]. Moreover, neutrophils are able to secrete MIG and IP-10 by stimulation with interferon γ in combination with lipopolysaccharide (LPS) or tumor necrosis factor (TNF) α [16], [17].

Tab. 1.2: Chemokines secreted by neutrophils

| chemokine | organism | secreted by | to attract | reference |
|-----------------------|----------|--------------------------|---------------|----------------|
| MIP-1 α (CCL3) | murine | neutrophils | DCs, M Φ | [13][14], [15] |
| MIP-1 β (CCL4) | murine | neutrophils | DCs, M Φ | [15] |
| MIG (CXCL9) | murine | neutrophils and M Φ | T-cells | [16] |
| IP-10 (CXCL10) | murine | neutrophils and M Φ | T-cells | [16] |

1.1.3 Phagocytosis and production of reactive oxygen species

Besides the recruitment of immune cells, neutrophils themselves fight against invading pathogens, which they recognize via pathogen associated molecular patterns (PAMPs). Therefore neutrophils express pattern recognition receptors (PRR) such as Fc γ and c-type lectin receptors. These receptors enclose pathogens within a vacuole in the neutrophil, called phagosome. Their granules contain hydrolytic enzymes and Nicotinamide adenine dinucleotide phosphate (NADPH) oxidase subunits, which are able to kill the pathogens [18]. In detail, molecular oxygen is reduced by NADPH oxidase to superoxids, which can form intermediates like hydrogen peroxide or hydroxyl radicals [19]. An advantage of neutrophil phagocytosis in comparison to M Φ is the high speed uptake. Thus, Segal *et al.* could show that immunoglobulin G (IgG) opsonized particle uptake and vacuole closure in human neutrophils can be completed within 20 seconds [20]. Nevertheless a drawback of this fast process is an incomplete phagosomal maturation, which releases ROS outside of the neutrophil, which might result in damage of the surrounding tissue.

1.2 The pathogen - *Helicobacter pylori*

Helicobacter pylori is a pathogen that effectively manages to prevent its elimination by the host immune system. The Gram-negative bacterium is visually characterized by its spiral shape and its six to eight flagella, which enable a strong motility of the bacteria. This is essential for the pathogen, which exists in microaerophilic conditions and is exclusively able to permanently colonize the human stomach. Originally *H. pylori*, formerly known as *Campylobacter pylori*, was discovered and verified as pathogen by Barry Marshall and Robin Warren in an experiment conducted on themselves in 1982. They could show that the bacterium was the trigger for the inflammation of the stomach. For their discovery, both researchers received the Nobel Prize in Physiology and Medicine in 2005.

Computer simulations on DNA of a large number of *H. pylori* strains have indicated that already 58.000 years ago the human stomach was colonized by *H. pylori* [21]. At that time, people emigrated from Africa to Europe. Even today, the infection rate in many African countries is still high at 80-90% of the population. However, in more industrialized countries only 20-40% of the population is infected with *H. pylori* [22]. DNA sequencing data of the bacterial genome revealed that every person holds its own individual *H. pylori* strain, because of its very high mutation rate [23]. This is facilitated by the fact that the pathogen is naturally competent and can absorb and actively take up DNA from the environment (natural competence of DNA transformation). Within families, the *H. pylori* strains are highly genetically similar. This might be due to the fact that *H. pylori* is probably efficiently transmitted by the oral-oral or fecal-oral route [24]. Usually a *H. pylori* infection already happens in childhood within families, probably by a transfer of the bacteria from the mother to the child [25], [26].

1.2.1 Clinical manifestation and treatment

Overall 50% of the world population is infected with *H. pylori*. An infection with *H. pylori* can be detected by a urease-breath test, by *H. pylori*-specific antibodies in the blood, a stool sample and/or by endoscopy and culture of the bacteria. After an acute *H. pylori* infection, almost all people develop gastritis [27]. Depending on the *H. pylori* strain the infection often results in an asymptomatic gastritis (80-90% of the infected persons) [28]. In up to 25% the infection results in a chronic atrophic gastritis and stomach ulceration [28]. Furthermore, infected individuals may rarely develop mucus associated lymphoid tissue (MALT) lymphoma or even gastric cancer [28]. For this reason the International Agency for Cancer Research (IARC) of the World Health Organization (WHO) classified *H. pylori* as a class I carcinogen [29]. Until now, no protective vaccination against *H. pylori* is available. However, an infection with *H. pylori* can be treated with antibiotics.

Bacteria can be eradicated with a triple or quadruple therapy consisting of two or three antibiotics in combination with an acid secretion inhibitor (proton pump inhibitor) after testing for antibiotic resistance of the bacteria.

1.2.2 Colonization of the human stomach by *H. pylori*

The stomach mucosa is the habitat of *H. pylori*. This human organ is characterized by its acidic pH, which increases from the lumen of the stomach in direction of the mucus layer to the surface of the epithelial cells. *H. pylori* is able to produce ammonium catalyzed by urease mediated cleavage of urea to neutralize the low gastric pH and to reduce the viscosity of the mucus to protect itself against the gastric acid [30]. Furthermore, the bacterium is able to orientate itself by chemotaxis within the pH gradient in the mucus layer [31], [32]. The bacteria move with their flagella from the lumen into the mucus layer. There the neutral pH protects the bacteria against the gastric acid [31]. Eaton *et al.* could show that the flagella are essential for gastric colonization of *H. pylori* [33]. After penetrating of the protective mucus layer, *H. pylori* binds to stomach epithelial cells. Therefore, the bacterium owns a set of different *H. pylori* outer membrane proteins (HOPs). They enable binding to epithelial cells, mucus and immune cells and, as a result, allow persistence of the bacteria. The best characterized and most important adhesins are: HopQ, (which will be described in section 1.4.6) [34], [35], the blood group antigen adhesin (BabA) [36] and the sialyl-Lewis x (sLex) adhesin SabA [37]. HopQ, BabA and SabA all cluster together and share up to 35% genetic similarity [38]. BabA enables binding to fucosylated Lewis B receptors on epithelial cells as well as on mucus glycoproteins such as MUC5AC [36], [39]. SabA mediates binding to sLex in membrane glycolipids and can be switched off by phase variation [40] to escape a contact with cells in a vigorous host defense [37]. Moreover, binding via SabA induces ROS production and phagocytosis [41]. Thus, SabA is actively involved in neutrophil recruitment and activation. Besides these outer membrane proteins (OMPs), *H. pylori* possesses further OMPs, but, for most of them the function as well as the respective receptor are not known.

1.2.3 CagA - The oncoprotein of *H. pylori*

The cytotoxin associated gene A (CagA) of *H. pylori* is considered to be responsible for a symptomatic progression of a *H. pylori* infection, besides other virulence factors and host specific factors, such as genetic predispositions. The oncoprotein CagA has a size of 120-145 kDa and is located on the cytotoxin associated pathogenicity island (Cag-PAI). *H. pylori* strains carrying the Cag-PAI with a size of 40 kb, called type I strains, are more virulent, whereas strains without the Cag-PAI were classified as type II strains

[42]. In addition to the main virulence factor CagA, the Cag-PAI contains 27-31 other genes, which form the type IV secretion system (T4SS) apparatus [43]. This needle-like structure encompasses the inner and outer bacterial membrane as well as the host membrane. Thereby, the T4SS enables *H. pylori* to translocate the only known effector protein CagA into host cells [44]. In the C-terminal region of CagA one or more EPIYA (Glu-Pro-Ile-Tyr-Ala) motifs can be found. These EPIYA motifs show variations in the surrounding amino acids and can be classified as EPIYA A-D. Inside the host cell CagA is phosphorylated on these EPIYA motifs by Src and c-Abl family kinases of the infected cell (see Fig. 1.3, A) [45], [46].

The phosphorylation of CagA is pivotal for triggering disease, as it could be shown by Ohnishi *et al.*. To prove the relevance of CagA phosphorylation, Ohnishi *et al.* generated transgenic mice expressing wt CagA and mice expressing a phosphorylation deficient CagA. Mice expressing a phosphorylation deficient CagA did not develop leukocytosis, myeloid leukemia, B-cell lymphoma and hematological malignancies, but mice expressing wt CagA suffered from such disease [47]. This proves the importance of the CagA phosphorylation for the carcinogenicity of *H. pylori*.

After phosphorylation CagA can interact with several different cellular proteins (see Fig. 1.3, A), which influences various signaling cascades in the host cell, leading to cytoskeleton rearrangements, disruption of cell junctions as well as changes in proliferation and the proinflammatory response [48].

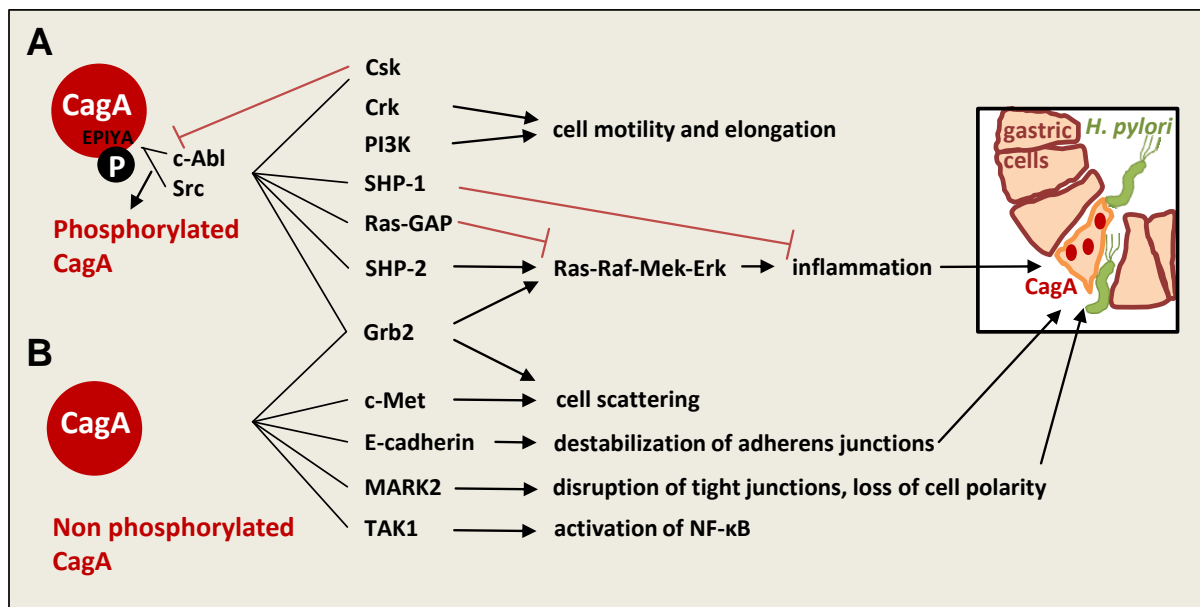


Fig. 1.3: The effect of CagA on host cells

Schematic view on the interaction of phosphorylated CagA (A) and non phosphorylated CagA (B) with several cellular proteins and their known consequences (arrow), (red line = inhibition). Modified from [48], [49]

The Src homology 2 (SH2) domain-containing protein 2 (SHP-2) was the first known protein to interact with phosphorylated CagA [50], [48]. Interaction of phosphorylated CagA with SHP-2 leads to cytoskeleton rearrangements and increased cell motility as well as cell elongation, forming the so called hummingbird phenotype of *H. pylori* infected cells [49], because of an inhibition of the focal adhesion kinase (FAK) [51]. Furthermore, the interaction of phosphorylated CagA with SHP-2 activates the RAS-Raf-Mek-Erk signaling pathway. However, binding of phosphorylated CagA to the Ras GTPase activating protein (Ras-GAP) can inhibit the activation of the pathway. In addition, binding of phosphorylated CagA to the C-terminal Src kinase (Csk) can inhibit the CagA SHP-2 interaction. Moreover, this interaction inactivates Src kinase activity, which results in a transient dephosphorylation of CagA. Nevertheless, CagA remains phosphorylated because of c-Abl takes over from Src and phosphorylates CagA [51]. In contrary to the activation of SHP-2 enhancing the oncogenic activity of CagA, Src homology 2 (SH2) domain-containing protein 1 (SHP-1) is able to dephosphorylate CagA and dampen its carcinogenic action in a *H. pylori* infection [52], as well as SHP-1 down regulates signals in hematopoietic and epithelial cells [53]. In addition, the phosphoinositide-3 (PI3)-kinase (PI3K) and Crk interact with phosphorylated CagA resulting in cell motility and elongation. The complex of the growth factor receptor-bound protein (Grb)2 and CagA activates Erk kinase signaling pathway and facilitates cell growth and cell scattering [54]. However, Grb2 also interacts with non phosphorylated CagA (see Fig. 1.3, B) resulting in cell scattering, as well as the binding of CagA to the tyrosine kinase c-Met, which binds to the hepatocyte growth factor and causes cell and massive tumor growth [55]. Destabilization also occurs when CagA interacts with E-cadherin and destabilizes E-cadherin- β -catenin complexes. Furthermore, the phosphorylation independent interaction of CagA with the microtubule affinity-regulating kinase 2 (MARK2) inhibits their activity and leads to disruption of tight junctions, loss of cell polarity and inhibits cellular proliferation. Apart from that infected cells might undergo apoptosis and do not differentiate anymore [56]. Moreover, CagA interacts with the host protein transforming growth factor- β -activated kinase (TAK) 1, which is essential for the induction of NF- κ B activation [57]. In addition to these interactions by CagA, which destroy the epithelial layer in particular, the injection of CagA via the T4SS results in release of proinflammatory chemokines such as IL-8, which attracts neutrophils [6], [7], [8]. Neutrophils release MIP-1 α and β attracting M Φ and DCs [13], [14], [15]. Those in turn also secrete chemokines recruiting B- and T-cells and activate the adaptive immune response (see section 1.3)

1.3 Immune response to *H. pylori*

The *H. pylori* infection is characterized by a high density of bacteria in the human stomach as well as its persistence and ongoing inflammation for years and decades. This suggests that the immune system is dysregulated and not able to eliminate *H. pylori*. An infection with the bacterium causes an inflammatory response as it was demonstrated by a massive neutrophil infiltration and the detection of proinflammatory cytokines such as IL-1 β , IL-6, IL-8 and TNF α in short term *in vitro* culture of biopsy samples of infected patients [58], [59]. However, the activation of immune cells does not remove the bacteria, instead the immune cells are manipulated by the bacteria resulting in damage and inflammation [60], [61], [62], [63].

It starts with a deficient recognition of the bacterium by the immune system. *H. pylori* makes use of modified PAMPs, which are not recognized by the immune system. Usually PAMPs such as LPS or flagella activate signal pathways via receptors like the toll like receptors (TLR) on epithelial cells, as well as on neutrophils. A dephosphorylation in the A domain of LPS of *H. pylori* results in a 1000-fold weaker activity compared to LPS of *Escherichia coli* [64], [65]. Therefore, the activation of TLR4 and the subsequent signaling cascades are weaker, too. Furthermore, other TLRs such as TLR5 are not able to recognize the flagella of *H. pylori*, because of a mutation in the N-terminal D1 domain of flagellin [66]. As a result the bacterium cannot be eliminated. Flagellin and the associated bacterial flagellar motility are required to establish and maintain colonization in the stomach [67].

On the epithelial surface the bacterium injects its oncoprotein CagA into gastric epithelial cells activating signaling cascades and resulting in inflammation (see section 1.2.3). In addition, injection via the T4SS activates epithelial cells to release proinflammatory chemokines such as IL-8. Thereby immune cells are recruited to the site of infection (see Fig. 1.4) [68].

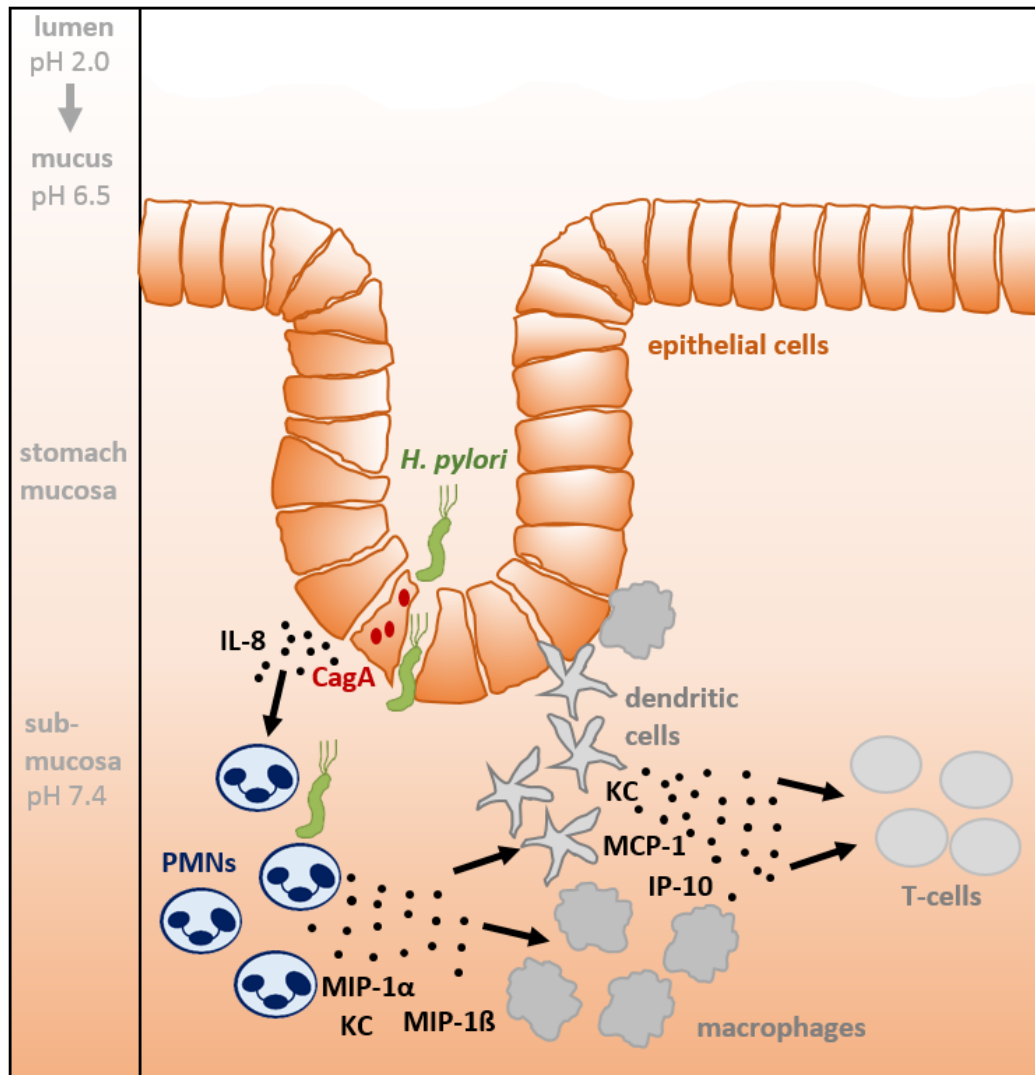


Fig. 1.4: Chemokine secretion after CagA injection

In the stomach *H. pylori* moves into the mucus layer and translocates its oncoprotein CagA into epithelial cells. Thus, the epithelial barrier may break open and *H. pylori* may enter the submucosa. As response to CagA translocation via the T4SS, epithelial cells secrete chemokines such as IL-8, thereby recruiting neutrophils. They release KC, MIP-1 α , MIP-1 β attracting M Φ and DCs. Those in turn secrete KC, MCP-1 and IP-10 to recruit T-cells and thus activate the adaptive immune response. Modified from [69]

H. pylori invade gastric epithelial cells and has direct contact to immune cells in the lamina propria [70]. Its interaction with PMNs, M Φ , DCs and T-cells is described in the following sections.

1.3.1 Massive recruitment of neutrophils

Neutrophils are the first cells recruited to the site of infection to initiate pathogen elimination. The massive recruitment of neutrophils is a hallmark of a *H. pylori* infection.

Neutrophils phagocytose pathogens and produce ROS. However, Allen *et al.* could show that *H. pylori* is able to disrupt NADPH oxidase activity leading to a strong extracellular oxidative burst and evading of killing [60]. In addition, Ramarao *et al.* demonstrated that *H. pylori* possesses an active antiphagocytic activity involving de novo protein synthesis by the bacterium and the T4SS [71]. The bacterium itself supports neutrophil recruitment and ROS production by activation of NADPH oxidase by secretion of *H. pylori* neutrophil activation protein (HP-NAP) [72] and SabA [41]. The massive infiltration of neutrophils results in tissue damage going along with a high number of apoptotic cells. One benefit for *H. pylori* is the release of nutrients from these apoptotic cells [69]. Apart from phagocytosis and ROS production, neutrophils secrete chemokines such as MIP-1 α and β (see section 1.1.2) to recruit further immune cells like M Φ and DCs to the site of infection (see Fig. 1.4).

1.3.2 Manipulation of macrophages and DCs

M Φ and DCs secrete KC to attract further neutrophils and the monocyte chemoattractant protein 1 (MCP-1/CCL2) to recruit more M Φ (see Fig. 1.4).

The main task of M Φ and DCs is phagocytosis of invading pathogens. Arnold *et al.* could show that CXCR1 positive M Φ and CD11b positive DCs are mainly responsible for phagocytosis of *H. pylori* [73]. However, Allen *et al.* demonstrated that phagosomes of M Φ infected with *H. pylori* strains fused and formed so-called megasomes containing live bacteria [61]. Furthermore, the bacterium can interfere with phagocytosis by M Φ involving bacterial de novo protein synthesis and the T4SS [71]. Moreover, *H. pylori* expresses an arginase enzyme inhibiting the nitric oxid (NO) production by activated M Φ and consequently preventing NO mediated killing of the bacterium [74]. Furthermore, *H. pylori* induces apoptosis of M Φ by activation of arginase II [75]. Apoptosis of M Φ recruits further PMNs.

DCs and M Φ are divided in immature and mature cells. After phagocytosis immature cells process phagocytosed antigens and present them on their surface. This results in maturation of the cells. It could be shown that the direct binding of neutrophils to DCs promotes their maturation and provides DCs access to phagocytosed pathogen products [18], [76], [77]. Once matured, DCs and M Φ are able to interact with CD4 positive T-cells and B-cells and initiate the adaptive immune response.

H. pylori is able to manipulate the maturation of DCs resulting in semimature DCs, which process antigens of pathogens, but do not present them to TLRs. These semimature DCs are called tolerogenic DCs and can initiate the differentiation of naive T-cells to regulatory T-cells with suppressed activity [78].

1.3.3 Downregulation of the adaptive immune response by T-cells

T-cells are recruited by M Φ and DCs via the secretion of IP-10 (see section 1.1.2 and Fig. 1.4). After activation CD4 positive T-cells can differentiate in T helper cells type 1 or type 2. T-cells isolated from infected gastric mucosa secrete high levels of IFN γ , indicating a T helper cell type 1 response [79]. This response is initiated by *H. pylori*. The bacterium stimulates via HP-NAP the production of IL-12 from DCs and M Φ as well as IL-23 from neutrophils. The release of IL-12 stimulates T helper cells type 1 to secrete IFN γ [80], which is linked to the development of peptic ulcers [63] and contributes to T-cell polarization [81]. The T helper cell type 1 immune response induced by *H. pylori* is a further explanation for the ineffectiveness to remove the bacterium.

Another important virulence factor of *H. pylori* is the vacuolating cytotoxin A (VacA). The main function of VacA is the induction of apoptosis, resulting in elimination of immune cells and release of nutrients [82]. Therefore, VacA binds to the cell surface and forms an anion selective channel in the endosome membrane. By osmotic swelling these channels transform to a vacuole [83]. The intoxication with VacA down regulates the IL-2 production. Thus, the viability and proliferation of T-cells [62] and thereby the adaptive immune response are influenced in a negative way.

All these examples show that the bacterium manipulates the host immune system and thereby prevents its elimination. An additional reason for the persistence of *H. pylori* in the stomach is its extreme adaptability to the host. *H. pylori* strains have a very high genetic variability, so that every infected person has its own genetically distinct *H. pylori* strain [23]. For this, membrane proteins enabling interaction with host cells play a key role. Important membrane proteins of epithelial cells and neutrophils, which function as pathogen receptors and initiate activating or inhibiting signaling pathways, are the so called CEACAMs.

1.4 CEACAMs

The carcino-embryonic antigen (CEA) was initially discovered in 1965 by Gold and Freedman and was also described in 1969 independently by Kleist and Burtin. Both described a new family of antigens, which only exists in colonic tumors, fetal gut, liver and pancreas [84], [85], [86]. At that time CEA expression could not be detected in healthy colonic mucosa. Later in 1989 Boucher *et al.* could show that CEA is expressed in healthy mucosa, too. However, there the expression was much lower [87]. In 1988, Thompson *et al.* identified CEA related genes and analyzed their sequences by cloning. This group localized CEA related genes on the human chromosome 19 in the region 19q13.1-3. and assigned

them to the immunoglobulin super family [88], [89]. On the basis of their sequence similarity they divided the CEA family in two groups: One consists of the classical CEA antigens and the other included the pregnancy-specific glycoproteins (PSG) [88]. This definition was confirmed by 26 CEACAM research groups in a workshop in Colorado in 1997. From then on, the classical CEA antigens were called CEA related cell adhesion molecules (CEACAMs) [90].

1.4.1 Structure and function of CEACAMs

Structural analysis revealed that CEACAMs are composed of several immunoglobulin like domains [89]. Many human CEACAMs consist of a N-terminal domain with 108-110 amino acids, whose secondary structure forms an immunoglobulin variable domain (IgV) following a variable number of immunoglobulin constant domains (IgC) (see sections 1.4.2-4 and Fig. 1.5 for details) [88].

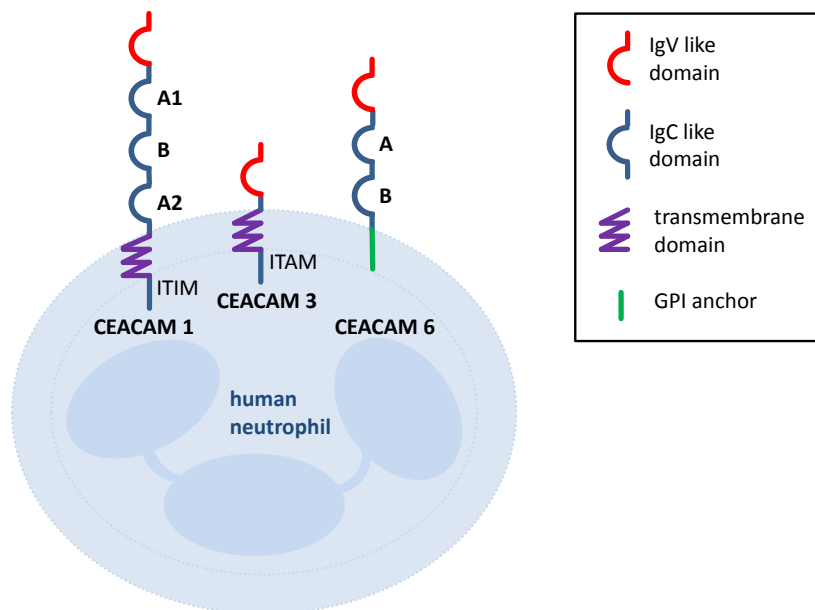


Fig. 1.5: Structure of human CEACAM1, 3 and 6 on neutrophils

Human neutrophils express CEACAM1, 3 and 6. CEACAM1 and 6 consist of several immunoglobulin like constant domains (IgC) (blue), followed by one immunoglobulin variable domain (IgV) (red), while CEACAM3 lacks the IgC domain. CEACAM1 and 3 own a transmembrane domain (purple), whereas CEACAM6 is anchored to the membrane by a glycosyl-phosphatidyl-inositol (GPI) anchor (green). Furthermore, human CEACAM1 possesses two ITIMs and human CEACAM3 has an ITAM. Modified from [91].

Today, twelve different CEACAMs are known [92]. They are highly conserved and can

be found so far in 27 mammals [93]. Beside different PSGs, humans harbour CEACAM 1, 3-8, 16 and 18-21. Whereas, in mice Kammerer *et al.* found only murine CEACAM1, 2 and 9-20 as well as different PSGs [93]. In general, the CEACAM tissue expression is very broadly distributed. Thus, CEACAMs are expressed on immune cells as well as epithelial cells of the gastrointestinal tract, the lung, the nasopharynx, the sweat and the urogenital tract [94], [95]. The IgV domain of CEACAMs functions as a pathogen receptor for cell adhesion of different Gram negative human pathogens, all colonizing the mucus layer, such as *E. coli*, *Haemophilus influenzae*, *H. pylori*, *Neisseria gonorrhoeae*, *Neisseria meningitidis*, *Moraxella catarrhalis* and different *Salmonella* strains [96], [97], [34], [98], [99]. Furthermore, in 2017 it was shown that CEACAM1, 3, 5 and 6 act as a receptor for the human pathogenic fungi *Candida albicans* and *Candida glabrata* via the N-terminal IgV domain [100]. Besides their function as pathogen receptors CEACAMs promote inter- and intracellular signaling [101], [102]. Moreover, the small glycoproteins influence the tissue architecture, differentiation and cell death, as described for CEACAM6 [103], as well as the insulin metabolism [104] and the neovascularization as described for CEACAM1 [105]. In medical science CEACAMs, especially CEACAM6, which is over-expressed in tumor tissue, function as important biomarkers and are promising therapeutics for cancer treatment.

In the following part CEACAMs that are important for this work, human CEACAM1, 3 and 6 on neutrophils, that are able to interact with *H. pylori*, are further characterized. Moreover, the two murine variants of human CEACAM1, murine CEACAM1 and 2 are discussed.

1.4.2 Human CEACAM1

Human CEACAM1, also called CD66a, is expressed almost in all cell types, e. g. on epithelial-, endothelial, lymphoid and myeloid cells [106]. It consists of three IgC domains (see Fig. 1.5, blue), one IgV like domain (red) and a transmembrane domain (purple). Because of alternative splicing of the primary mRNA, several different isoforms of CEACAM1 occur, some of them with a cytoplasmic tail have two Immunoreceptor tyrosine-based inhibitory motifs (ITIMs) [107], characterized by the following sequence (I/L/V/S)xYxx(L/V) [93]. In general, CEACAM1 can exist as a monomer or a dimer. It interacts with other CEACAMs or homodimerizes with CEACAM1 molecules via the N-terminal part of the IgV domain [108]. This is important for the communication with immune cells. In its dimerized form, the receptor can recruit SHP-1 via its ITIMs, which are phosphorylated by Src kinases [109]. Thereby, inhibitory signals are mediated, which limit the immune response. This mechanism is exploited by bacterial species such as *Neisseria* or *Moraxella*. Binding of *N. gonorrhoeae* to CEACAM1 leads to inhibition of

the CD4+ T-cell response via the ITIM. Furthermore, the B-cell response is suppressed as well [101]. In addition, *M. catarrhalis* and *N. meningitidis* bypass the immune response by binding to CEACAM1 on bronchial epithelial cells, whereby the ITIM-mediated inhibition of the TLR2 activated transcription factor NF- κ B prevents an adequate immune response [102]. Whether pathogens also inhibit the immune response through CEACAM1 on neutrophils is so far unknown. In general, Singer *et al.* could show that CEACAM1 delays apoptosis in rat granulocytes, thereby resulting in longer survival [110]. Especially for neutrophils it could be shown that CEACAM1 supports the bacterial internalization depending on the phosphatidylinositol-3'kinase (PI3K) [111]. But, overexpression of CEACAM1 Ig_{C2} domains stops CEACAM1 mediated internalization [111]. Moreover, CEACAM1 is partly responsible for granulopoiesis of neutrophils [112] and in combination with CEACAM3 and 6 CEACAM1 boost the neutrophil response against *Neisseria* [113].

1.4.3 Human CEACAM3

Human CEACAM3 (CD66d) is exclusively expressed on human granulocytes [114], [115]. It consists of one IgV like domain (see Fig. 1.5, red) and one transmembrane domain (purple). The cytoplasmic tail of CEACAM3 consists of an ITAM like motif (see Fig. 1.5), (YXXL/Ix₆₋₈YXXL/I), that gets phosphorylated by Src kinase, inducing activating signals. This stimulates the small GTPase Rac, which is responsible for actin cytoskeleton dynamics and the production of ROS [116]. Sarantis *et al.* could show that the ITAM of CEACAM3 is responsible for neutrophil activation, ROS production and degranulation of cells infected with *Neisseria* [113]. Furthermore, the interaction of *N. gonorrhoeae*, *N. meningitidis*, *M. catarrhalis* or *H. influenzae* with CEACAM3 leads to opsonin independent phagocytosis [116]. This process is ITAM independent [113] and compared to CEACAM1 induces phagocytosis much more efficiently [116]. Moreover, the phagocytosis is independent of PI3K, however, it is essential for ROS production [117]. Compared to other CEACAMs, CEACAM3 does not interact with itself or other CEACAMs. Furthermore, coexpression of CEACAM3 with the inhibitory CEACAM1 does not result in an inhibition of the immune response [113].

1.4.4 Human CEACAM6

Characteristic for the CEACAM6 molecule, consisting of two IgC (see Fig. 1.5 blue) and one IgV like domain (red), is the fixation via a GPI anchor (green) to the plasma membrane. Only primates own CEACAMs with a GPI anchor [93]. CEACAM6 is expressed on human neutrophils and different epithelial cells, for example in stomach epithelial cells

[95]. Moreover, soluble CEACAM6 was detected in the blood. CEACAM6 acts as an important marker in medical science and diagnostics, because it is overexpressed in tumors [95], which led to its discovery. Furthermore, CEACAM6 is held responsible for the development of tumors, because the overexpression of CEACAM6 destroys the tissue architecture, blocks differentiation and induction of the programmed cell death (anoikis) [103]. All these functions depend on the GPI anchor of CEACAM6 [118], which has probably developed by changes in the transmembrane domain of CEACAM1 [119]. The transmembrane domain of CEACAM1 has a contrary inhibitory anti tumorigenic effect as compared to CEACAM6. Like CEACAM1, CEACAM6 supports bacterial internalization [111] and interacts with itself (homophilic interaction) as well as with other CEACAMs (heterophilic interaction). The exact function of CEACAM6 on neutrophils and its role in the interaction with pathogens is so far unknown.

1.4.5 Murine CEACAM1 and 2

In contrast to humans, mice express two different variants of CEACAM1: murine CEACAM1 (formerly called as biliary glycoprotein (Bgp)1) and murine CEACAM2 (Bgp2). Both are located on murine chromosome seven and share conserved exon and intron structures [120], [121] and have a sequence structure similarity of 79,6 % [122]. However, Robitaille *et al.* could show that murine CEACAM1 and 2 produce different splice variants, which differ in their gene expression pattern and therefore in their function [123]. Murine CEACAM1 is expressed during embryonal development and in the adult organism in different tissues, such as: the liver, the small intestine, the prostate and the spleen [122]. However, murine CEACAM2 is expressed in the crypts of epithelial- and intestine tissue, in the kidney, in the uterus, in gut-resident MΦs [123], in the liver, the brain [120], in the testicle, in the spleen (low expression) [122] and on murine blood platelets [124]. On granulocytes murine CEACAM1 was detected, but not murine CEACAM2 [123]. The different functions of murine CEACAM1 and 2 were analyzed in aggregation experiments: It could be shown that only murine CEACAM1 functions as a homophilic binding molecule [123]. All in all, murine CEACAM1 is more similar to human CEACAM1 in comparison to murine CEACAM2 [122]. However, the differences in the sequence of human and murine CEACAM1 are considered to be sufficient to cause different functions, as it is exemplified by the fact that murine CEACAM1 does not support bacterial internalization [125]. Moreover, murine CEACAM1 does not function as a receptor for human pathogens like *H. pylori* and *Neisseria* [34], [126]. Another difference between human and murine CEACAM1 is the immunorezeptor tyrosine based switch motif (ITSM), TxYxx(V/I), which characterizes murine CEACAM1 besides its ITIM. Similar to the ITIM, SHP1 and SHP2 bind to the ITSM after phosphorylation by Src kinase. The difference between

the ITIM and the ITSM is the necessity of an adapter molecule bound by the ITSM. Then, depending on the adapter molecule the ITSM gets phosphorylated or dephosphorylated and results in activating or inhibitory signals. Evolutionary speaking, CEACAM1 of *Catarrhini apes* (also called as old world monkeys), including humans, in former times also possessed an ITSM. This ITSM was replaced by the second ITIM in CEACAM1 of *Homo sapiens* [93]. An other model organism in *H. pylori* research the Mongolian gerbil (*Meriones unguiculatus*) (see section 1.5) which also contains an ITSM in its CEACAM1. Thus, it would be interesting to know more about the Mongolian gerbil CEACAMs, especially their CEACAM1, since little is known about CEACAM1 in Mongolian Gerbils so far.

1.4.6 *H. pylori* - CEACAM interaction

H. pylori recognizes human CEACAM1, 3, 5 and 6 via the IgV like N-terminal domain [34]. For this the bacterium uses HopQ, which was identified to be the main and so far only known binding adhesin of *H. pylori* for CEACAMs [34], [35]. In other bacteria such as *Neisseria* several different opacity proteins (Opa) proteins interact with CEACAMs. Moreover, Opa proteins are phase-variable. Although, *H. pylori* is able to turn off SabA, the bacterium cannot switch off HopQ. The protein exists in two forms HopQI and HopQII [127]. Some studies have linked the occurrence of HopQI and the oncoprotein CagA of *H. pylori* and demonstrated a stronger binding and CagA phosphorylation in HopQI strains [127]. HopQ interacts with human CEACAMs via the interface between two CEACAM molecules and inhibits CEACAM dimerization [38]. However, murine, bovine and canine CEACAMs are not recognized by HopQ [34]. An explanation could be the high adaptability to humans and the differences in CEACAMs in different species. In murine neutrophils only murine CEACAM1 is expressed, whereas in human neutrophils CEACAM1, 3 and 6 were detected. Human CEACAMs function as pathogen receptors for *H. pylori* and are essential for CagA translocation [128]. No other functions of CEACAMs in the interaction with *H. pylori* are known so far.

1.5 *H. pylori* infection model systems

Besides *in vitro* infection experiments and analysis of biopsy-derived tissues, also *in vivo* infection experiments are performed in research on *H. pylori*. For these, the most common model organism in infection research is *Mus musculus*. But, human clinical isolates of *H. pylori* do not colonize mice [129]. Only a few mouse adapted strains, such as the Sydney strain (SS1), were successfully isolated from the murine stomach after experimental infections [130]. Colonization of C57BL6 mice with the SS1 strain resulted after six month in an active chronic gastritis [130]. In comparison to humans, the mouse adapted *H. pylori* strain only cause a mild pathology in mice. Thus, the mouse is a not suitable animal model to study a *H. pylori* induced gastric pathology.

In 1996, Hirayama *et al.* could show that *H. pylori* colonize in Mongolian gerbils (*Meriones unguiculatus*) and cause an infiltration of PMNs and mononuclear cells in the mucus layer of the gastric epithelium indicating a gastritis [131]. Other researcher confirmed these results and demonstrated the development of intestinal metaplasia, gastric ulcer [132] and after 18 month of infection gastric cancer [133]. Moreover, Matsumoto *et al.* showed that it is possible to clear the infection by an eradication of the bacterium by antibiotic therapy using amoxycillin [134]. Thus, the pathology of an infection of the Mongolian gerbil with *H. pylori* is more comparable to the human situation [135]. However, Mongolian gerbils are not an ideal model organism, because nearly no antibodies or transgenic animals are available. In addition, the genome of the Mongolian gerbil is only known since 2019 [136]. In order to establish a better model system, different humanized mouse lines are now being investigated.

A possible model system for *H. pylori* research could be humanized CEACAM mice. Originally, Eades *et al.* generated transgenic CEA mice expressing human CEACAM5 to establish an animal model for tumor immunotherapy, because CEACAMs were overexpressed in tumor tissue [137]. Ten years later, Chan *et al.* transferred a CEA bacterial artificial chromosome (CEABAC) in mice, which consists of the complete genes for human CEACAM3, 5, 6 and 7 [138]. Their aim was to perform preclinical testing of CEA-targeted therapies as well as studies with *N. gonorrhoeae*, which interacts with CEACAM receptors [138]. In addition, Gu *et al.* established a transgenic mouse expressing human CEACAM1, named tg418, to study the interaction of human pathogens with human CEACAM1 [126]. Furthermore, Gray-Owen and his team combined both mouse lines and generated a mouse expressing human CEACAM1, 3, 5, 6 and 7 (unpublished).

1.6 Aims of this work

H. pylori, classified by the WHO as a class I carcinogen, persistently colonizes the stomach of half of the world's population. Characteristic of a *H. pylori* infection is a massive infiltration of neutrophils, which are the first recruited immune cells getting in touch with the bacterium. Their task is to initiate the removal of invading pathogens, but the innate immune cells and the following immune response are apparently successfully manipulated by *H. pylori* and not able to eliminate the bacterium. The massive production of ROS of the PMNs destroys the surrounding tissue, but not the bacteria. In humans the ongoing infection can result in various malignancies such as gastric cancer, whereas mice infected with *H. pylori* show only a mild pathology. Humans express several CEACAMs on the surface of different cell types. They function as pathogen receptors and promote intra- and intercellular signaling, such as human CEACAM1 expressed on B- and T-cells inhibiting the immune response and CEACAM6 promoting the development of tumors [101], [103]. Moreover, CEACAM3, which is exclusively expressed on granulocytes, enhance ROS production and promote phagocytosis of human pathogens such as *N. gonorrhoeae* [116]. For *H. pylori* human CEACAMs are essential to translocate CagA into gastric epithelial cells [128]. However, their role on neutrophils has not been investigated so far. On human neutrophils CEACAM1, 3 and 6 are expressed. Previous work demonstrated the interaction of *H. pylori* with human CEACAM1, 5 and 6 [34]. In contrast, murine neutrophils express only murine CEACAM1, which does not function as a receptor for *H. pylori* [34]. The aim of this work was to study the role of human CEACAMs for the interaction of *H. pylori* with neutrophils. Thus, migration, ROS production, binding, phagocytosis, chemokine secretion and CagA translocation and phosphorylation were studied in human, murine and humanized CEACAM neutrophils, DCs and M Φ . Furthermore, neutrophils of naive and chronically infected humans and mice have been investigated. This might facilitate the understanding of the host pathogen interaction. Moreover, it may lead to a more suitable humanized mouse model to study the *H. pylori* infection *in vivo*.

2. Material and methods

2.1 Isolation and cultivation of cells

2.1.1 Mouse lines

Tab. 2.1 lists all mouse lines used in this work.

Tab. 2.1: Overview of all mouse lines used in this work

| name | description | reference |
|----------------|---|------------------------------------|
| wt | C57BL/6 mice | |
| hCEACAM1 | Human CEACAM1 transgenic mice cross bred with C57BL/6 2D2 to eliminate murine CEACAM1 | [126] |
| hCEACAM3, 6 | Human CEACAM3, 5, 6, 7 transgenic mice cross bred with C57BL/6 2D2 to eliminate murine CEACAM1 | [138] |
| hCEACAM1, 3, 6 | Human CEACAM1, 3, 5, 6, 7 transgenic mice cross bred with C57BL/6 2D2 to eliminate murine CEACAM1 | kindly provided by Prof. Gray Owen |

All procedures with these specific-pathogen-free mice (see Tab. 2.1) were performed according to the guidelines for care and use of laboratory animals by a veterinarian. They were approved by the Regierung von Oberbayern (ROB-55.2-2532.Vet_02-18-189).

The humanized CEACAM mouse lines were kindly provided by Prof. Dr. John E. Shively, Prof. Dr. Clifford Stanners and Prof. Gray Owen. All humanized CEACAM mouse lines were crossed with the C57BL/6 2D2 mouse line. In this mouse line the murine CEACAM1 gene is inactive. Thus, negative effect of two different CEACAM1 versions in one mouse can be avoided.

For infections two times a dose of 10^9 bacteria of the *H. pylori* strain PMSS1 (see Tab. 2.6) were injected orogastrically in mice. After four weeks the animals were killed with

CO₂. To prove the infection with *H. pylori*, stomach tissue was homogenized and colony forming units (CFUs) of the bacteria were calculated.

2.1.2 Isolation of murine neutrophils

The isolation of murine bone marrow derived neutrophils from wt and different humanized CEACAM mice (see Tab. 2.1) was performed according to the method of Schymeinsky *et al.* by density gradient centrifugation [139], [140]. In detail, first the hind leg bones (femur and tibia) of the mice were prepared. Then the intact bones were incubated in 70% ethanol in a sterile Petri dish for a few min for disinfection. Both ends of the bones were cut with a sterile scalpel, so that the bones could be flushed with a needle using phosphate buffered saline (PBS) without calcium and magnesium (Life Technologies). The cell suspension resulting of flushing the bones was centrifuged. The obtained cell pellet was resuspended and applied on a Percoll gradient consisting of 72%, 64% and 52% Percoll. After 30 min centrifugation at 1000 x g at 4 °C without using brake different cell types were separated by their density in the Percoll gradient. The cell layer between 64% and 72% Percoll was cultivated in RPMI 1640 cell culture medium supplemented with 10% FCS (Life Technologies) and 20% supernatant of WEHI3B cells producing IL-3 overnight.

2.1.3 Isolation of human neutrophils

Human neutrophils were obtained from blood of healthy adult volunteers by density gradient centrifugation, as described before by [141]. All volunteers signed a written approval. The collection was conducted according to the Declaration of Helsinki and was approved by the Ethics Committee of the LMU Munich. Briefly, 40 ml of human blood was taken and heparinized with 10 U/ml. One fifth of the total volume was centrifuged at 1000 x g for 5 min at room temperature (RT). The serum was added to the human blood and incubated at RT to separate red from white blood cells. After 1.5 h the white blood cells were layered on top of a Percoll gradient consisting of 4 ml 74% and 3 ml 55% Percoll (Sigma). The gradient was centrifuged at 600 x g for 20 min at RT without a brake. Afterwards the human neutrophils were taken from the interphase between the two Percoll layers and washed with PBS.

2.1.4 Isolation of murine DCs and M Φ

Murine DCs and M Φ were received from murine bone marrow after eight to twelve days of differentiation in media with GM-CSF or M-CSF, according to the protocol of Lutz *et al.* [142]. In detail, the bone marrow was flushed with PBS from femur and tibia similar

to the isolation of bone marrow-derived neutrophils (see section 2.1.2). Afterwards 5×10^6 cells of the murine bone marrow were cultivated in a petridish at 37°C and 5% CO_2 in RPMI 1640 supplemented with 20 ng/ml rm GM-CSF to differentiate to DCs and in Dulbecco's Modified Eagle medium (DMEM) supplemented with 10 ng/ml rm M-CSF to differentiate to $\text{M}\Phi$ (see Tab. 2.2). After three and seven days of cultivation new media were added to the cells. DCs were harvested 8-10 days and $\text{M}\Phi$ 10-12 days after stimulation.

Tab. 2.2: Medium of murine DCs and $\text{M}\Phi$

| cells | medium | company |
|----------------|--------------------------------------|-------------------|
| DCs | RPMI 1640 1640 with 2 mM L-glutamine | Life Technologies |
| | + 10% FCS | Life Technologies |
| | + 20 ng/ml rm GM-CSF | PeperoTech |
| $\text{M}\Phi$ | DMEM with 2 mM L-glutamine | Life Technologies |
| | + 5% horse serum (heat inactivated) | PAA |
| | + 10 mM HEPES | Life Technologies |
| | + 1 mM pyruvate | Life Technologies |
| | + 10 ng/ml rm M-CSF | ImmunoTools |

2.1.5 Isolation of human DCs and $\text{M}\Phi$

Human monocytes were obtained from blood of healthy, adult volunteers according to ethical guidelines (see section 2.1.3) and were differentiated to DCs and $\text{M}\Phi$. Briefly, 20 ml blood were taken and heparinized (see section 2.1.3). The blood was mixed with 30 ml PBS and layered on 15 ml Ficoll. After 30 min centrifugation at $400 \times g$ without brake at RT monocytes were collected from the interphase. They were washed with PBS and resuspended in $100 \mu\text{l}$ PBS. Then, $20 \mu\text{l}$ human CD14 MACS beads (Milteny Biotec) were added, followed by 15 min incubation at 4°C and a subsequent washing with PBS. Afterwards cells bound to the MACS beads were isolated using the magnetic force in an equilibrated MACS column. After three washing steps the cells were detached with mechanical force. They were washed again and were incubated in RPMI 1640 with 2% FCS, 50 ng/ml rh GM-CSF (ImmunoTools) and 1000 Units IL-4 for six days to differentiate to DCs. $\text{M}\Phi$ were isolated according to the same protocol except media usage. $\text{M}\Phi$ media contained 50 ng/ml rh M-CSF (ImmunoTools). Media were changed every two days.

2.1.6 Cell lines and their cultivation

Tab. 2.3 lists all cell lines used in this work.

Tab. 2.3: Cell lines used in this work

| cell line | description | reference |
|--|---|--|
| B16-GM-CSF | murine melanoma cell line B16-F10 with retroviral vector for rm GM-CSF | kindly provided by Ms. Anding |
| CHO-SCF | immortalized cell line from hamster ovaries (CHO) transfected with SCF cDNA | kindly provided by Ms. Anding |
| HM5 | GM-CSF producing CHO cell line | kindly provided by Prof. Gray Owen |
| Hoxb8 wt neutrophils without murine CEACAM1 | neutrophil cell line of murine bone marrow of C57BL/6 2D2 mice | generated in this work |
| Hoxb8 CEACAM1, 3, 6 neutrophils | neutrophil cell line of murine bone marrow of C57BL/6 2D2 tg418 CEABAC mice | generated in this work |
| MPRO | murine bone marrow cell line | ATCC CRL 11422 |
| MPRO CEACAM 1 | murine bone marrow cell line expressing human CEACAM 1 | [113] |
| MPRO CEACAM 3 | murine bone marrow cell line expressing human CEACAM 3 | [113] |
| Phoenix Eco | human kidney cell line (packaging cell line) | kindly provided by Ms. Anding |
| WEHI3B | murine myelomonocyte leukemia, IL-3 producing cell line | ACC 26 |

Cells were cultivated at 37 °C and 5% CO₂ in 75 cm² tissue culture flasks (BD Falcon) and subcultured every 2-3 days. In detail, the adherent cell lines B16-GMCSF, CHO-SCF and

HM5 were washed with PBS. Then 0.5% Trypsin/EDTA (Life Technologies) was added and the cells were incubated for a few minutes at 37 °C and 5% CO₂. After detachment of the cells the reaction was stopped with media (see Tab. 2.4), and the cell suspension was splitted 1:4 to 1:8 and supplemented with fresh media. WEHI3B cells were scraped off with a cell scraper, splitted 1:3 and supplemented with fresh media (see Tab. 2.4). The suspension cell lines Hoxb8 and MPRO cell lines were splitted 1:4 to 1:8 and new media were added.

Tab. 2.4 lists all cell culture medium for cell lines used in this work.

Tab. 2.4: Cell culture medium used in this work

| cell line | medium | company |
|-----------|--|-------------------|
| B16-GMCSF | RPMI 1640 | Life Technologies |
| | + 10% FCS | Life Technologies |
| CHO-SCF | Opti-MEM GlutaMAX | Life Technologies |
| | + 10% FCS | Life Technologies |
| | + 3 μ M β -Mercaptoethanol | Gibco |
| HM5 | DMEM | Life Technologies |
| | + 10% FCS | Life Technologies |
| | + 1% GluatMAX | Gibco |
| WEHI3B | RPMI 1640 | Life Technologies |
| | + 10% FCS | Life Technologies |
| Hoxb8 | Optimem Glutamax | Life Technologies |
| | + 10% FCS | Life Technologies |
| | + 0.06% β -Mercaptoethanol | Life Technologies |
| | + 1% supernatant of SCF cells | |
| | + 0.01% β -Estradiol | Sigma |
| MPRO | Isocov's modified Dulbeccos media (IMDM) | Life Technologies |
| | + 20% horse serum (heat inactivated) | PAA |
| | + 1.5 g/L sodium bicarbonat | Sigma |
| | + 1% Gluatmax | Gibco |
| | + 2.5% supernatant of HM5 cells | |

For determination of cell numbers the cells were counted with a Casy cell counter (OLS OMNI Life Science). Apart from that cell numbers were calculated by a life/death staining using a Neubauer cell counting chamber. Then, defined cell numbers were seeded in

cell culture plates and used for experiments.

2.1.7 Immortalization and differentiation of cells

Neutrophils, M Φ and DCs arise from a hematopoietic stem cell and have a limited life time. In order to cultivate these cells they have to be immortalized. Before the experiments immortalization is canceled by adding or removing medium components as described in the following part and cells differentiate again. In detail, Hoxb8 cells were arrested by β -estradiol (Sigma) and differentiate in media without β -estradiol. MPRO cells were immortalized by a dominant negative retinoic acid receptor. After 72 h in medium with a physiological dose of retinoic acid they start differentiation again. Differentiation of isolated blood or bone marrow cells are described before (see section 2.1.2-5).

2.1.8 Cryoconservation of cells

For cryoconservation, a defined number of cells was centrifuged and resuspended in their respective cell culture medium supplemented with 20% FCS and 10% DMSO (Sigma) in cryogenic tubes (Nalgene, Thermo Fisher Scientific). Those tubes were stored for at least 24 h at -80°C and then for long term storage, in liquid nitrogen at -196°C .

For thawing of cells, the cryogenic tubes were incubated at 37°C until the cells were nearly completely thawed. Then cell culture medium was added and the cell suspension was centrifuged. Afterwards the supernatant was discarded. The cell pellet was resuspended in cell culture medium and transferred to a 75 cm^2 tissue culture flask, which was incubated at 37°C as described in section 2.1.6.

2.1.9 Generation of ER-Hoxb8 neutrophil cell lines

Neutrophils isolated from the bone marrow have a short life time, their number is limited and their isolation is time consuming and expensive. Therefore, progenitor cells of neutrophils were immortalized according to Wang *et al.* by retroviral transfection with ER-Hoxb8. Thus, unlimited amounts of progenitor cells of this cell line can be cultured and differentiated to neutrophils [143]. In detail, Wang *et al.* fused the estrogen binding domain of an estrogen receptor (ER) to the N-terminus of Hoxb8. Then the fusion cDNA was cloned in a retroviral vector [143], which was transfected in stimulated progenitor cells. Estrogen added to the neutrophil cell culture media arrests the cells by binding to the fusion product of the estrogen receptor and Hoxb8. Whereas in neutrophil cell culture media without estrogen cells differentiate to neutrophils.

In this work ER-Hoxb8 neutrophils were generated from C57BL/6 2D2 mice, which do not express murine CEACAM1 anymore. In addition, ER-Hoxb8 neutrophils were generated from C57BL/6 2D2 mice, expressing human CEACAM1, 3 and 6. Briefly, bone marrow was isolated from femur and tibia. Afterwards cells were stimulated with 10 ng/ml murine IL-3 (PeperoTech), 20 ng/ml murine IL6 (PeperoTech) and 1% SCF for two days. Meanwhile 19.4 μ l of the vector and 10 μ g DNA were transfected with 25 μ l Lipofectamin2000 (Life Technologies) in 58.5 μ l in pCLEco, Top 10 packing vector. This was transfected in a Phoenix Eco packing cell line, thereby producing virus particles. After two days, the prestimulated cells were infected with 3 ml virus containing supernatant. Then, 5 μ g/ μ l polybrene (Millipore) was added for a higher efficiency of gene transfer. Thus, the fusion product of ER and Hoxb8 randomly integrate in the genome of the cells. By adding SCF, gained from CHO cells, the cells develop to progenitor cells, which were arrested by β -estradiol in the cell culture media.

2.2 Microbiological methods

2.2.1 Bacterial strains

Tab. 2.5-2.6 show all bacterial strains used in this work.

Tab. 2.5: *H. pylori* strains used in this work part I

| strain | internal ID | description | reference |
|----------------------------|-------------|---|---------------------------|
| 26695 | VKH5 | wildtype; clinical isolate | [144] |
| 26695 Δ <i>hopQ</i> | VKH18 | Δ <i>hopQ</i> mutant of 26695 | Odenbreit (not published) |
| G27 | LHP20 | wildtype; clinical isolate | [145] |
| G27 Δ <i>hopQ</i> | VKH70 | Δ <i>hopQ</i> mutant of G27 | Königer (not published) |
| B8 | EL5 | gerbil adapted | [146] |
| SS1 | UB242 | murine, passaged isolate of the clinical isolate 10700, the PMSS1 | [130] |
| X47 | UB24 | mouse adapted | [147] |
| PMSS1 | UB47 | clinical isolate, parental strain of SS1 | [148] |

Tab. 2.6: *H. pylori* strains used in this work part II

(CmR: Chloramphenicol resistance, KanR: Kanamycin resistance, ErmR: Erythromycin resistance, strepR/S: streptomycin sensitivity)

| strain | internal ID | description | reference |
|------------------------------|--------------------|--|---------------------------|
| P12 | WSP12 | wildtype; clinical isolate (888-0) from the University of Hamburg | [149] |
| P12 $\Delta cagI$ | WSP556 | P12 transformed with pWS320; ErmR; $\Delta cagI$ | [150] |
| P12 $\Delta hopQ$ | WSP1254 | P12 transformed with pFS10; ErmR; $\Delta hopQ$ | [38] |
| P12 $\Delta cagA$ | PJP52 | P12 transformed with pWS30; KanR; $\Delta cagA$ | [44] |
| P12 $\Delta vacA$ | P163 | clinical isolate lacking <i>vacA</i> ; ErmR | Fischer |
| P12 $\Delta cagA\Delta vacA$ | P165 | P12 $\Delta vacA$ (P163), ErmR, transformed with pWS130 | Haas (not published) |
| P12 strep wt GFP | LH-P229 | pHel4-GFP | [34] |
| P12 strep $\Delta hopQ$ GFP | LH-P230 | $\Delta hopQ$; pHel4-GFP | [34] |
| P12 TEM-CagA | FSP1 | P12[pWS373] transformed with pWS486; CmR; expressing TEM-CagA | [151] |
| P12 TEM-CagA; $\Delta cagI$ | FSP2 | P12[pWS486] transformed with pWS320; CmR, ErmR; TEM-CagA expression, $\Delta cagI$ | [151] |
| P12 TEM-CagA; $\Delta hopQ$ | FSP21 | P12[pWS486] transformed with pFS10; CmR, ErmR; TEM-CagA expression, $\Delta hopQ$ | Schindele (not published) |

2.2.2 Cultivation of bacteria

H. pylori were streaked from a glycerol stock on a serum plate and were cultivated under microaerobic conditions at 37 °C and 5% O₂, 10% CO₂, 85% N₂. After 48 h, bacteria were passaged on a new serum plate every day. For experiments *H. pylori* were used after one passage on a new serum plate. Serum plates consists of GC agar base (Oxoid) supplemented with 8% horse serum (PAA) and 1% vitamin mix. The vitamin mix consists of 100 g/L α -D-glucose, 10 g/L L-glutamine, 26 g/L L-cysteine, 1.1 g/L L-cystine, 0.15 g/L L-arginine, 0.1 g/L cocarboxylase, 20 mg/L iron(III)nitrate, 3 mg/L thiamine, 13 mg/L p-aminobenzoic acid, 0.25 g/L nicotinamide adenine dinucleotide, 10 mg/L vitamin B12, 1 g/L adenine, 30 mg/L guanine and 0.5 g/L uracil.

For experiments, bacteria were taken off a serum plate with a sterile cotton swab and resuspended in PBS with 10% FCS. Then the optical density of the bacteria suspension was determined with a spectrophotometer (DR 2000, Hach). For *H. pylori*, the optical density was measured at a wave length of 550nm. At this wavelength, an optical density of 0.1 correlates to approximately 2.5×10^7 CFU/mL.

2.2.3 Cryoconservation of bacteria

Bacteria from serum plates were resuspended in 70% Brucella Broth (BB) (Becton Dickinson) supplemented with 10% FCS (heat inactivated 20 min at 56 °C) and 20% glycerol in cryogenic tubes (Nalgene, Thermo Fisher Scientific) and were stored at -80 °C.

2.3 *In vitro* infection

For an *in vitro* infection the optical density of the bacteria was measured with a spectrophotometer (see section 2.2.2) and the number of cells was determined (see section 2.1.6). Then, the bacteria were incubated with cells in PBS supplemented with 10% FCS (heat inactivated 20 min at 56 °C) at a defined multiplicity of infection (MOI) at 37 °C and 5% CO₂.

2.3.1 Survival assay

Survival of phagocytosed bacteria was studied according to Odenbreit *et al.* [152]. Briefly, 2×10^5 cells were infected with an MOI of 25 for 0.5, 1 or 1.5 h with *H. pylori* P12, a *H. pylori* P12 Δ *hopQ*, a *H. pylori* P12 Δ *cagA*, a *H. pylori* P12 Δ *vacA* or a *H. pylori* P12

$\Delta cagA\Delta vacA$ mutant. Afterwards adherent extracellular bacteria were killed by 1 h incubation with $100 \mu\text{g ml}^{-1}$ gentamicin. After one hour cells were washed with PBS and the cell membrane was permeabilized using PBS with 0.1% saponin. Then the supernatant was plated on serum plates and after three days of incubation, the number of CFUs was determined.

2.4 Biochemical methods

2.4.1 Bacterial and cellular lysates

For generation of bacterial and cellular lysates a defined number of bacteria or cells was harvested by centrifugation. For chemokine measurements the supernatant was saved and stored until further use, otherwise it was discarded. The pellet was resuspended in 2 x SDS loading buffer and PBS* (Tab. 2.7). After an incubation at 95°C for 10 min the samples were stored at -20°C until further analysis.

Tab. 2.7: Solutions for lysates

| solution | components |
|-----------------------------------|--|
| PBS* | PBS + 1 mM phenylmethylsulfonyl fluoride + 1 mM sodium vanadate + 1 μM leupeptin + 1 μM pepstatin |
| 2 x SDS-PAGE sample buffer | 100 mM Tris-HCl pH 6.8 + 4% (w/v) SDS + 20% (v/v) glycerol + 10% (v/v) β -mercaptoethanol + 0.2% (w/v) bromphenol blue |

2.4.2 Sodium dodecyl sulfate polyacrylamide gel electrophoresis

Sodium dodecyl sulfate polyacrylamide gel electrophoresis (SDS-PAGE) is a common technique for separation of proteins. The proteins can then be immobilized and detected in an immunoblot with specific antibodies. For separation of proteins, a resolving and a

stacking gel were prepared. The components sufficient for one gel are listed in Tab. 2.8.

Tab. 2.8: SDS gel mixture

| substance | resolving gel (8%) | stacking gel |
|---|--------------------|--------------|
| ddH ₂ O | 2.3 ml | 0.68 ml |
| acrylamide (Rotiphorese® Gel 30 (37.5:1)) | 1.3 ml | 0.17 ml |
| 1.5 M Tris/HCl, pH 8.8 | 1.3 ml | |
| 1.0 M Tris/HCl, pH 6.8 | | 0.13 ml |
| 10% SDS | 0.05 ml | 0.01 ml |
| ammonium persulfate | 0.05 ml | 0.01 ml |
| trichloroethanol | 0.05 ml | 0.01 ml |
| tetramethylethylenediamine | 0.003 ml | 0.001 ml |

The resolving gel mixture was filled in the mini gel polymerization cassette between two glass plates. After polymerization the stacking gel was loaded on top and a comb was inserted for formation of slots. The samples were loaded in the polymerized SDS gel. Page Ruler™ Prestained Protein Ladder, 10 to 180 kDa (Fermentas) was used for a marker. Electrophoresis was performed in SDS-PAGE running buffer with a voltage of 130 V in the mini-PROTEAN 3 Cell chamber gel electrophoresis system of BioRad. After electrophoresis, protein bands of the SDS-PAGE were visualized using trichloroethanol in the SDS gel on the ChemiDoc MP device from BioRad. Pictures were taken with the Image Lab software.

2.4.3 Immunoblot

An Immunoblot, also known as Western blot, is an antibody based technique for detection of proteins, which are separated by SDS-PAGE and immobilized on a membrane.

Blotting

After separation of proteins by SDS-PAGE, the proteins were transferred on a polyvinylidene fluoride (PVDF) membrane using a semi dry blotting system (all buffers are listed in Tab. 2.9).

Tab. 2.9: Blotting buffer

| solution | anode I | anode II | cathode |
|----------------------|----------------|-----------------|----------------|
| Tris HCl | 300 mM | 25 mM | 25 mM |
| | pH 10.4 | pH 10.4 | pH 9.6 |
| 6-amino caproic acid | - | - | 40 mM |
| methanol | 10 % | 10 % | 10 % |

For blotting thick Whatman papers saturated in anode I buffer followed by thin Whatman papers soaked in anode II buffer were placed in a blotting chamber. The SDS gel were put on a PDVF membrane activated in methanol (Sigma) and placed on the Whatman papers. On top Whatman papers saturated in cathode buffer were stacked. Then a current of $1.25mA/cm^2$ for 70 min was applied to transfer the proteins from the gel to the membrane. Afterwards the membrane was dried to fix proteins.

Detection of immobilized proteins

Next, the dried membrane was activated with methanol. Then, the membrane was blocked with TBS-Tween buffer (TBS-T) supplemented with 3% BSA (see Tab. 2.10) for at least 1 h at RT. Primary antibody was added and incubated over night at $4^\circ C$ or for at least 3 h at RT. After washing four times with TBS-T the blot was incubated with the secondary antibody for 45 min at RT, followed by washing four times. For the development of blots incubated with a horseradish peroxidase (POX) coupled secondary antibody, Immobilon Chemiluminescent HRP Substrate (Millipore) was used. The chemiluminescence reaction was detected on an X-ray film (Fuji Medical X-Ray Films Super RX, Fujifilm). The development solution of alkaline phosphatase (AP) blots is shown in Tab. 2.10. The blots were incubated in the AP detection solution until the bands were visible. For detection of another protein on the same membrane after chemiluminescence development the membrane was incubated for 1 h using stripping solution (see Tab. 2.10).

Tab. 2.10: Solutions for immunoblots

| solution | components |
|--------------------------------|--|
| 10x TBS | 1.5 M NaCl + 200 mM Tris/HCl, pH 7.5 |
| TBS-Tween buffer(TBST) | 100 mL 10x TBS + 0.75 mL Tween 20 filled up to 1 L dH ₂ O |
| AP development solution | 100 mM Tris/HCl, pH 9.6 + 7 mM MgCl ₂ + 50 mg/L 5-Bromo-4-chloro-3-indolyl-phosphate (BCIP) + 0.1 g/L Nitro blue tetrazolium (NBT) |
| stripping solution | 25 mM glycine + 1% SDS pH 2 with HCl |

2.4.4 CagA phosphorylation

To test CagA phosphorylation, cells were infected with *H. pylori* for 3 h with a MOI 60. The pellet was resuspended in PBS* (Tab. 2.7) and an immunoblot was performed as described in 2.4.2-3. First, phosphorylated proteins were detected using the α -P-Tyr antibody PY99 and then CagA was detected with the α -CagA antibody 299 (Tab. 2.11-12).

2.4.5 Antibodies - Immunoblots

All antibodies used for immunoblots in this work are listed in Tab. 2.11 and 2.12.

Tab. 2.11: Primary antibodies - immunoblots

| antibody | description | finale concentration | company/ reference |
|-----------------|---|-----------------------------|-------------------------------|
| AK299 | α - <i>cagA</i> (EPIYA peptide) | 1:10000 | W. Fischer |
| PY99 | monoclonal α -P-Tyr antibody (murine) | 1:5000 | Santa Cruz Biotechnologies |

Tab. 2.12: Secondary antibodies - immunoblots

| antibody | description | finale concentration | company reference |
|---------------------|--|----------------------|-------------------|
| α -mouse POX | POX coupled polyclonal α -mouse IgG (goat) | 1:10000 | Sigma |
| ProteinA-AP | AP coupled to proteinA | 1:5000 | Sigma |

2.4.6 *In vitro* phosphorylation

An *in vitro* phosphorylation assay was performed to study whether kinases within the cells are active and are able to phosphorylate CagA. Therefore 6×10^6 cells were centrifuged and resuspended in NP40 cell lysis buffer (Tab. 2.13). $45 \mu\text{l}$ cells lysates, $45 \mu\text{l}$ *H. pylori* and $11 \mu\text{l}$ phosphorylation buffer (Tab. 2.13) were incubated at 30°C for 10 min. Afterwards $28 \mu\text{l}$ 5 x SDS sample buffer were added. After an incubation at 95°C for 10 min, the samples were analyzed in an immunoblot as described in section 2.4.2-3.

Tab. 2.13: Solutions for the *in vitro* phosphorylation

| solution | components |
|-------------------------------|--|
| NP40 cell lysis buffer | 20 mM Tris/HCl pH 7.5 + 150 mM NaCl + 1% noident-P40 + 1 mM EDTA + 1 mM PMSF + 1 mM sodium vanadate + $1 \mu\text{M}$ leupeptin + $1 \mu\text{M}$ pepstatin |
| phosphorylation buffer | 250 mM Tris/HCl pH 7.2 + 312.5 mM $\text{MgCl}_2 \cdot 4\text{H}_2\text{O}$ + 1 mM sodium vanadate + $400 \mu\text{M}$ ATP |

2.4.7 Src homology protein tyrosine phosphatase-1 inhibition

Protein phosphatases dephosphorylate proteins and regulate thereby signaling within the cells. Src homology (SH2) protein tyrosine phosphatase-1 (SHP-1) down regulates signals in hematopoietic cells [53]. According to Pathak *et al.*, 99% of SHP-1 activity can be inhibited by 5 min incubation of the cells with 10 $\mu\text{g}/\text{ml}$ sodium stibogluconate (Cayman chemicals) [153]. Additionally, the SHP-1 activity was inhibited according to Cho *et al.* by incubating the cells with 100 μM hydrogen peroxide for 30 min at 37 °C [154].

2.5 Flow cytometry

Flow cytometry is a technique to detect the size, the granularity and the fluorescence of single cells. The cells are separated by high pressure in the flow cytometer, all passing a forward scatter, detecting their size, a sideward scatter, detecting their granularity and a laser light exciting fluorophores in the cells or bacteria producing fluorescence emission.

2.5.1 Antibodies - flow cytometry

Tab. 2.14 lists all antibodies used for flow cytometry in this work.

Tab. 2.14: Antibodies - flow cytometry

(APC = allophycocyanin, FITC = fluoresceinisothiocyanat, PE = phycoerythrin)

| antibody | clon | company |
|---|-------------|----------------|
| FITC anti mouse/human CD11b | M1/70 | Biologend |
| PE anti mouse CD11c | HL3 | BD Bio Science |
| α -human CD66abce-APC | TET2 | Miltenybiotec |
| α -human CEACAM1 | 4/3/17 | Aldevron |
| α -human CEACAM3 | col1 | Aldevron |
| α -human CEACAM6 | 9A6 | Aldevron |
| APC rat anti mouse Ly6G | 1A8 | Biologend |
| PE Cy5 anti mouse F4/80 | Bm8 | e Bio Science |
| Rat IgG2a κ isotype control APC | eBR2a | Biologend |
| Rat IgG2a κ isotype control FITC | | BD Bio Science |
| Rat IgG2a κ isotype control PE | eBR2a | e Bio Science |
| Rat IgG2a κ isotype control PE Cy5 | eBR2a | e Bio Science |

2.5.2 Cell characterization

Neutrophils, M Φ and DCs were characterized by flow cytometry analysis. After blocking of FC receptors using goat serum, 2×10^5 cells were stained with antibodies (see Tab 2.14) according to the guidelines of the manufacturer. The primary or conjugated antibodies were incubated for 1 h at 4 °C and the secondary antibodies for 45 min at 4 °C. In between and afterwards the cells were washed three times with flow cytometry buffer consisting of PBS + 2 mM EDTA + 0.1% BSA and 0.5% FCS. Finally, the sample analysis was performed at the BD CantoII flow cytometer and the data were studied using FlowJo software (Tree Star).

2.5.3 CEACAM expression

The CEACAM expression was measured via flow cytometry analysis, too. Therefore the assays were performed as described in section 2.5.2. The antibodies used are listed in Tab 2.14. They were used according to the instruction of the manufacturer with $1.2 \mu\text{g}/10^6$ cells. Goat α -mouse Alexa488 was used as secondary antibody.

2.5.4 Interaction experiment

For analysis of the interaction of *H. pylori* and immune cells in general, 2×10^5 cells were infected with an MOI of 10 for 1 h with *H. pylori* P12 wt GFP and *H. pylori* P12 ΔhopQ GFP. Strains, which do not express GFP, were stained with 5 mg/ml 4, 6-Diamidin-2-phenylindol (DAPI) for 10 min and afterwards washed with PBS to be used for infection. After 1 h of infection cells were washed with flow cytometry buffer. Finally, the GFP or DAPI signal was detected by flow cytometry. Fluorescence intensities were normalized to uninfected cells. In addition, the GFP or DAPI intensities were normalized to the P12 wt strain.

2.5.5 Binding assay

Binding of *H. pylori* to cells was analyzed using flow cytometry. For this phagocytosis was inhibited by adding $10 \mu\text{g}/\text{ml}$ cytochalasin D. In detail, neutrophils were infected with an MOI of 25 for 1 h with *H. pylori* P12 wt GFP and *H. pylori* P12 ΔhopQ GFP. Afterwards cells were washed with flow cytometry buffer and binding was measured by flow cytometry.

2.5.6 Phagocytosis assay

Phagocytosed bacteria were detected by flow cytometry using trypan blue according to the protocol of Pils *et al.* [155]. For this PMNs were infected with an MOI of 25 for 1 h with *H. pylori* P12 wt GFP and *H. pylori* P12 Δ *hopQ* GFP. Then the cells were washed and the permeable substrate trypan blue was added to quench the green fluorescent signal of adherent bacteria. Finally, the green fluorescence signal of intracellular, phagocytosed bacteria was analyzed by flow cytometry.

2.5.7 Detection of ROS

ROS were detected according to the method of Chen *et al.* by flow cytometry. In detail, neutrophils infected with *H. pylori* with an MOI of 60 were incubated for 20 min at 37°C with dihydrorhodamine123. Meanwhile by production of ROS, the non fluorescent dihydrorhodamine is oxidized to green fluorescent rhodamine. Afterwards, the cells were centrifuged and fixed with 4% paraformaldehyd in flow cytometry buffer (see section 2.5.2) on ice. Finally, the green fluorescence was analyzed by flow cytometry [156].

2.5.8 Quantification of CagA translocation

For quantification of CagA translocation the method of Schindele *et al.* was used [151]. *H. pylori* P12 [TEM-CagA] strains were incubated for 1.5 h in PBS with 10% FCS at 37°C. Afterwards cells were infected for 2.5 h with the preincubated *H. pylori* strains. After centrifugation the supernatant was discarded and a CCF4-AM loading solution (Live-BLAzer-FRET B/G loading kit, Invitrogen) supplemented with 1 mM probenecid (Sigma) was added (Tab. 2.15). The samples were incubated for 1.5 h at RT in the dark on a shaker. Then, the samples were washed three times with flow cytometry buffer and analyzed by flow cytometry.

The CCF4-AM is colorless outside of the cell. Within the cell CCF4-AM is activated by cellular esterases and shows a green fluorescence. If TEM-CagA is translocated into the cell, CCF4-AM is cleaved and shows a blue fluorescence. Cells containing TEM-CagA show in addition a blue fluorescence. Whereas cells without CagA are not fluorescent in blue.

Tab. 2.15: Components of the CCF4-AM loading solution

| solution | components |
|--------------------------------|--|
| CCF4-AM loading solution [1ml] | 828 μ l DPBS + 1 μ l 1 mM CCF4-AM + 10 μ l solution B + 156 μ l solution C + 5 μ l 200 mM probenecid |

2.5.9 Chemokine measurement

For analysis of chemokine production, the supernatant of infected neutrophils, M Φ and DCs was collected. Chemokine measurements were performed with the LEGENDplex kit (BioLegend) according to the manufacturers instructions. The principle of the LEGENDplex kit is a bead-based sandwich immunoassay. The chemokines bind to a specific antibody conjugated to beads, which were detected by biotinylated antibodies (Streptavidin, R-Phycoerythrin Conjugate (SAPE)). The samples were measured using flow cytometry and the data were analyzed with the LEGENDplex software.

2.6 Microscopy

2.6.1 Confocal microscopy of *H. pylori* - neutrophil interaction

Besides flow cytometry, the interaction of *H. pylori* with neutrophils was studied by confocal microscopy. Therefor neutrophils were infected for 1 h with an MOI of 10 with a *H. pylori* wt strain. Afterwards 2×10^5 neutrophils were transferred to a microscopy slide by using a cytospin3 (Shandon) and were fixed with 4% formaldehyde (PFA) solution. For immunostaining non-specific binding sites of the cells were blocked with 5% goat serum over night. CEACAMs were stained in red with the pan CEACAM antibody (D14HD11, Genovac, 1:200) and a goat anti mouse Alexa555 secondary antibody (Invitrogen). *H. pylori* was stained in green with a rabbit anti-*H. pylori* (AK175, 1:400) and a goat α rabbit Alexa488 secondary antibody (Invitrogen). Moreover, the nuclei were stained with DAPI (5 μ g/ml) and the cell shape with wheat germ agglutinate (WGA)-Alexa647 (5 μ g/ml) for 10 min. Then cells were mounted with mounting medium (Dako) and were analyzed using a 63x oil immersion objective of the confocal Laser Scanning Microscope (LSM880, Zeiss) with Airyscan Module. Micrographs were analyzed with ImageJ/Fiji.

In addition, to distinguish between extra- and intracellular bacteria immune stainings

were performed with extracellular bacteria stained with rabbit anti-*H. pylori* (AK175, 1:400) and a goat α rabbit Alexa555 secondary antibody in red. Afterwards the cell shape of the nuclei were stained with WGA-Alexa647. Extra- and intracellular bacteria were stained after cell permeabilization with Triton X-100 using the same primary antibody and a goat α rabbit Alexa488 secondary antibody in green. Furthermore, cell nuclei were stained with DAPI. Micrographs were taken with the 63x oil immersion objective of the confocal Laser Scanning Microscope (LSM880, Zeiss) with Airyscan Module. In addition to ImagJ/Fiji, the Imaris software (Bitplane AG) was used to analyze the micrographs.

2.6.2 Giemsa staining

The differentiated MPRO neutrophil cell lines (Tab. 2.3) and bone marrow derived neutrophils were stained with Giemsa solution to check for differentiation of the cells. For this 2×10^5 cells were centrifuged, the supernatant was discarded and the cell pellet was resuspended in 100 μ l PBS supplemented with 0.5% BSA. Then, the cells were centrifuged in a cytospin3 at 1500 rpm for 5 min. The sample was incubated for 5 min in methanol, followed by an incubation for 30 min in Giemsa solution. Afterwards, the sample was washed in ddH₂O.

2.7 CRISPR/Cas9

The specific genome editing technique CRISPR/Cas9 was used in this work to delete SHP-1 and/or murine CEACAM 1 in MPRO and MPRO CEACAM cells. CRISPR stands for Clustered Regularly Interspaced Short Palindromic Repeats. These are gene sequences in bacteria that are able to destroy phage DNA. For the knockout the CRISPR guide RNAs were designed to lead the Cas9 nickase to the target sequence of exon 2 of SHP-1 (see Fig. 2.1 A) or exon 1 of murine CEACAM1 (see Fig. 2.1 B), where a double strand break is induced. This break gets repaired by non-homologous end-joning repair, which results in mutations in the gene of interest.

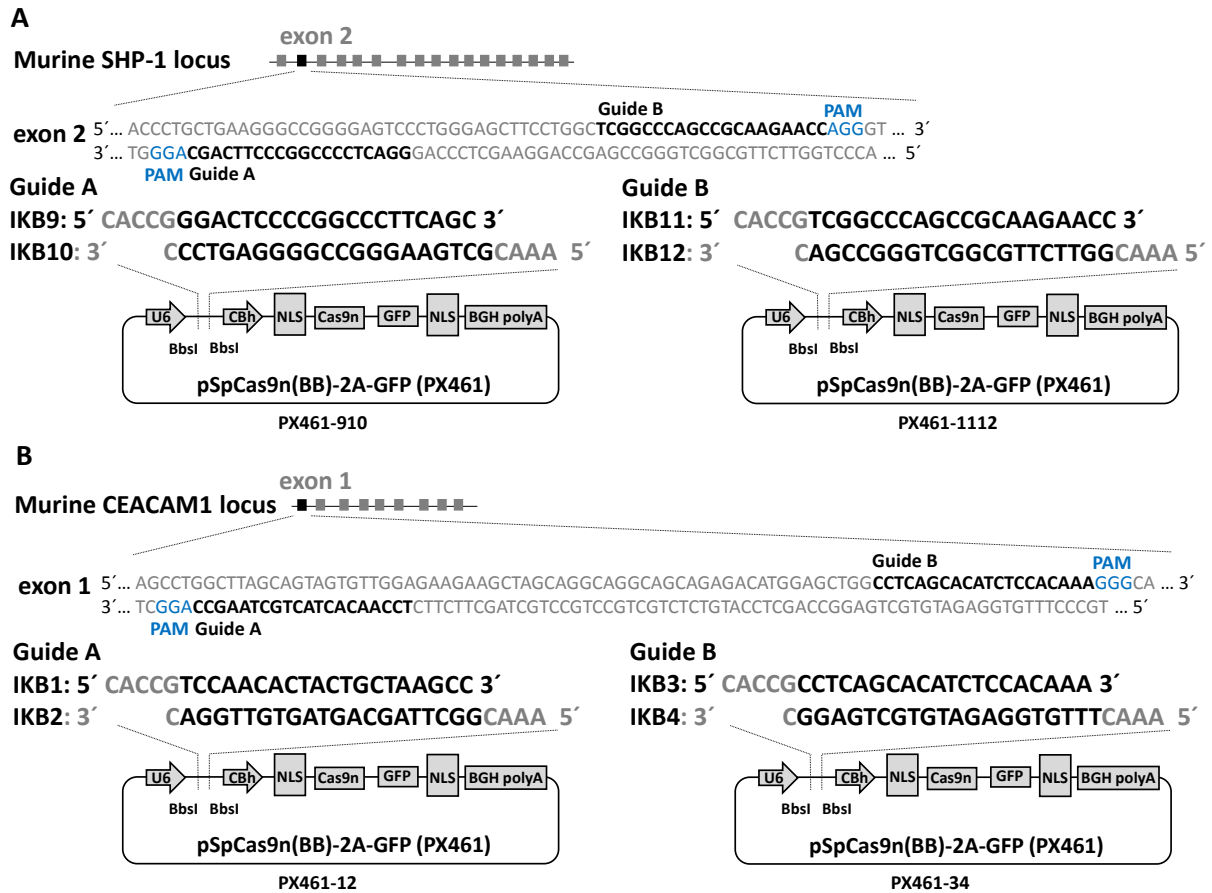


Fig. 2.1: CRISPR/Cas9 deletion strategy for SHP-1 and murine CEACAM1

CRISPR/Cas9 deletion strategy: For murine SHP-1 (A) guide RNA, located in exon 2 and for murine CEACAM1 (B), guide RNAs in exon 1, followed by the 5'NGG PAM (protospacer adjacent motif) (blue). All this was cloned in the vector pSpCas9n(BB)-2A-GFP (PX461).

For this study the CRISPR guide RNAs were designed using the online tool <http://tools.genome-engineering.org/> (see Tab. 2.16).

Tab. 2.16: CRISPR/Cas9 primer list

| primer | sequence | target/reference |
|---------------|---------------------------|-------------------------|
| IKB9 | CACCGGGACTCCCCGGCCCTTCAGC | SHP-1 |
| IKB10 | AAACGCTGAAGGGCCGGGGAGTCCC | SHP-1 |
| IKB11 | CACCGTTCGGCCAGCCGCAAGAACC | SHP-1 |
| IKB12 | AAACGGTTCTTGCGGCTGGGCCGAC | SHP-1 |
| IKB1 | CACCGTCCAACACTACTGCTAAGCC | murine CEACAM1 |
| IKB2 | AAACGGCTTAGCAGTAGTGTTGGAC | murine CEACAM1 |
| IKB3 | CACCGCCTCAGCACATCTCCACAAA | murine CEACAM1 |
| IKB4 | AAACTTTGTGGAGATGTGCTGAGGC | murine CEACAM1 |
| ZQ66 | GAGGGCCTATTTCCCATGATTCC | [128] |

The two oligos were annealed using 1 μl of each oligo, 2 μl T4 ligase buffer (NEB), 1 μl T4 ligase and 16 μl ddH₂O for 5 min at 95 °C and stored at 4 °C. The Cas9 nickase-GFP vector Px461 (Cas9n-GFP) (pSpCas9n(BB)-2A-GFP (PX461)) [157] was digested with BbsI for 3 h at 37 °C (see Tab. 2.17). Then the ligation components were added to the digestion.

Tab. 2.17: Components of the Cas9n-GFP vector digestion

| components | |
|--------------------------------|--|
| digestion of the vector | 2 μl 10x cut smart buffer (Biolabs) + 4.22 μl vector Px461 (Cas9n-GFP) (1 $\mu\text{g}/\mu\text{l}$) + 13.78 μl ddH ₂ O + 0.3 μl BbsI (NEB) |

Next 1 μl annealed oligos were incubated with 2.5 μl 10x ligase buffer and 1.2 μl T4 DNA ligase (NEB) for 1 h at RT. For transformation 2 μl were added to 10 μl stbl3 chemical competent *E. coli* cells. After a heatshock at 42 °C for 30 s they were incubated for 2 min on ice. 500 μl SOCS medium was added and 100 μl of the sample was plated on a LB Ampicillin (100 mg/L) plate. After one day clones were picked and the plasmids were extracted using the Qia prep Spin Mini prep Kit 250 following the instructors manual. The extracted plasmids were sequenced using ZQ66 (see Tab. 2.16, primer list) to check the right insertions of the oligos.

Then 1 μg (or 0.5 μg by double deletions) of the sgRNAs and 0.5 μg of the plasmid containing the Cas9 nickase-GFP vector Px461 (Cas9n-GFP) (pSpCas9n(BB)-2A-GFP (PX461)) construct were transfected in MPRO, MPRO CEACAM 1 and MPRO CEACAM 3 cells by electroporation using program T-20 according to Cullere *et al.* [158].

Afterwards the cells were sorted by GFP signals using fluorescence activated cell sorting at the flow cytometry unit of the TU Munich. Finally, the sorted cells were cultured and cells were cryconserved (see section 2.1.7).

2.8 2D migration

The under agarose migration assay is a method to study the 2D migration of cells. It was performed according to the protocol of Heit and Kubes An 8 well chamber slide (ibidi) was coated for 30 min at 37 °C with 0.1% BSA in HBSS, pH 7.2 (Sigma). 400 μl agarose solution consisting of 2 x HBSS, RPMI 1640 + 20% FCS in a 1:1 mixture and 1.6% ultra pure agarose (Invitrogen) were filled in the 8 wells chamber slide (ibidi), which were then incubated for 1 h at 37 °C under wet conditions. Then, two slots with a diameter of 3.5 mm were punched in the agarose of one well of the 8 Well chamber slide and the slide were incubated again for 1 h. Afterwards a chemoattractant were filled in one slot. After 1 h the chemoattractant gradient was formed and 1×10^6 cells were filled in the other slot. The migration of the cells under the agarose gel was studied by time-lapse microscopy using a 10x objective of the SP5 confocal microscope (Leica). The analysis was performed with the Manual Tracking Plugin for ImageJ and the Chemotaxis and Migration Tool (ibidi).

2.9 Statistics

All experiments were performed independent at least three times. Data sets show average values with the standard error of mean. For data analysis GraphPadPrism 5 software (GraphPad) was used. Other analysis programs are mentioned in the different sections. Statistical analysis of independent groups was performed using Two way ANOVA, with a Bonferroni post hoc test.

3. Results

3.1 The role of human CEACAMs for the interaction of *H. pylori* with neutrophils

3.1.1 CEACAM expression in neutrophils

For analysis of the role of human CEACAMs for the interaction of *H. pylori* with PMNs, bone-marrow derived neutrophils were isolated from murine wt and different humanized-CEACAM mice expressing: hCEACAM1, hCEACAM3, 6 and hCEACAM1, 3, 6 (see section 2.1.2, Tab. 2.1). In addition, neutrophils, isolated from human blood of healthy adult volunteers were used as controls. The isolated neutrophils were characterized and their expression of human CEACAMs was studied by flow cytometry (Fig. 3.1 and 3.2).

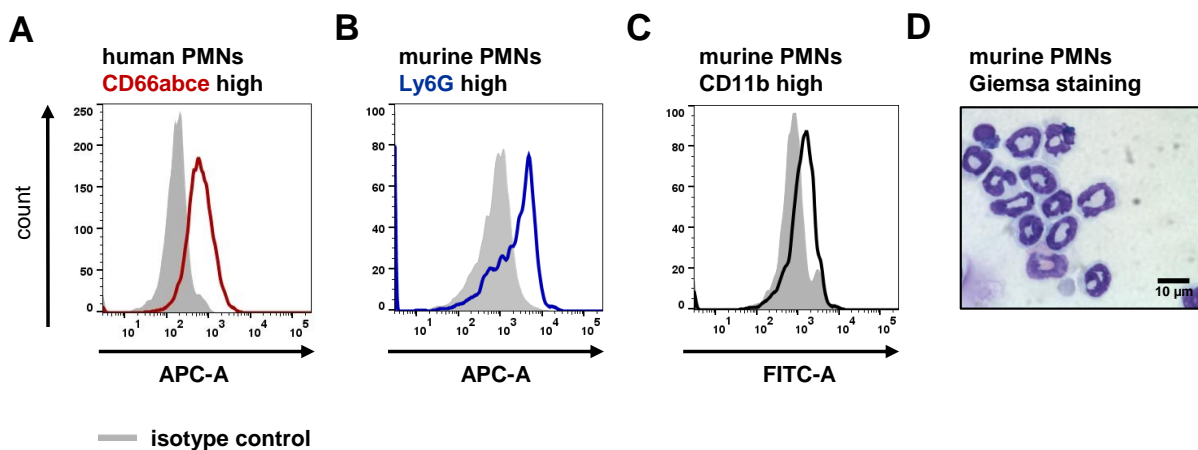


Fig. 3.1: Characterization of isolated neutrophils

A-C) Isolated human (A) and murine (B and C) neutrophils were characterized by flow cytometry using the following antibodies: CD66abce-APC (TET2) (Miltenybiotec) (red), Ly6G-APC (1A8) (Biolegend) (blue), CD11b-FITC (M1/70) (Biolegend) (black) and the isotype controls rat IgG2a κ FITC (BD BioScience) as well as rat IgG2a κ APC (Biolegend) (shaded histograms). The graphs in A-C show a representative experiment of at least three.

D) The typical donut shaped nuclei of neutrophils were observed using Giemsa staining.

The isolated human neutrophils expressed the characteristic surface marker CD66abce

(see Fig. 3.1 A, red), while the murine neutrophils were identified by the typically murine neutrophil markers Ly6G (Fig. 3.1 B, blue) in combination with CD11b (black). Moreover, the hallmark of differentiated neutrophils, the donut shaped nuclei, was shown by a staining with Giemsa (Fig. 3.1 D).

Next, Fig. 3.2 illustrates the result of the CEACAM expression analysis.

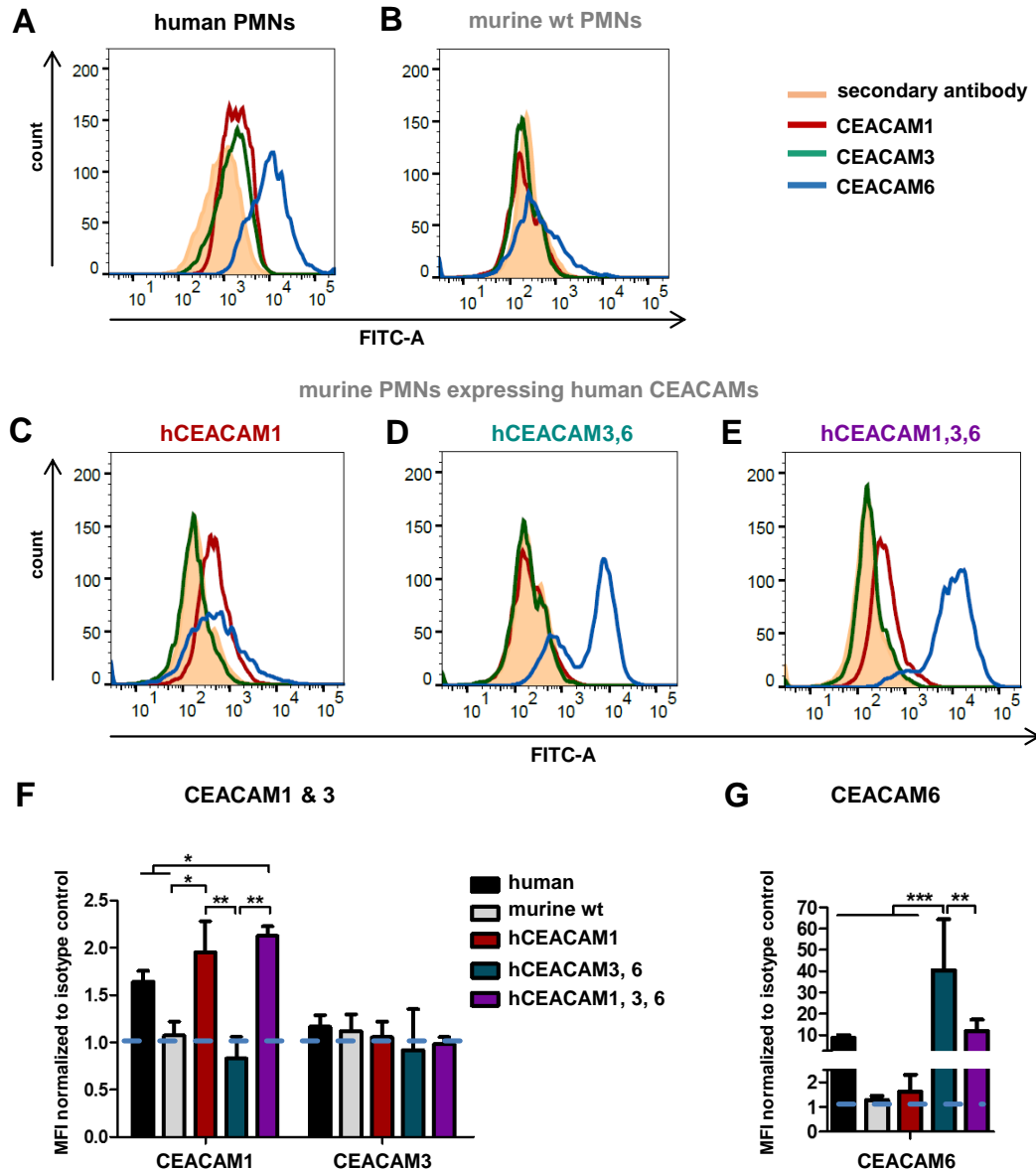


Fig. 3.2: CEACAM expression of human, murine and humanized neutrophils

CEACAM expression was studied by flow cytometry using the following antibodies: CEACAM1 (3/4/17, Genovac) (red), CEACAM3 (col-1, Thermo Fisher) (green), CEACAM6 (9A6, Genovac) (blue) and a Alexa488 conjugated secondary antibody (isotype control) (shaded histogram).

A-E) The graphs show a representative experiment of at least three independent experiments.

F, G) Quantification of CEACAM expression. All bars over the dashed blue line show CEACAM expression. Statistics was performed using Two way ANOVA, with a Bonferroni post hoc test. The error bars show the standard error of mean (SEM), * < 0.05, ** < 0.01, *** < 0.001.

Human CEACAM1 (see Fig. 3.2 F) was detected in low levels in human (black), hCEACAM1 (red) and hCEACAM1, 3, 6 neutrophils (purple). High expression levels were measured for human CEACAM6 (Fig. 3.2 G) in human (black), hCEACAM3, 6 (turquoise) and hCEACAM1, 3, 6 neutrophils (purple). Here, the CEACAM6 expression of hCEACAM3, 6 PMNs (Fig. 3.2 G, turquoise bar) shows a significant higher level in comparison to human PMNs (black bar) and hCEACAM1, 3 and 6 PMNs (purple bar).

All in all, flow cytometry analysis revealed that human and humanized neutrophils expressed human CEACAM1 and 6 (Fig. 3.2), whereas murine wt PMNs (gray bar) do not express human CEACAMs. The expression of human CEACAM3 (Fig. 3.2 F) was weak. Chan *et al.* already reported about difficulties in the detection of human CEACAM3 [138].

3.1.2 Interaction of *H. pylori* with neutrophils

Binding of pathogens to host cells is an initial step in an infection process. Thus, human, murine and the different humanized CEACAM neutrophils were infected with *H. pylori* wt GFP or $\Delta hopQ$ GFP mutant strains for 1 h with an MOI of 10 to analyze their interaction by flow cytometry and confocal microscopy (see Fig. 3.3-4).

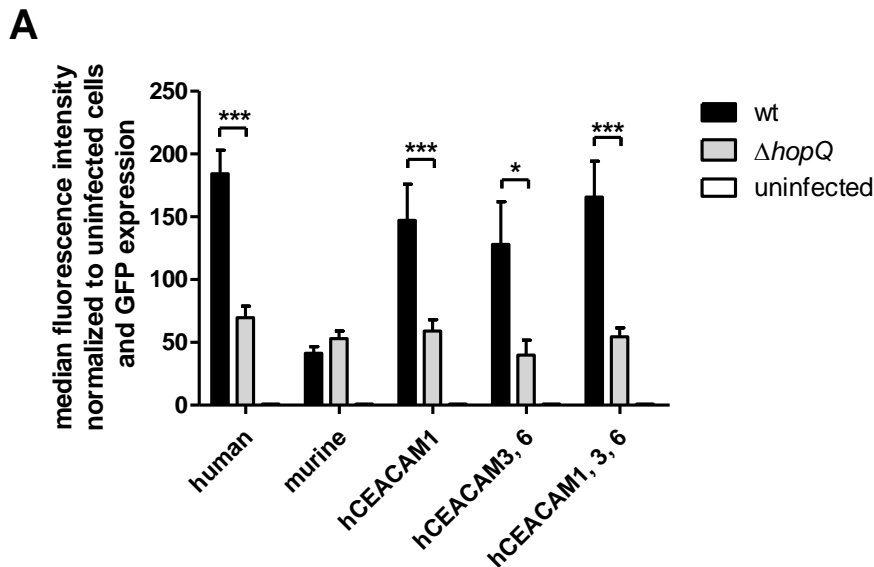


Fig. 3.3: Analysis of the interaction of *H. pylori* with PMNs by flow cytometry

Flow cytometry analysis of different PMNs infected with P12 wt GFP (black) or a P12 $\Delta hopQ$ GFP mutant strain (gray) or left uninfected (white) by flow cytometry. Statistics was performed using Two way ANOVA, with a Bonferroni post hoc test. The error bars show the SEM of at least three independent experiments, * < 0.05, ** < 0.01, *** < 0.001.

High fluorescence intensities were seen in human and humanized neutrophils infected with *H. pylori* P12 wt GFP (see Fig.3.3 A, black). Murine PMNs without human CEACAMs

showed three to four times lower fluorescence intensities than human or humanized PMNs. These data indicated a CEACAM dependent increase of the interaction of *H. pylori* with neutrophils expressing human CEACAMs. This result was supported by the significantly reduced fluorescence signal in an infection with the P12 $\Delta hopQ$ GFP mutant strain (gray), lacking the adhesin to interact with CEACAMs. Consistent with these results, in murine wt PMNs no difference was revealed between the P12 wt GFP (black) and the P12 $\Delta hopQ$ GFP mutant strain (gray). When comparing several groups of humanized CEACAM PMNs, it can be seen that they do not differ in their interaction with the bacterium. Next, Fig. 3.4 shows micrographs of infected humanized-CEACAM and murine PMNs.

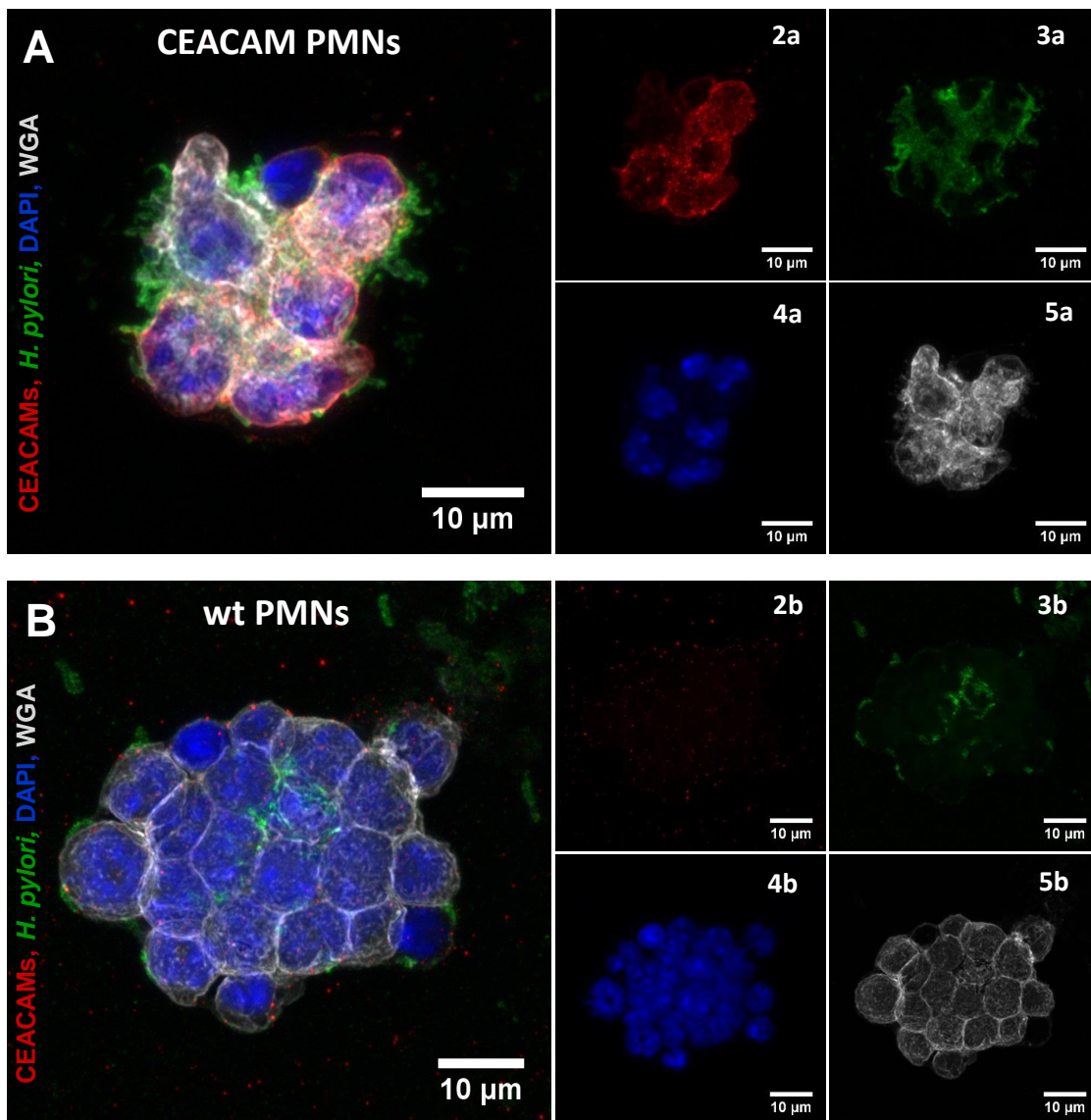


Fig. 3.4: Confocal microscopy of CEACAM expression and binding of *H. pylori* to PMNs HCEACAM1, 3, 6 (A) and murine PMNs (B) were infected with *H. pylori*, fixed on microscopy slides and stained with antibodies. Merged (1), α -CEACAM and Alexa555 (2), *H. pylori* α -AK175 and Alexa488 (3), nuclei DAPI (4), cell shape WGA-Alexa647 (5). Shown are 3D image projections of z-stacks from the confocal microscopy images.

The confocal microscopy of infected hCEACAM1, 3, 6 PMNs (see Fig.3.4, A), expressing all human CEACAMs on PMNs, and murine PMNs (B) stained with antibodies against CEACAMs (red) and *H. pylori* (green) demonstrates differences in the interaction of *H. pylori* with neutrophils. Many bacteria (green) interact with hCEACAM1, 3, 6 PMNs, expressing a high amount of CEACAMs (red), while only a few bacteria interact with murine PMNs. Thus, the flow cytometry analysis data were confirmed by confocal microscopy images of infected humanized-CEACAM and murine PMNs. Taken together, human CEACAMs enhance the interaction of *H. pylori* P12 with PMNs.

Furthermore, it was studied whether other *H. pylori* strains show the same CEACAM dependent effect in the interaction with the bacterium (see Fig. 3.5).

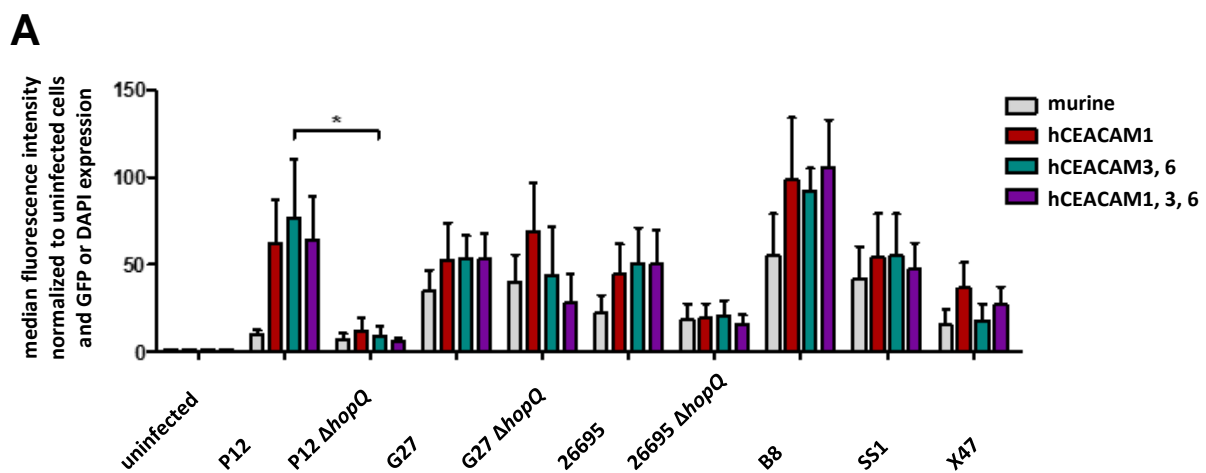


Fig. 3.5: Study of the interaction of different *H. pylori* strains with PMNs

The interaction of several *H. pylori* wt or Δ hopQ mutant strains either expressing GFP or stained with DAPI with the different neutrophil populations was analyzed after an infection for 1 h with an MOI of 10 by flow cytometry. Statistics was performed using Two way ANOVA, with a Bonferroni post hoc test. The error bars show the SEM of at least three experiments, * < 0.05, ** < 0.01, *** < 0.001.

The analysis of the interaction of several *H. pylori* strains with PMNs showed high fluorescence intensities in infections with humanized neutrophils, demonstrated by a CEACAM dependent increase of the interaction with PMNs, which is independent of the *H. pylori* strain. These result were supported by lower fluorescence intensities in murine PMNs without human CEACAMs. In addition, the different interaction experiments with murine wt PMNs did not show a difference between an infection of the *H. pylori* wt or Δ hopQ mutant strains. However, in an infection of humanized PMNs with the 26695 Δ hopQ mutant strain the fluorescence intensity was reduced. These results support the CEACAM effect. Only in infections of the G27 Δ hopQ mutant strains with hCEACAM1 and hCEACAM3, 6 PMNs the fluorescence intensity of the bacteria did not show a reduction. However, further experiments are necessary to prove this finding. Interestingly, neutrophils infected with the gerbil adapted B8 strain showed a high fluorescence intensity. Moreover, a low

CEACAM effect was observed in the infection with the mouse adapted SS1 strain. In conclusion, experiments with various independent *H. pylori* strains revealed that human CEACAMs increase the interaction of *H. pylori* with neutrophils. However, with this approach it was not possible to distinguish between adhesion and phagocytosis. Thus, other experiments were performed to study this aspect separately (see Fig. 3.6).

3.1.3 Binding versus phagocytosis of *H. pylori*

Besides binding of *H. pylori* to neutrophils, these cells are able to phagocytose the bacterium. Fig. 3.6 A demonstrates binding of *H. pylori* to neutrophils incubated with cytochalasin D, a drug, which inhibits the process of phagocytosis. Fig. 3.6 B quantifies phagocytosis of the bacteria by neutrophils using trypan blue to quench the signal of external bacteria.

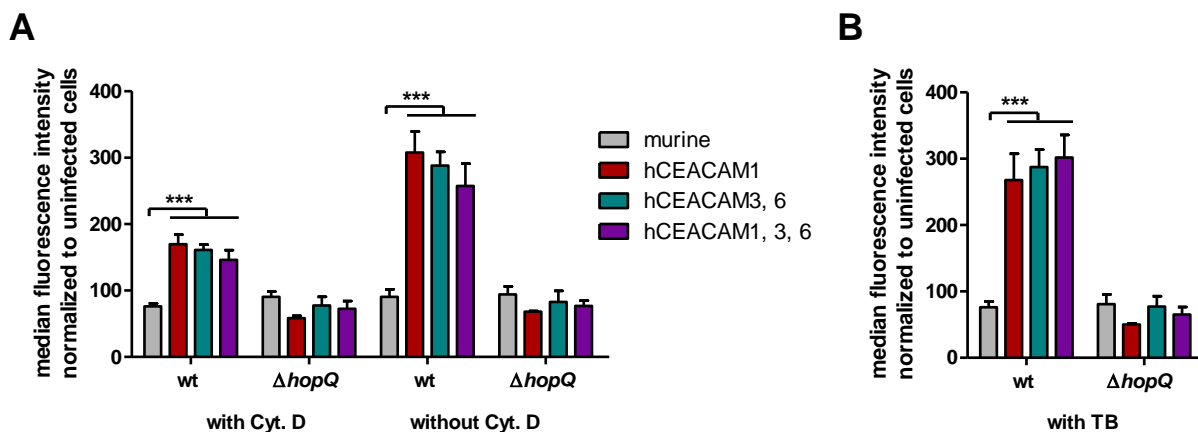


Fig. 3.6: Analysis of binding versus phagocytosis of *H. pylori*

- A) Binding was analyzed after an infection with a P12 GFP and $\Delta hopQ$ GFP mutant strain with an MOI of 25 for 1 h using neutrophils incubated with cytochalasin D (Cyt. D) to inhibit phagocytosis by flow cytometry. Statistics was performed using Two way ANOVA, with a Bonferroni post hoc test. The error bars show SEM of at least three experiments, * < 0.05, ** < 0.01, *** < 0.001.
- (B) Phagocytosis was studied under the same conditions without cytochalasin D addition. To quench the signal of adherent bacteria trypan blue (TB) was added shortly before flow cytometry analysis.

Humanized neutrophils incubated with cytochalasin D showed a significant higher fluorescence intensity compared to murine neutrophils (see Fig. 3.6 A). Moreover, the fluorescence intensity was reduced in an infection with the $\Delta hopQ$ mutant strain. This indicated that *H. pylori* binds to neutrophils depending on CEACAMs. Humanized neutrophils, which were not incubated with cytochalasin D, exhibit a higher fluorescence intensity compared to humanized neutrophils with inhibited phagocytosis. Therefore, it could be concluded that neutrophils phagocytose *H. pylori*. Notably, no difference was detected

in the fluorescence intensity of PMNs treated with cytochalasin D compared to PMNs without cytochalasin D infected with the $\Delta hopQ$ mutant strain.

In Fig. 3.6 B the signal of adherent bacteria was quenched by trypan blue. Here, the humanized neutrophils showed a significantly higher fluorescence intensity, whereas the fluorescence intensity in murine neutrophils and in an infection with the $\Delta hopQ$ mutant strain was three times lower. Accordingly, phagocytosis of the bacteria is dependent on CEACAMs. When comparing several groups of humanized CEACAM PMNs, it can be seen that they do not differ in their binding and phagocytosis. All in all, consistent with the results of the interaction experiments, binding and phagocytosis of *H. pylori* are enhanced in PMNs expressing human CEACAMs.

3.1.4 Survival of *H. pylori* after phagocytosis by PMNs

Allen *et al.* reported that *H. pylori* is able to evade killing by disrupting NADPH oxidase [60]. Humanized neutrophils phagocytose *H. pylori* more efficiently compared to murine neutrophils, as it was demonstrated in the previous section. Thus, a plating assay was performed to quantify bacteria surviving the phagocytosis of murine versus the different humanized CEACAM neutrophils. Therefore, PMNs were infected with *H. pylori* P12 and $\Delta hopQ$ mutant strain for 30 min, 1 h and 1.5 h with an MOI of 25. Then, after eliminating extracellular bacteria with gentamicin and permeabilization of cells with saponin, samples were plated on serum plates. After three days, the CFUs were counted (Fig. 3.7).

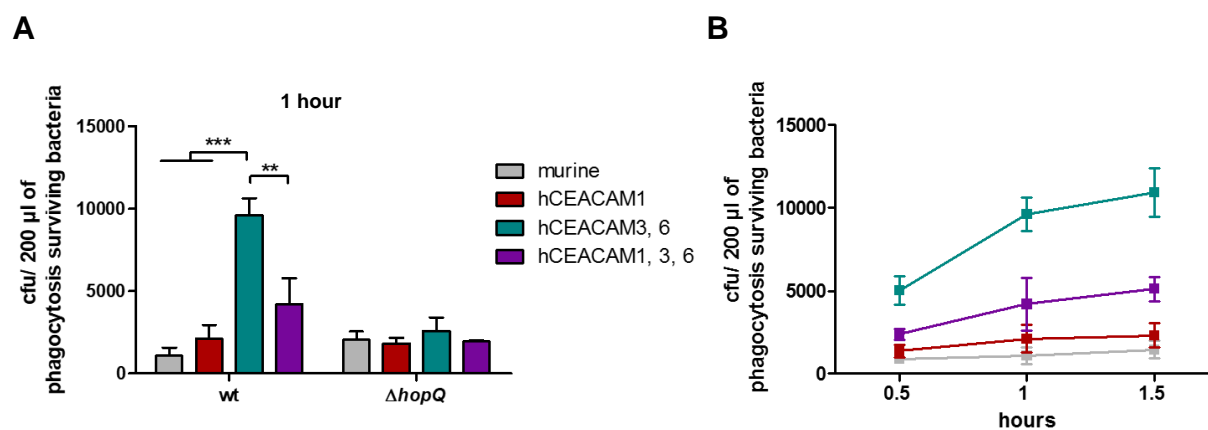


Fig. 3.7: Study of survival of *H. pylori* after phagocytosis by PMNs

Survival of phagocytosis were analyzed using the gentamicin killing assay. Statistics of at least three independent experiments was performed using Two way ANOVA, with a Bonferroni post hoc test. The error bars show the SEM, * < 0.05, ** < 0.01, *** < 0.001.

A) The bar chart shows the CFUs after 1 h of infection.

B) The dot plot shows the phagocytosis surviving bacteria after an infection of neutrophils for 0.5, 1 and 1.5 h with *H. pylori*.

The survival assay indicates that *H. pylori* survives phagocytosis of neutrophils. Remarkably, in neutrophils of humanized CEACAM3, 6 mice (turquoise bar) ten times more *H. pylori* (wt) survive phagocytosis compared to murine PMNs (gray), five times more bacteria survive compared to hCEACAM1 (red bar) and two times more *H. pylori* survive compared to hCEACAM1, 3, 6 PMNs (Fig. 3.7 A, purple bar). Furthermore, survival depends on CEACAMs as it was confirmed by the results of the infection using the $\Delta hopQ$ mutant strain.

Notably, an infection with P12 wt of hCEACAM1 neutrophils (red) showed a five times lower survival rate of *H. pylori* compared to hCEACAM3, 6 neutrophils (turquoise). Moreover, hCEACAM1 PMNs infected with the P12 $\Delta hopQ$ mutant strain did not show a reduced survival and consequently no CEACAM effect. A hallmark of hCEACAM1 are the two ITIM motifs (see section 1.4.2) leading to inhibitory signaling cascades. Thus, hCEACAM1 seems to play an opposite role in surviving phagocytosis. Furthermore, even hCEACAM1, 3, 6 neutrophils demonstrated a reduced survival rate compared to hCEACAM3, 6 PMNs. But, comparing both humanized PMNs with lower surviving rates, the survival in hCEACAM1, 3, 6 is two times higher compared to hCEACAM1 PMNs.

Next, the survival of *H. pylori* in PMNs was analyzed over a time period up to 1.5 h. The survival rate of the bacterium in hCEACAM3, 6 PMNs strongly increased in the first hour of infection (see Fig. 3.7 B). After 1 h the amount of surviving bacteria doubled compared to 0.5 h, whereas after 1.5 h nearly the same amount of bacteria survives in hCEACAM3, 6 PMNs compared to the results after 1 h of infection. In murine and hCEACAM1 PMNs only a few bacteria survive phagocytosis independent of the time period of infection, while in hCEACAM1, 3, 6 PMNs the amount of surviving bacteria increase up to one hour and reaches a plateau as well as hCEACAM3,6 PMNs. However, after 1.5 h of infection two times more bacteria survive in hCEACAM3, 6 PMNs compared to hCEACAM1, 3, 6 PMNs. Taken together, these data suggest that CEACAM3 and/or 6 seem to support survival of *H. pylori* in PMNs.

Allen *et al.* could demonstrate differences in phagocytosis by M Φ of strains, which do not contain CagA and VacA [61]. Raising the question, whether CagA and VacA are also involved in the survival of phagocytosis in neutrophils. However, Odenbreit *et al.* did not detect differences in phagocytosis by M Φ of strains, which do not contain CagA and VacA [152]. Thus, the gentamicin killing assay were performed with *H. pylori* $\Delta cagA$ and $\Delta vacA$ mutant strains (see Fig. 3.8).

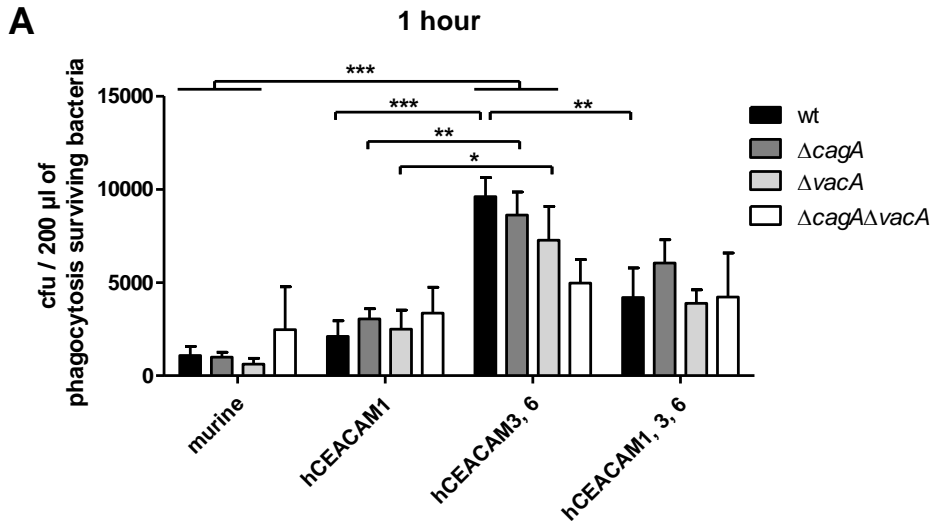


Fig. 3.8: Study of survival of *H. pylori* $\Delta cagA$ and $\Delta vacA$ after phagocytosis by PMNs
Survival of phagocytosis of *H. pylori* $\Delta cagA$ and $\Delta vacA$ were analyzed using the gentamicin killing assay. Statistics of at least three independent experiments was performed using Two way ANOVA, with a Bonferroni post hoc test. The error bars show the SEM, * < 0.05, ** < 0.01, *** < 0.001. The dot plot shows the phagocytosis surviving bacteria after an infection of PMNs for 1 h.

The survival assay showed that infections with a *H. pylori* $\Delta cagA$ and/or $\Delta vacA$ mutant strain of murine and hCEACAM1 PMNs showed lower survival rates of the bacteria compared to hCEACAM3, 6 PMNs. In an infection of hCEACAM3, 6 PMNs with a *H. pylori* $\Delta cagA$ mutant strain (dark gray) the survival probability is approximately 10% lower in comparison to P12 wt bacteria (black). Furthermore, in an infection of PMNs with a *H. pylori* $\Delta vacA$ mutant strain (light gray) the probability of survival of phagocytosis drops about 25% in comparison to P12 wt bacteria. Notably, in an infection of hCEACAM3, 6 PMNs with a $\Delta cagA\Delta vacA$ mutant strain (white) only half of the amount of bacteria survive phagocytosis in comparison to P12 wt bacteria. Thus, CagA and VacA seems to have an influence on survival of phagocytosis in hCEACAM3, 6 PMNs. In hCEACAM1, 3, 6 PMNs a deletion of CagA did not influence survival of phagocytosis, while a deletion of VacA leads to a small reduction of survival of phagocytosis in comparison to P12 wt bacteria. Surprisingly, even more *H. pylori* with a deletion of CagA survive phagocytosis in hCEACAM1, 3, 6 PMNs. In murine and hCEACAM1 neutrophils no difference can be seen between *H. pylori* wt and $\Delta cagA$ or $\Delta vacA$ mutant strains. All in all, the data suggest that especially VacA is involved in survival of phagocytosis by humanized PMNs.

3.1.5 Production of reactive oxygen species

As mentioned in section 3.1.4, *H. pylori* is able to disrupt NADPH oxidase resulting in a strong extracellular release of ROS. Thus, ROS production was analyzed in murine and

humanized neutrophils measuring NADPH oxidase activity using dihydrorhodamine (see Fig. 3.9).

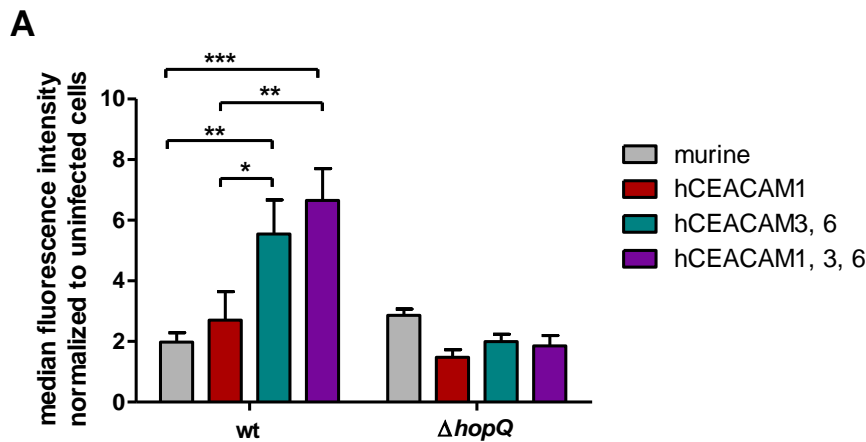


Fig. 3.9: Analysis of ROS production by PMNs

ROS production was studied using dihydrorhodamine, which reacts in the presence of ROS to green fluorescent rhodamine. Statistics was performed using Two way ANOVA, with a Bonferroni post hoc test. The error bars show the SEM of at least three experiments, * < 0.05, ** < 0.01, *** < 0.001.

The ROS analysis showed that hCEACAM3, 6 (see Fig. 3.9, turquoise bar) as well as hCEACAM1, 3, 6 PMNs (purple bar) showed two to three times higher fluorescence intensity compared to hCEACAM1 neutrophils (red bar) and murine PMNs (gray bar). Thus, hCEACAM3, 6 and hCEACAM1, 3, 6 PMNs produced significantly more ROS (2-3 times) compared to hCEACAM1 neutrophils and murine PMNs. Incubation of *H. pylori* $\Delta hopQ$ with neutrophils led to a reduced fluorescence intensity and consequently a lower ROS release. This indicated that, consistent with the survival of phagocytosis, ROS production is CEACAM3 and 6 dependent. However, the interaction of *H. pylori* with human CEACAM1, consisting of two ITIM motifs, resulted in a lower ROS production, eventually due to the general inhibitory function of human CEACAM1.

3.1.6 Confocal microscopy studies of the interaction of *H. pylori* and PMNs

Besides flow cytometry and the survival assay the interaction of *H. pylori* and neutrophils was studied using confocal microscopy (see Fig. 3.9). In addition, it was differentiated between extracellular *H. pylori* stained in green with red dots by a double staining with an anti-*H. pylori* antibody and a secondary Alexa555 as well as an anti-*H. pylori* antibody and a secondary Alexa488 antibody, while intracellular *H. pylori* were stained after permeabilization in green by an anti-*H. pylori* antibody and a secondary Alexa488 antibody.

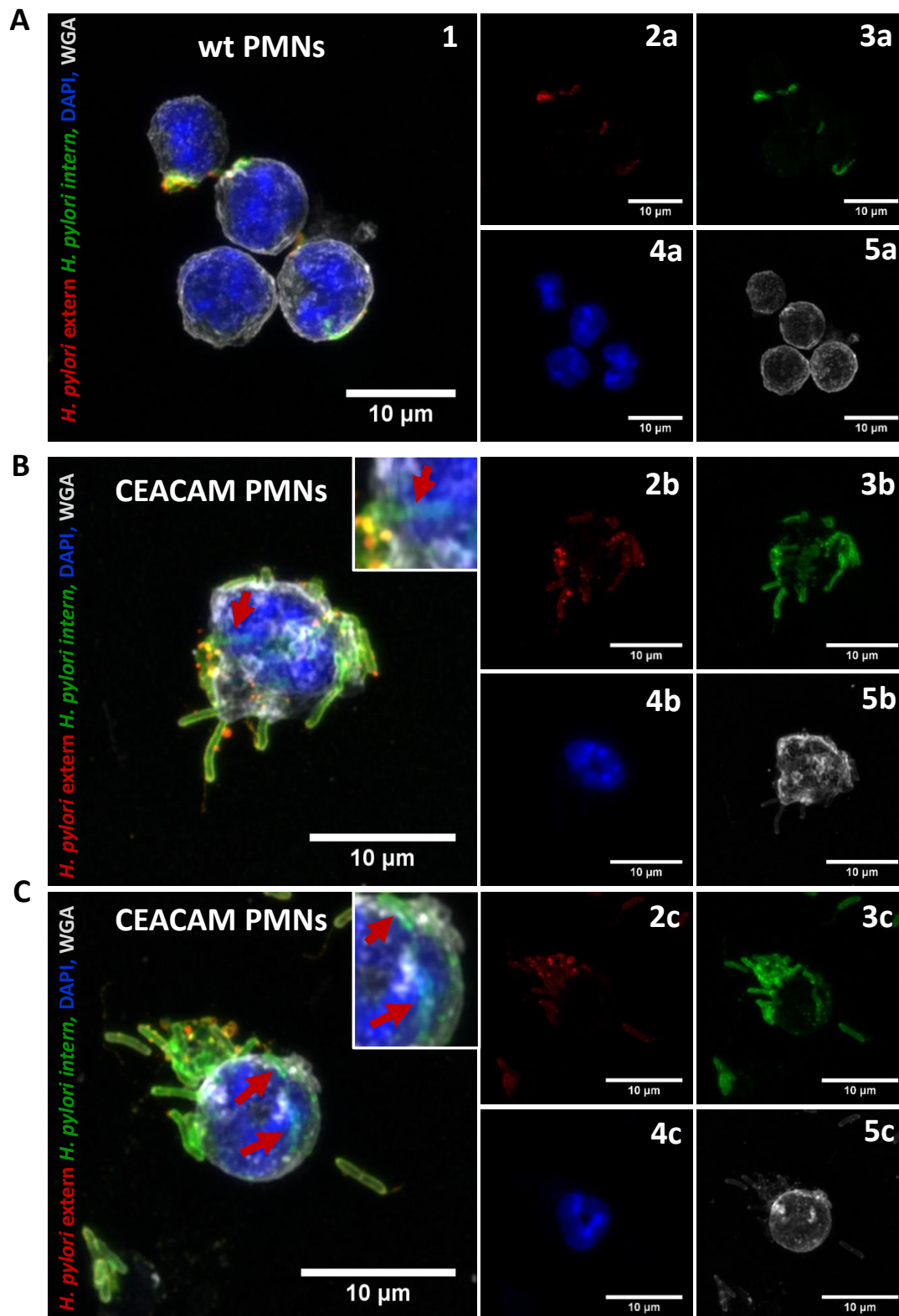


Fig. 3.10: Interaction of *H. pylori* and PMNs studied by confocal microscopy

Murine (A) and hCEACAM1, 3, 6 (B, C) PMNs were infected with *H. pylori*, fixed on microscopy slides and stained with antibodies. Merged with zoom in (1), *H. pylori* extern α -AK175 and Alexa555, (2) after permeabilization *H. pylori* extern and intern α -AK175 and Alexa488, (3) nuclei DAPI, (4) cell shape WGA-Alexa647. Shown are 3 D image projections of z-stacks from the confocal microscopy images.

Confocal microscopy of infected murine wt PMNs (see Fig. 3.10, A) showed binding of a few *H. pylori* (green with orange dots) to murine wt neutrophils. All bacteria were stained in red (2) and in green (3). But, no bacteria were colored in green (3) only indicating that *H. pylori* was not phagocytosed by murine wt neutrophils. In contrast, humanized CEACAM1, 3 and 6 PMNs (B, C) showed binding of many *H. pylori* (green with orange dots) and a high amount of green fluorescence (3) inside the cells. Inside of the cell only green fluorescence (3), but no red fluorescence (2) was detected. This demonstrates that the bacteria were phagocytosed by humanized hCEACAM1, 3 and 6 PMNs.

In addition, to show that *H. pylori* is located within the cell, reconstructions of the micrographs were performed using the imaris software (see Fig. 3.11).

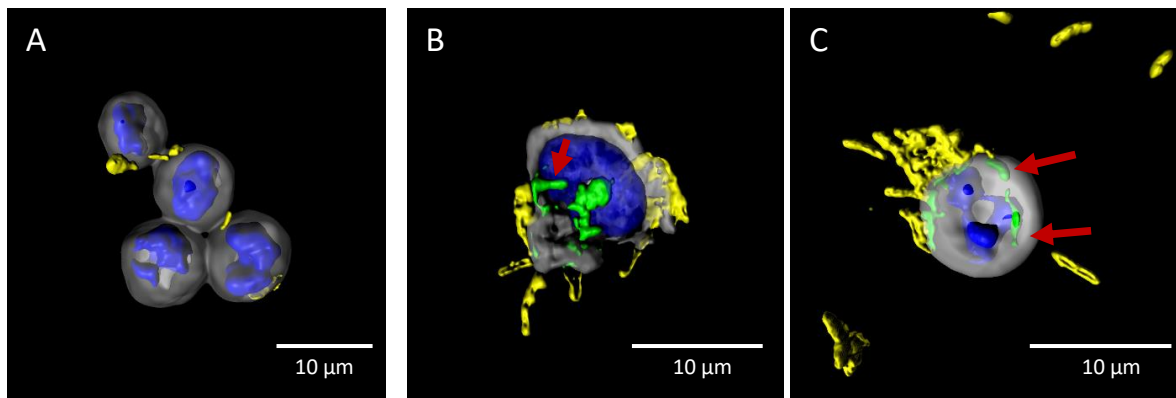


Fig. 3.11: Reconstructions of confocal microscopy images of PMNs infected with *H. pylori* Micrographs of confocal microscopy of murine (A) and humanized hCEACAM1, 3, 6 (B, C) neutrophils infected with *H. pylori* were rendered in 3D.

The reconstructions of the confocal microscopy images clearly show *H. pylori* (green) (see red arrows) inside of humanized neutrophils, but not in wt neutrophils. Taken together, the confocal microscopy confirmed the flow cytometry and survival assay data.

3.1.7 The role of human CEACAMs on CagA translocation and phosphorylation

A key event in the infection process of *H. pylori* is the translocation and subsequent phosphorylation of CagA resulting in an activation of CagA inside the host cell. Thus, human, murine and humanized neutrophils were infected with *H. pylori* and an immunoblot of the infected cells (Fig. 3.12 A, B) using CagA and phosphotyrosine antibodies was performed. In addition, *in vitro* phosphorylation of CagA from cell lysates of infected murine neutrophils (Fig. 3.12 C) was performed and tested by an immunoblot. Furthermore, the CagA translocation was quantified with a β -lactamase dependent reporter system by flow cytometry (Fig. 3.12 D). For this, human, murine and humanized neutrophils were

infected with a P12 TEM-CagA, a P12 $\Delta cagI$ TEM-CagA and a P12 $\Delta hopQ$ TEM-CagA *H. pylori* strain and were stained with CCF4. Cells containing translocated CagA show a blue and green fluorescence.

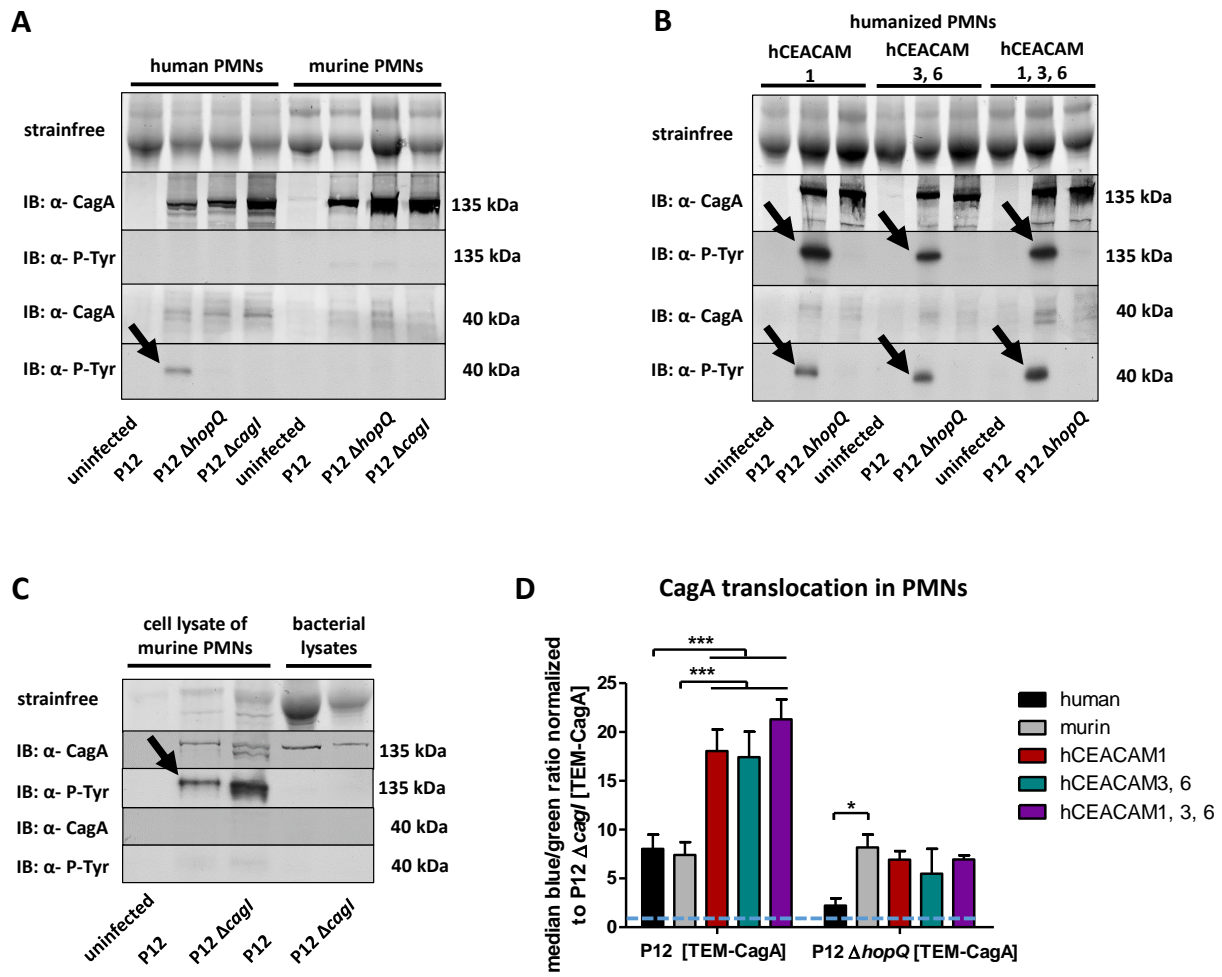


Fig. 3.12: CagA phosphorylation and quantification of CagA translocation in human, murine and humanized PMNs

A, B) Immunoblot analysis of CagA phosphorylation in PMNs using α -CagA (AK299) and α -phosphotyrosine (PY99) antibodies.

A) Human and murine PMNs

B) CEACAM humanized PMNs

C) Immunoblot analysis of the *in vitro* phosphorylation of CagA in cell lysates of murine PMNs.

D) Quantification of TEM-CagA translocation in PMNs. CagA translocation was studied using a β -lactamase dependent reporter system. Shown are mean values of the ratio of blue and green fluorescence of at least three independent experiments normalized to the translocation deficient strain *H. pylori* P12 $\Delta cagI$ TEM-CagA. Error bars show the SEM. Statistical analysis was performed using two way ANOVA, with a Bonferroni post hoc test with * < 0.05, ** < 0.01, *** < 0.001. All bars over the dashed blue line are positive for CagA translocation.

The immunoblot analysis detected a 40 kDa phosphorylated fragment of CagA (see Fig. 3.12 A, left side, black arrow) as a result of an infection of human PMNs with P12. This shows that CagA is translocated in human PMNs and is completely cleaved into a phosphorylated C-terminal 40 kDa CagA fragment, because no phosphorylated full length CagA (135 kDa) was detected. In human neutrophils infected with P12 $\Delta hopQ$ or P12 $\Delta cagI$ (phosphorylation deficient control) no phosphorylated CagA could be detected.

In contrast to human PMNs, murine PMNs infected with P12 did not show CagA phosphorylation (see Fig. 3.12 A, right side). However, in all murine neutrophils expressing human CEACAMs infected with P12 a full length (135 kDa) and a cleaved (40 kDa) phosphorylated CagA band was detected (see Fig. 3.10 B black arrows). In these cells CagA is not completely cleaved in 40 kDa fragments. Taken together, the CagA phosphorylation and cleaving of CagA (processing) in human and humanized neutrophils is mediated by CEACAMs. In addition this finding is supported by the fact that no CagA phosphorylation was seen in an infection of humanized PMNs with P12 $\Delta hopQ$ strain (see Fig. 3.12 B).

Notably, CagA is not phosphorylated in murine PMN infected with P12 (see Fig. 3.12 A). To prove, whether kinase are active in murine neutrophils, an *in vitro* phosphorylation assay was performed. In cell lysates of murine PMNs full length CagA (135 kDa) is phosphorylated (see Fig. 3.12 C). Consequently, host kinases are active in murine PMNs. This leads to the question, whether CagA is translocated into murine PMNs.

Quantification of CagA translocation revealed that CagA is translocated in all different PMNs, even in murine wt PMNs (see Fig. 3.12 D, gray bar). However, the amount of CagA in hCEACAM1, 3, 6 neutrophils (purple bar) was three times and in hCEACAM1 (red bar) and hCEACAM3, 6 (turquoise bar) two times higher in comparison to human (black bar) and murine (gray bar) neutrophils. This indicates that CagA is translocated into murine PMNs, but not phosphorylated or rapidly dephosphorylated. The CEACAM effect in CagA translocation was supported by a two to three times reduced CagA translocation in humanized neutrophils infected with P12 $\Delta hopQ$ TEM-CagA. Furthermore, this is consistent with the result that murine neutrophils without human CEACAMs showed no HopQ dependent reduction in CagA translocation. In addition, consistent with humanized neutrophils, the CagA translocation in human neutrophils was reduced depending on HopQ.

In conclusion, these results demonstrate that CagA is translocated in all different types of PMNs. But, human CEACAMs are necessary to enable CagA phosphorylation and processing of CagA in PMNs. This demonstrates the physiological relevance of CEACAMs.

3.1.8 Influence of SHP-1 on CagA phosphorylation

Although, CagA is translocated into murine PMNs, and it was proven that host kinases are active in murine PMNs (see section 3.1.7 C, D), no phosphorylated CagA was observed in murine PMNs. It is known, that CagA interacts with different proteins in the host cell (see section 1.2.3). Saju *et al.* could show that phosphorylated CagA interacts with SHP-1 and SHP-2. SHP-2 enhance the oncogenicity of CagA, whereas SHP-1 dampens the oncogenicity of CagA by dephosphorylation of its EPIYA motifs [52].

Thus, SHP-1 was blocked in murine PMNs using two different inhibitors sodium stibogluconat or hydrogen peroxide and an infection experiment, followed by an immunoblot analysis using CagA and phosphotyrosine antibodies was performed (see Fig. 3.13).

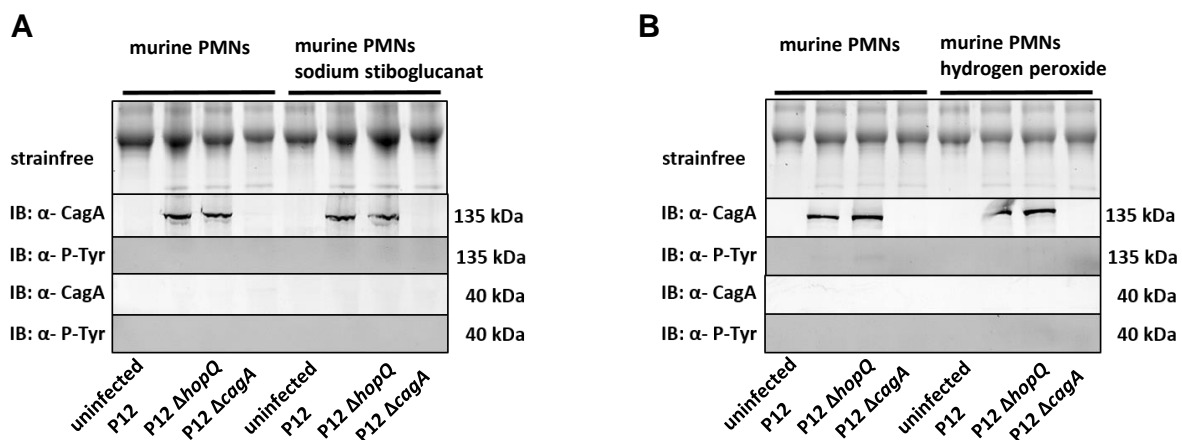


Fig. 3.13: Chemical inhibition of SHP-1 in murine PMNs

CagA phosphorylation in infected PMNs with an inhibition of SHP-1 either with sodium stibogluconat (A) or hydrogen peroxide (B) was analyzed in an immunoblot.

Inhibition of SHP-1 using either sodium stibogluconat or hydrogen peroxide did not result in detection of phosphorylated CagA in murine PMNs.

As inhibition of SHP-1 seems to have no influence on CagA phosphorylation in murine PMNs, the possible effect of CEACAM1 in combination with SHP-1 on CagA phosphorylation was analyzed. It is known that CEACAM1 in its dimerized form can recruit SHP-1 via its ITIMs, which subsequently are phosphorylated by Src kinases [107]. *Bonsor et al.* could show that HopQ can inhibit CEACAM1 dimerization (see section 1.4.6) [38]. A possible mechanism could be that SHP-1 recruited to dimerized CEACAM1 could dephosphorylate CagA, whereas HopQ interrupts the CEACAM1 dimerization and SHP-1 signaling and CagA is not dephosphorylated. To analyze this aspect further, SHP-1 was deleted in a murine neutrophil cell line expressing human CEACAMs using the CRISPR Cas9 technology (see section 2.7). Moreover, murine CEACAM1 was deleted in the same cell line to avoid negative influences of both murine and human CEACAM1 in combina-

tion. For these experiments, the MPRO neutrophil cell lines expressing human CEACAMs was used, which was kindly provided by Prof. Dr. Scott Gray Owen [113]. Phosphorylation of CagA was determined in an immunoblot analysis of the generated cells infected with P12 wt (see Fig. 3.14).

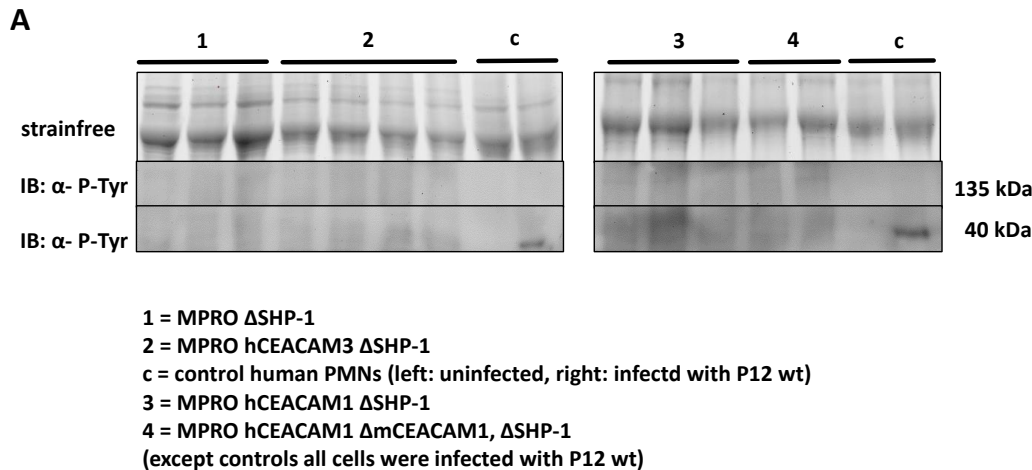


Fig. 3.14: Immunoblot analysis of different MPRO cells with a deletion in SHP-1

SHP-1 was deleted in MPRO, MPRO hCEACAM1 and MPRO hCEACAM3 cells using the CRISPR Cas9 technology. Moreover, murine CEACAM1 was deleted in MPRO CEACAM1 cells. Cells with SHP-1 and/or murine CEACAM1 deletion were infected for 3 h with an MOI of 60 with *H. pylori* P12. Then, an immunoblot was performed analyzing phosphorylation.

However, a SHP-1 deletion in MPRO, MPRO hCEACAM3 and MPRO hCEACAM1 cells as well as an additional deletion of murine CEACAM1 did not result in CagA phosphorylation in murine neutrophils. Therefore, further experiments have to be performed to understand this phenomenon in the future.

3.1.9 2D migration of murine and humanized PMNs

Next, to study whether the expression of human CEACAMs influence 2D migration of neutrophils, an under agarose assay was performed using LTB4 as a chemoattractant, which should result in swarming of neutrophils (see Fig. 3.15). *In vivo*, PMNs use chemoattractant gradients to find their way to the site of infection (see section 1.1.2).

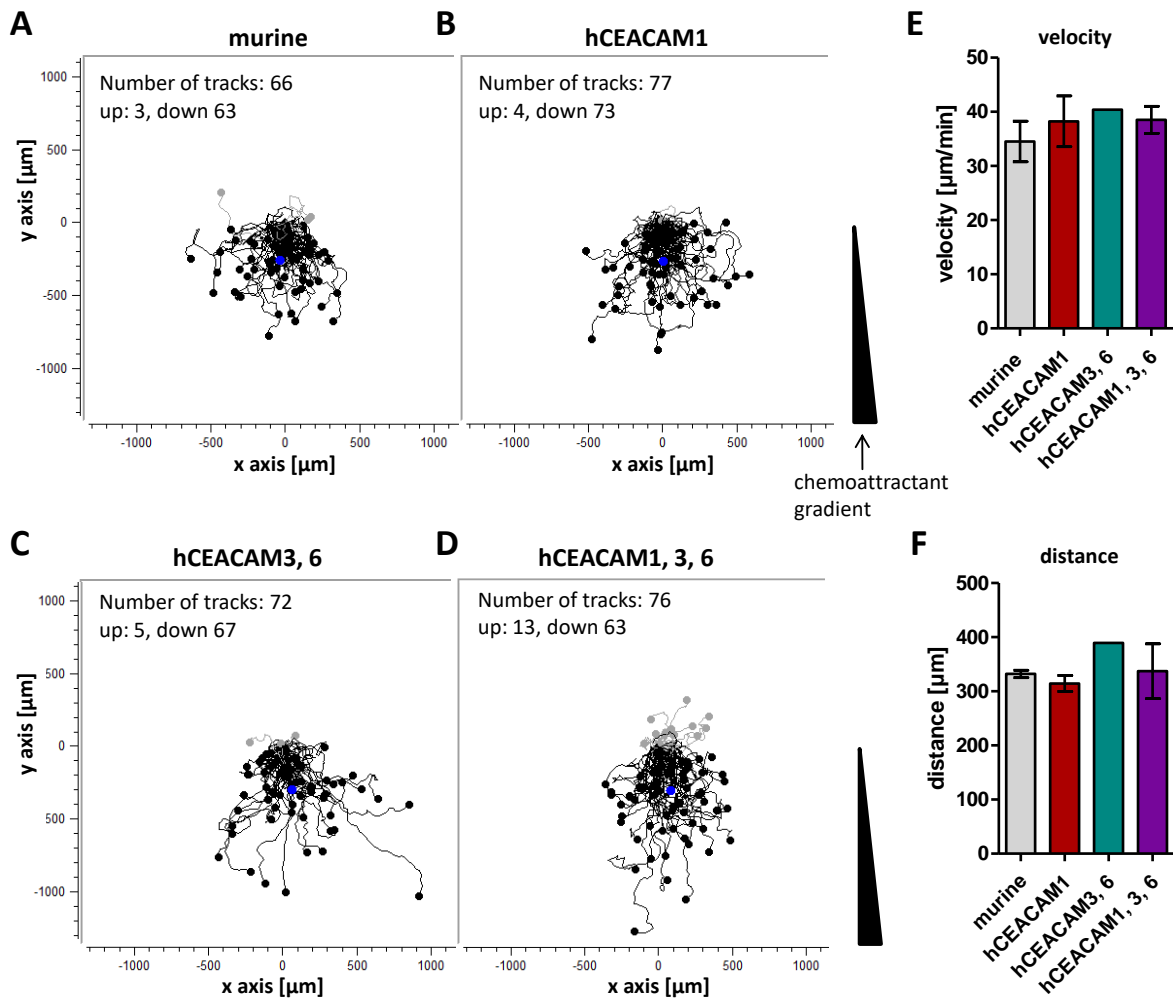


Fig. 3.15: 2D migration of murine and humanized PMNs

Murine or humanized PMNs were filled in one slot of an agarose gel and in another slot the chemoattractant LTB₄. After 1 h, the chemoattractant gradient was formed and migration was studied using time-lapse microscopy. Error bars show the SEM of two independent experiments.

A-D) Plots showing the migration of PMNs

A) murine B) hCEACAM1 C) hCEACAM3, 6 D) hCEACAM1, 3, 6

E) Quantification of the velocity of migration

F) Quantification of the migrated distance

The plots of the 2D migration assay illustrate that murine as well as humanized neutrophils swarmed towards the chemoattractant LTB₄ (see Fig. 3.15 A-D). In this regard the humanized cells do not show differences compared to murine wt PMNs. To further prove this observation, the velocity (Fig. 3.15 E) and distance (F) of swarming towards the chemoattractant LTB₄ was quantified. Consistent with the results of the plots the swarming did not differ significantly between the cells. This indicates that CEACAM expression does not influence the migration behavior towards LTB₄. However, further chemoattractive substances have to be tested in the future. Besides migrating towards a chemoattractant gradient to the site of infection or inflammation, neutrophils themselves

are able to secrete chemical attractants to recruit further immune cells.

3.2 The role of human CEACAMs on the secretion of chemokines

3.2.1 Chemokine secretion of PMNs infected with *H. pylori*

In a further experiment the chemokine secretion of neutrophils was studied with a bead based sandwich immunoassay (see Fig.3.16).

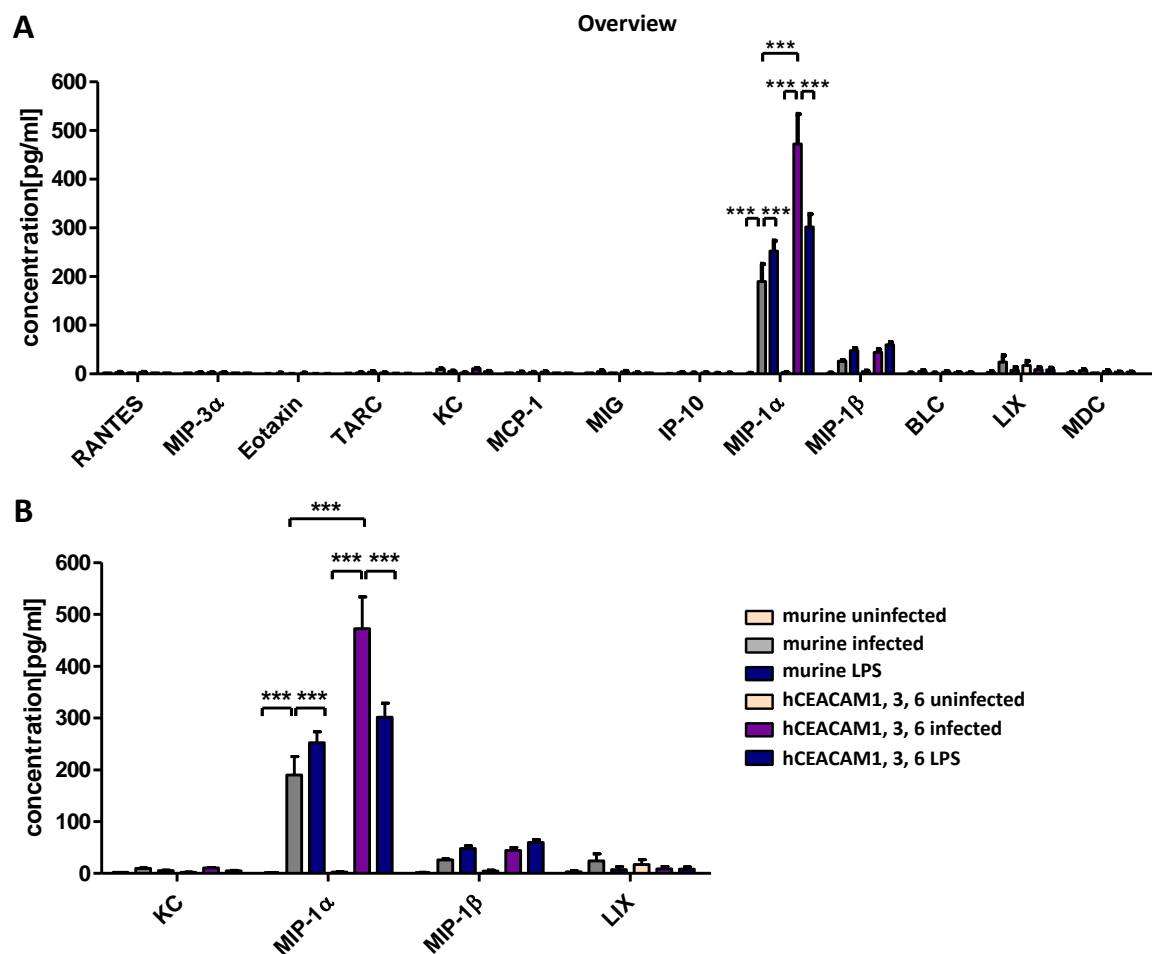


Fig. 3.16: Chemokine secretion of PMNs infected with *H. pylori*

Murine and hCEACAM1, 3, 6 PMNs were infected with *H. pylori* with an MOI of 60. As a control PMNs were incubated with LPS or uninfected. After 3 h the supernatant of the infection was collected. Chemokine concentrations of two replicates of two independent experiments of murine wt PMNs and four independent experiments of humanized PMNs were determined using the Legendplex proinflammatory chemokine panel 13 plex by flow cytometry. Error bars show the SEM. The statistics were analyzed using two way ANOVA, with a Bonferroni post hoc test, * $p < 0,05$, ** $p < 0,01$, *** $p < 0001$.

A) Overview of all 13 different chemokines

B) KC, MIP-1α, MIP-1β, LIX concentrations

Figure 3.16 shows the chemokine concentrations in supernatants of murine or humanized neutrophils infected with *H. pylori* for 3 h, incubated with LPS or uninfected to verify whether CEACAMs influence the physical behavior of neutrophils in an inflammatory response. The chemokine measurement of infected neutrophils detected MIP-1 β and MIP-1 α in a high concentration (see Fig. 3.16 A). Scapini *et al.* could show that human PMNs secrete IL-8, Gro α , MIP-1 α , MIP-1 β , IP-10 and MIG. Functionally homologues of IL-8 and Gro α in the murine organism are KC, MIP2 and LIX. MIP2 was not analyzed in this thesis. KC and LIX were detected in this experiments only in very low concentrations, whereas MIP-1 β was found in low and MIP-1 α in high concentrations. IP-10 and MIG could not be detected in these experiments, because IP-10 and MIG need a costimulation with IFN- γ in combination with LPS or TNF- α , as it was shown by Gasperini *et al.* [17]. The concentration of MIP-1 α in humanized PMNs (purple) was increased 2.5 times compared to murine wt neutrophils (gray) (see Fig. 3.16 B). An incubation with LPS (blue) increased the amount of MIP-1 α secreted by murine wt PMNs. This concentration of MIP-1 α after LPS stimulation was similar to humanized PMNs incubated with LPS. However, humanized neutrophils infected with *H. pylori* secreted 1.7 times more MIP-1 α than neutrophils incubated with LPS. The function of secreted MIP-1 α is the recruitment of further immune cells to the site of infection. Here, the secretion of MIP-1 α in high concentrations indicates an enhanced proinflammatory response initiated by humanized neutrophils, which might influence the pathology in an infection with *H. pylori*. Moreover, it highlights the role of CEACAMs on neutrophils in the interaction with *H. pylori*. Furthermore, this result raises the question, whether the CEACAM expression also has an effect on cells recruited by neutrophils like DCs and M Φ .

3.2.2 Chemokine secretion of DCs and M Φ infected with *H. pylori*

Similar to murine and humanized neutrophils chemokine secretion was measured in supernatants of murine and humanized DCs and M Φ , which were infected with *H. pylori* (see Fig. 3.17).

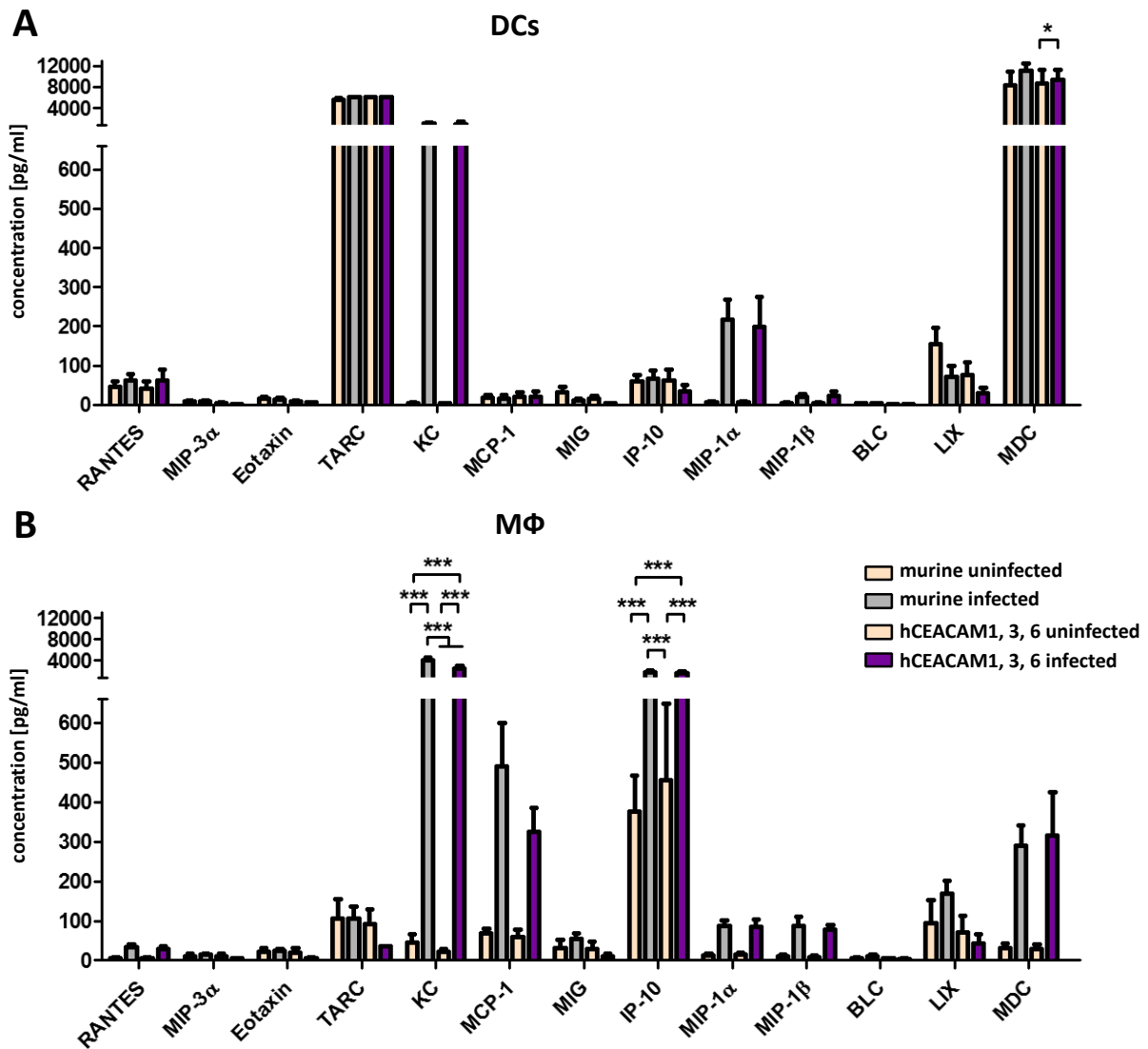


Fig. 3.17: Chemokine secretion of DCs and MΦs infected with *H. pylori*

Murine DCs (A) and MΦs (B) and humanized DCs (A) and MΦs (B), expressing human CEACAM1, 3 and 6 were infected with *H. pylori* with an MOI 60 for 3 h. Afterwards, the supernatant was collected. Chemokine concentrations of two replicates of three independent experiments were measured with the Legendplex proinflammatory Chemokine panel 13 plex by flow cytometry. Error bars show the SEM. Statistical analysis was performed using ANOVA, Two way, with a Bonferroni post hoc test, * $p < 0,05$, ** $p < 0,01$, *** $p < 0001$

DCs infected with *H. pylori* release KC in high and MIP-1 α in moderate concentrations (see Fig. 3.17 A). However, the secretion seems to be independent of CEACAMs, because murine (gray bar) and humanized (purple bar) DCs release the same amount of KC and MIP-1 α . The function of KC is the recruitment of neutrophil, whereas MIP-1 α attracts DCs. The amount of MIP-1 α produced from murine DCs is comparable to murine neutrophils (see Fig. 3.17 A). However, humanized DCs secrete only half of the

amount of MIP-1 α compared to humanized neutrophils. Furthermore, DCs produce other chemokines independent of an infection with *H. pylori* like TARC and MDC in high concentrations and RANTES, IP-10 and LIX in low concentrations.

Infected M Φ secrete high concentrations of KC and IP-10 (see Fig. 3.17 B). As already mentioned, the function of KC is the attraction of neutrophils, whereas IP-10 recruits T-cells. Furthermore, M Φ release moderate concentrations of MCP-1 and MDC and low concentrations of MIP-1 α , MIP-1 β , LIX and, independent of the infection with *H. pylori*, TARC. KC is significantly down regulated in humanized M Φ (see Fig. 3.17, purple bar) compared to murine M Φ (gray bar). Moreover, MCP-1 was downregulated in humanized M Φ compared to murine M Φ . The opposite phenomenon was seen in MDC. There, the MDC secretion was upregulated in humanized M Φ compared to murine M Φ . However, the differences in production of MCP-1 and MDC are not significant. The amount of MIP-1 α was five times lower compared to humanized neutrophils (see Fig. 3.16).

All in all, it seems that the chemokine secretion of infected DCs and M Φ is mostly independent of CEACAMs. In comparison to neutrophils CEACAMs do not influence the chemokine secretion of immature DCs and M Φ . One exception is the release of KC, which was lower in humanized M Φ in comparison to murine wt M Φ . So, these data support the special role of CEACAMs on neutrophils in the proinflammatory response. However, so far only the proinflammatory response was analyzed. Thus, the role of CEACAMs in the interaction of *H. pylori* with DCs or M Φ was further investigated.

3.3 Interaction of *H. pylori* with DCs and M Φ

Neutrophils recruit DCs and M Φ to the site of infection. In the previous section it was already shown that chemokine secretion of DCs and M Φ infected with *H. pylori* was not strongly influenced by CEACAMs. In the following section the CEACAM expression, the interaction with *H. pylori* and the CagA translocation and phosphorylation in DCs and M Φ were studied. This is important to verify, whether the CEACAM effect is unique for neutrophils or not.

3.3.1 CEACAM expression of DCs and M Φ

First DCs and M Φ were characterized and their CEACAM expression was analyzed by flow cytometry as it was described before for isolated neutrophils (see Fig. 3.18).

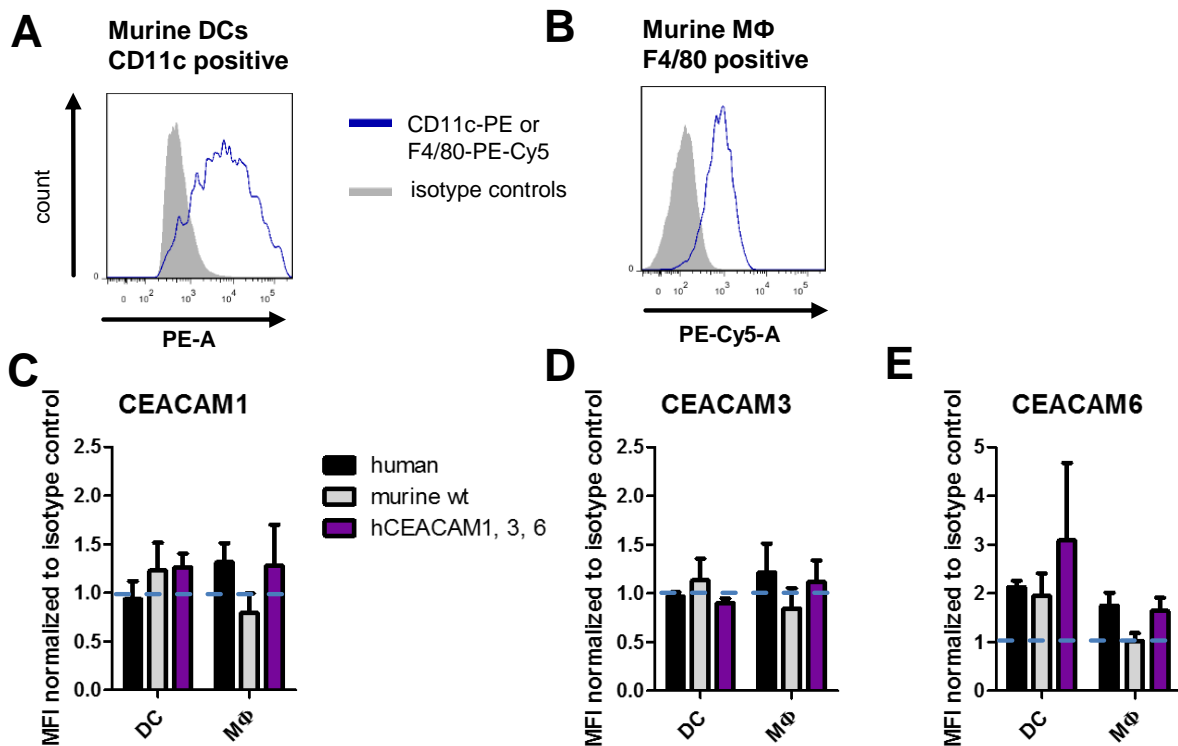


Fig. 3.18: Characterization and CEACAM expression of DCs and MΦ

DCs and MΦ were characterized by flow cytometry using the following antibodies: CD11c PE anti mouse, PE-Cy5 conjugated with F4/80 and the isotype controls PE rat IgG2a and rat IgG2a PE-Cy5. Graphs show one representative experiment. CEACAM expression was analyzed using the following antibodies: CEACAM1 (3/4/17, Genovac), CEACAM3 (col-1, Thermo Fisher), CEACAM6 (9A6, Genovac) and a ALEXA488 conjugated secondary antibody (isotype control). Moreover, CEACAM expression was quantified (see C-E). All bars over the dashed blue line show CEACAM expression. Statistics was performed using Two way ANOVA, with a Bonferroni post hoc test. The error bars show the SEM of at least three independent experiments, * < 0.05, ** < 0.01, *** < 0.001.

A) Murine bone marrow derived DCs

B) Murine bone marrow derived MΦ

C-E) Quantification of CEACAM expression

DCs showed a positive signal for CD11c and MΦ for F4/80 (see Fig. 3.18). Thus, both expressed their characteristic cell surface markers. Generally, the CEACAM expression levels were low on DCs and MΦ. Human and humanized DCs expressed low levels of human CEACAM6. In humanized DCs the amount of CEACAM6 expression was a bit higher compared to human DCs. Human and humanized MΦ did not differ in their CEACAM expression levels. Both expressed very low levels of CEACAM1 and 6. In total, CEACAM expression of naive DCs and MΦ was very low compared to human and humanized neutrophils (see section 1.1.1).

3.3.2 Interaction of *H. pylori* with DCs and M Φ

Next, the interaction of *H. pylori* with DCs and M Φ was analyzed (see Fig. 3.19).

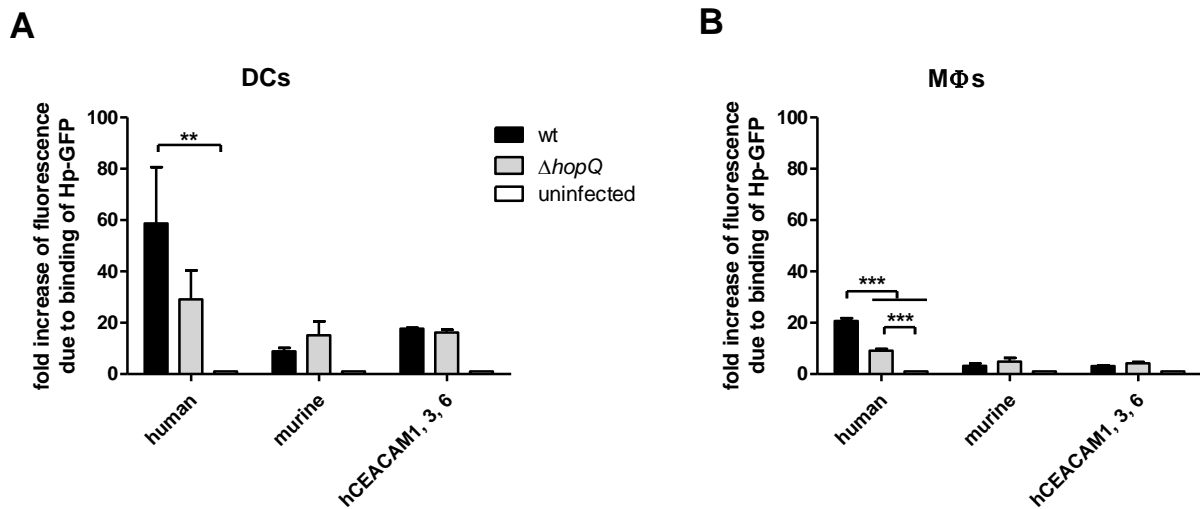


Fig. 3.19: Interaction of *H. pylori* with DCs and M Φ

The interaction was analyzed after an infection for 1 h with an MOI of 10 using a P12 GFP (black bars) or a P12 $\Delta hopQ$ GFP mutant strain (gray bars) or left uninfected (white bar) by flow cytometry. Statistics was performed using Two way ANOVA, with a Bonferroni post hoc test. The error bars show the SEM, * < 0.05, ** < 0.01, *** < 0.001.

Human DCs and M Φ infected with P12 wt (see Fig. 3.19, black bars) show an increased fluorescence intensity compared to murine and humanized cells. However, the fluorescence intensity of human DCs is three times higher compared to human M Φ . The difference between human and murine cells indicates a CEACAM effect in DCs and M Φ . This effect is supported by a reduced fluorescence intensity in an infection with the P12 $\Delta hopQ$ mutant strain (gray bar).

Murine and humanized DCs as well as M Φ interact independently of CEACAMs with the bacterium, because an infection of human DCs and M Φ with the P12 $\Delta hopQ$ mutant strain (gray bar) does not results in a reduced fluorescence intensity compared to an infection with P12. Generally, murine and humanized DCs show a low interaction with *H. pylori* after 1 h infection and the interaction of murine and humanized M Φ is even lower. All in all, the interaction of *H. pylori* with DCs or M Φ is three to four times lower compared to neutrophils (see Fig. 3.4).

3.3.3 CagA translocation and phosphorylation

The translocation and subsequent phosphorylation of CagA are associated with a more serious progression of an *H. pylori* infection (see section 1.2.3). In this work it could be

shown, that CagA is not phosphorylated in murine PMNs, but in murine PMNs expressing human CEACAMs (see Fig. 3.12). Thus, the CagA translocation and phosphorylation in DCs and M Φ was analyzed (see Fig. 3.20).

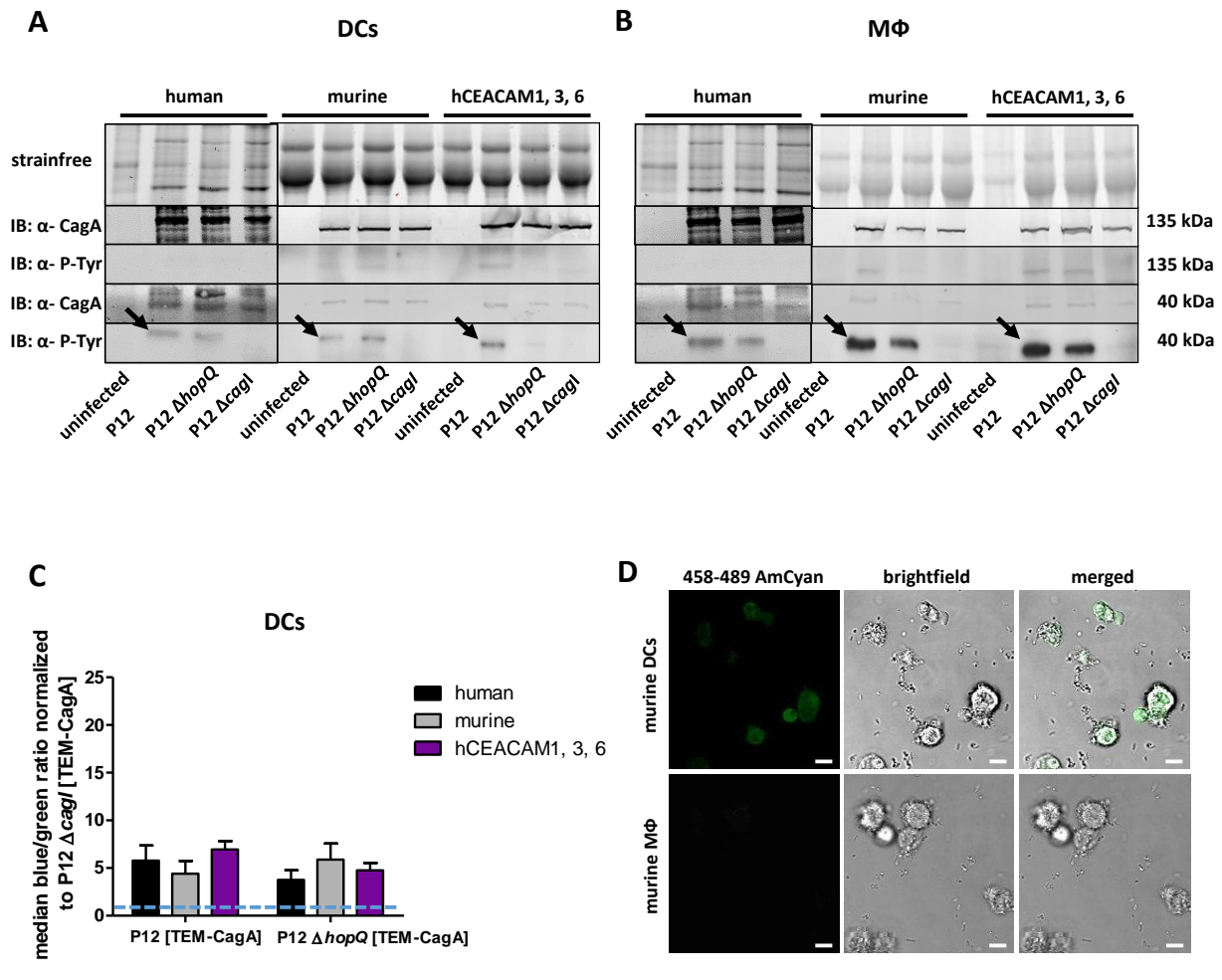


Fig. 3.20: CagA phosphorylation and quantification of CagA translocation in human, murine and humanized DCs and M Φ

A, B) Immunoblot analysis of CagA phosphorylation in human, murine and humanized DCs and M Φ .

Cells were infected for 3 h with an MOI of 60 with *H. pylori* P12, P12 Δ hopQ and P12 Δ cagI.

A) Human, murine and humanized DCs

B) Human, murine and humanized M Φ

C) Quantification of TEM-CagA translocation in DCs. CagA translocation was studied using a β -lactamase dependent reporter assay. Graphs displays mean values of the ratio of blue to green fluorescence of at least three independent experiments normalized to the translocation deficient strain *H. pylori* P12 Δ cagI TEM-CagA. Error bars show the SEM of at least three independent experiments. Statistical analysis was performed using two way ANOVA, with a Bonferroni post hoc test with * < 0.05, ** < 0.01, *** < 0.001. All bars over the blue dashed line are positive for CagA translocation.

D) Fluorescence microscopy of DCs and M Φ infected with *H. pylori* P12 TEM-CagA and stained with CCF4

CagA is phosphorylated in human, murine and humanized DCs and M Φ (see Fig. 3.20 A and B). M Φ showed a stronger CagA phosphorylation compared to DCs. However, CagA phosphorylation in M Φ is independent of CEACAMs, because similar amounts of phosphorylated CagA were detected in cells infected with the P12 Δ *hopQ* mutant strain. Quantification revealed that CagA is translocated in human, humanized and murine DCs (see Fig. 3.20 C). Human (black) and humanized (purple) DCs show a higher amount of translocated CagA in comparison to murine (gray) DCs. Again, compared to neutrophils the amount of translocated CagA is much lower in DCs. CagA translocation could not be detected in M Φ using the β -lactamase dependent reporter assay, as no signal can be detected. To study this, microscopy of the cells infected with *H. pylori* P12 TEM-CagA and labeled with CCF4 was performed. Fig. 3.20 D shows green fluorescent DCs, whereas M Φ exhibit no fluorescence.

Taken together, CEACAMs do not influence CagA translocation and phosphorylation in humanized DCs and M Φ . These data highlight the special role of CEACAMs on neutrophils in the interaction with *H. pylori*.

3.4 Impact of a chronic infection with *H. pylori* on the interaction with neutrophils

Finally, it was evaluated whether human CEACAMs on neutrophils have an effect *in vivo*, too. Thus, it was analyzed whether neutrophils from humanized mice, which were chronically infected with *H. pylori*, show a different behavior compared to neutrophils from humanized naive mice. Murine wt neutrophils of naive and chronically infected mice were used as controls. It was known before, that pre- and coinfections of *H. pylori* reduce the amount of CagA translocation in host cells [159].

3.4.1 Effect on CagA translocation and phosphorylation

Firstly, the CagA translocation into neutrophils from chronically infected mice was studied. Therefore, mice were infected for four weeks with the mouse adapted *H. pylori* strain PMSS1. Afterwards, neutrophils were isolated and used in translocation experiments (see Fig. 3.21).

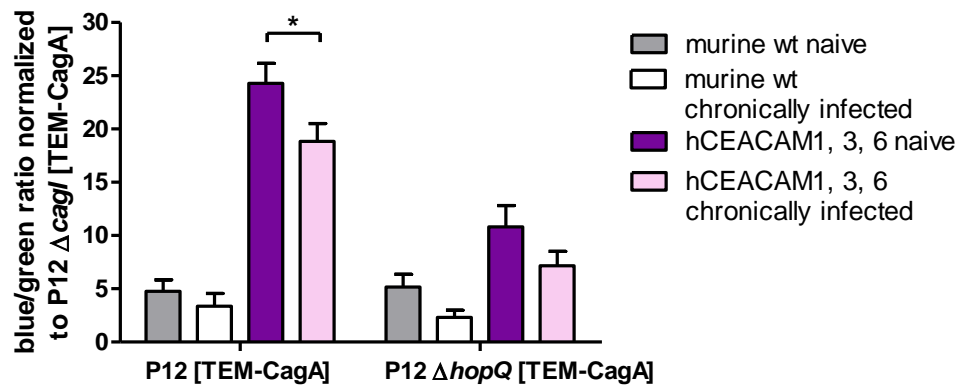


Fig. 3.21: Translocation of CagA into neutrophils isolated from chronically infected mice CagA translocation was quantified using the β -lactamase dependent reporter assay. Before, mice were infected for four weeks with the *H. pylori* PMSS1 strain. Afterwards, neutrophils were isolated and then, a translocation assay was performed. Shown are mean values of the ratio of blue to green fluorescence of at least three independent experiments normalized to the translocation deficient strain *H. pylori* P12 Δ cagI TEM-CagA. Error bars show the SEM. Statistical analysis was performed using Two way ANOVA, with a Bonferroni post hoc test with * < 0.05, ** < 0.01, *** < 0.001.

After an infection with *H. pylori* P12 TEM-CagA a significantly reduced amount of CagA was detected in humanized hCEACAM1, 3, 6 neutrophils from chronically infected mice (see Fig. 3.20, pink bar) in comparison to neutrophils from naive mice (purple). In murine wt neutrophils (gray) from chronically infected mice (white) a low reduction of CagA translocation can be seen. A reduced amount of CagA translocation was also seen in an infection with P12 Δ hopQ TEM-CagA. This indicates that *H. pylori* changes its behavior towards PMNs coming from an infected host. This result suggests that there might be a difference between naive and chronically infected PMNs and that the bacterium can distinguish between both.

Therefore, it was further analyzed whether the effect could be seen in human neutrophils as well (see Fig. 3.22). Moreover, it was studied whether human CEACAM1 plays a special role in this context (see Fig. 3.20), as previous results from phagocytosis survival assay suggest (see section 3.1.4).

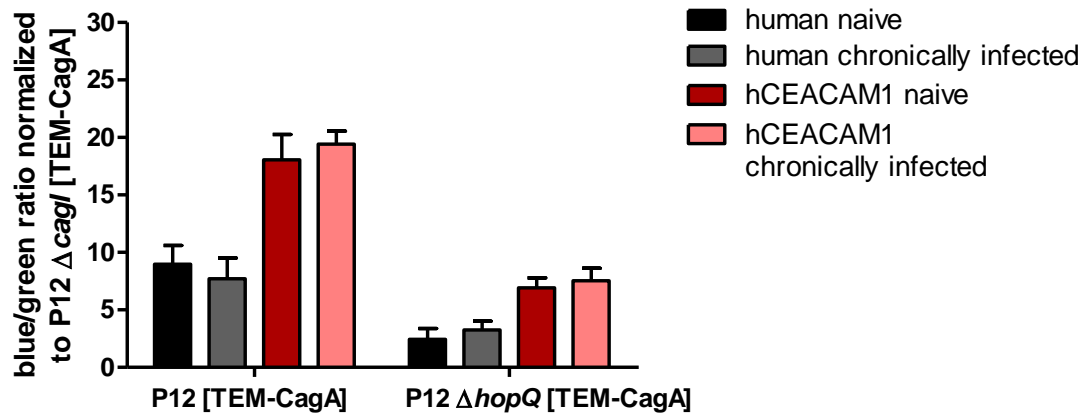


Fig. 3.22: Translocation of CagA into neutrophils isolated from naive versus chronically with *H. pylori* infected humans

CagA translocation was quantified with the β -lactamase dependent reporter assay by flow cytometry. For this, neutrophils were isolated from blood of naive as well as chronically infected individuals without symptoms. Afterwards, a translocation assay was performed. Shown are mean values of the ratio of blue to green fluorescence of at least three independent experiments normalized to the translocation deficient strain *H. pylori* P12 $\Delta cagI$ [TEM-CagA]. Lighter colors show the chronically infected neutrophils. Error bars show the SEM. Statistic analysis was performed using Two way ANOVA, with a Bonferroni post hoc test with * < 0.05, ** < 0.01, *** < 0.001.

In human neutrophils (black) isolated from blood of chronically infected individuals (dark gray) without symptoms a weak reduction in CagA translocation was revealed in comparison to human neutrophils of naive individuals (darker hue). An infection of human chronically with *H. pylori* infected individuals with the P12 $\Delta hopQ$ TEM-CagA strain shows a reduction in CagA translocation in comparison to P12 wt. Notably, neutrophils of chronically infected mice expressing only human CEACAM1 (red) infected with P12 TEM-CagA did not show a reduced CagA translocation as it was seen for chronically infected hCEACAM1, 3, 6 PMNs. The amount of CagA of these chronically infected hCEACAM1 PMNs is similar to neutrophils of naive mice expressing only human CEACAM1 (red). This again highlights a special role of human CEACAM1.

Further, it was evaluated whether a chronic infection also has an effect on CagA phosphorylation (see Fig. 3.23).

A

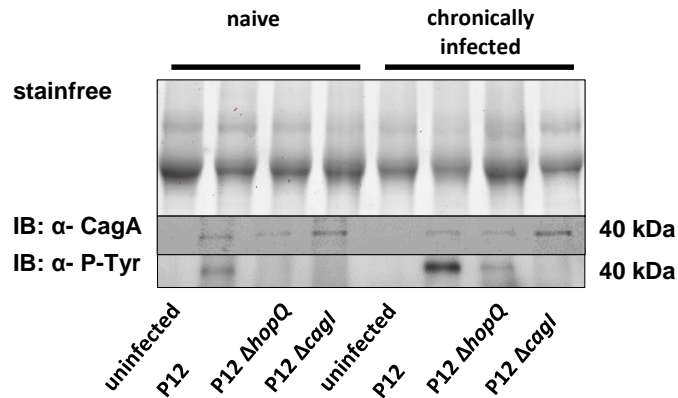


Fig. 3.23: CagA phosphorylation in neutrophils from naive versus chronically with *H. pylori* infected individuals

Immunoblot analysis of neutrophils infected with *H. pylori* from a naive person and a chronically with *H. pylori* infected person.

In human PMNs of naive and chronically infected individuals CagA phosphorylation was detected. The CagA band of the chronically infected individuals is stronger as compared to the CagA band of the naive individuals. Moreover, neutrophils from chronically infected individuals show a weak CagA phosphorylation band in an infection with the P12 $\Delta hopQ$ mutant strain, indicating differences between naive and chronically infected PMNs.

3.4.2 Effect on CEACAM expression

Consequently, the expression of CEACAMs in chronically infected murine, human and humanized neutrophils was analyzed (see Fig. 3.24).

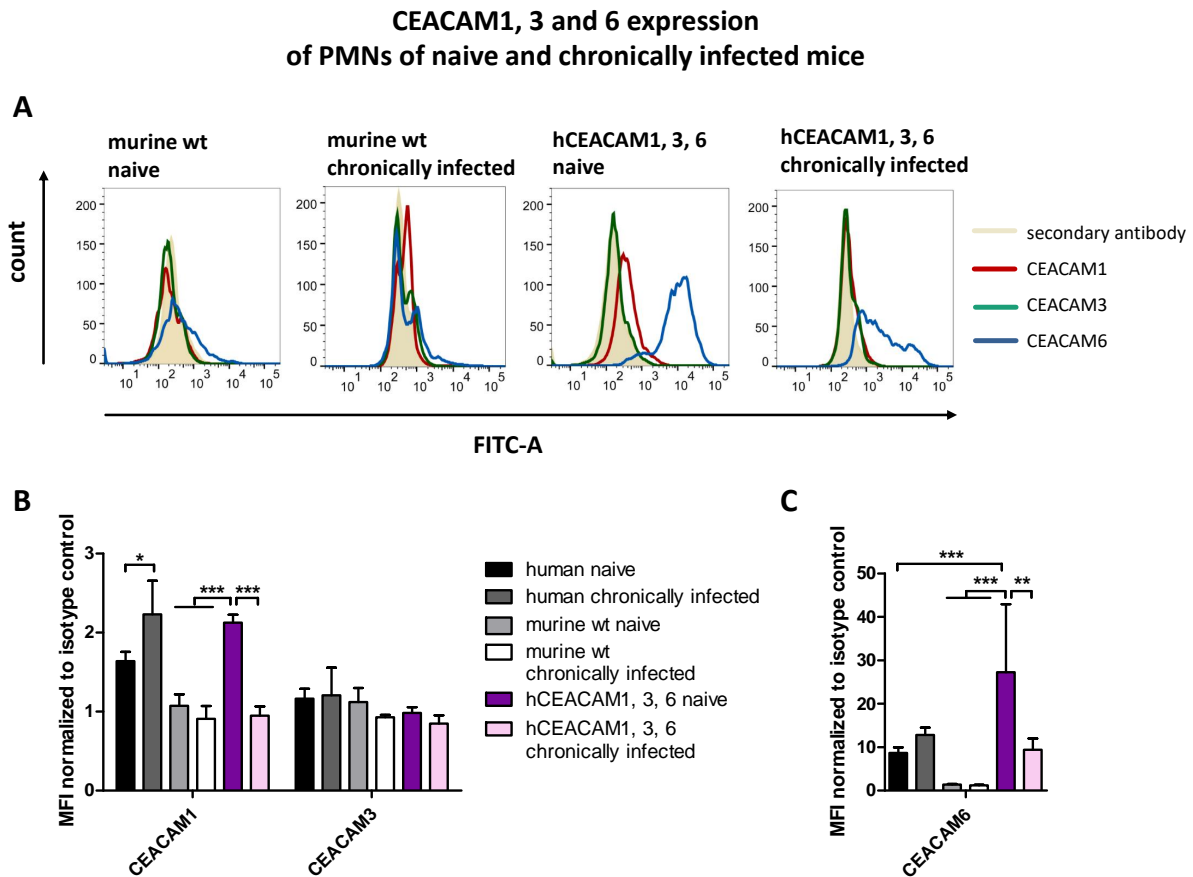


Fig. 3.24: CEACAM expression of neutrophils from naive and chronically infected humans
CEACAM expression was studied by flow cytometry using the following antibodies: α -CEACAM1 (4/3/17), α -CEACAM3 (col-1) und α -CEACAM6 (9A6).

A) The graphs show a representative experiment CEACAM1 (red), CEACAM3 (green), CEACAM6 (blue) and isotype control (beige).

B) Quantitative analysis of CEACAM expression normalized to isotype control. Error bars show the SEM of at least three independent experiments. Statistical analysis was performed using Two way ANOVA, with a Bonferroni post hoc test with * < 0.05 , ** < 0.01 , *** < 0.001 .

Naive PMNs (darker hue) express a significantly higher level of CEACAM1 (Fig. 3.24 B) and CEACAM6 (C) as compared to PMNs of chronically infected (lighter hue) humanized neutrophils. But, in human neutrophils the CEACAM1 and 6 expression was significantly higher in neutrophils of chronically infected individuals.

These data suggest that a CEACAM effect is also seen under *in vivo* infection conditions. Moreover, they show that *H. pylori* is able to manipulate neutrophils. All in all, it could be shown that human CEACAMs on neutrophils can drastically influence the interaction with *H. pylori*.

4. Discussion

Today, the interaction of CEACAMs with more than ten different pathogens such as *E. coli*, *H. influenzae*, *H. pylori*, *N. gonorrhoeae*, *N. meningitidis*, *M. catarrhalis*, and different *Salmonella* strains [96], [97], [34], [98], [99], as well as human pathogenic fungi such as *Candida albicans* [100] are known. All started in 1965 with the discovery of CEA, which was found overexpressed in tumor tissue. To establish an animal model for tumor immunotherapy, transgenic CEA mice expressing human CEACAM5 were generated [137]. At that time it was already known that binding to host cells is a key event in the infection process of bacteria [160], [161]. In addition, *in vitro* experiments showed that bacteria such as *N. gonorrhoeae* bind via its Opa proteins to CEACAMs expressed on epithelial cells as well as on neutrophils [114], [162], [163]. The Gram-negative bacterium *N. gonorrhoeae* colonizes the mucosa of the human urogenital tract, which is characterized by massive infiltration of neutrophils and can cause gonorrhoea. In 2005, *in vitro* studies demonstrated that bacteria such as *N. gonorrhoeae* induce detachment of epithelial cells [164], as a reaction of the innate immune response. To study the role of CEA *in vivo* Muenzer *et al.* worked with transgenic CEA mice. They discovered that *N. gonorrhoeae* interact with CEA resulting in colonization of the urogenital tract of transgenic CEA mice after 24 h of infection, whereas wild-type mice were not colonized [164]. The bacteria suppress exfoliation by triggering *de novo* expression of CD105, which blocks cell migration and promotes adhesion [165].

The transgenic CEA mice were also used for an infection with *H. pylori*, which is a Gram-negative, mucus-associated human pathogen like *N. gonorrhoeae*. Koeniger *et al.* studied the interaction of *H. pylori* with CEACAMs on epithelial cell lines *in vitro* as well as in the transgenic CEA mice expressing CEACAM5 *in vivo*. For *H. pylori* it was shown that its adhesin HopQ interacts with human CEACAM1, 5 and 6 on epithelial cells [34]. However, HopQ is not able to recognize murine CEACAMs [34]. The role of human CEACAMs for the interaction of *H. pylori* with neutrophils was not studied so far.

Massive infiltration of neutrophils is a hallmark of a *H. pylori* infection as well as an infection of *N. gonorrhoeae*. But, the PMNs and the corresponding immune response are manipulated by *H. pylori* as well as *N. gonorrhoeae* and the immune system cannot clear the infection. Instead inflammation occurs, which can result in case of *H. pylori* in MALT lymphoma and stomach cancer.

To learn more about the role of CEACAMs and to create a model system to study human pathogens binding to CEACAMs such as *N. gonorrhoeae in vivo*, Chan *et al.* included a CEABAC in mice and generated transgenic mice expressing CEACAM3, 5, 6 and 7 [138]. Moreover, Gu *et al.* generated transgenic mice expressing human CEACAM1 [126]. Islam *et al.* used these transgenic CEACAM mice and studied the role of CEACAMs in an infection of *N. gonorrhoeae in vivo*. They could support the initial findings of Muenzer *et al.* by showing that CEACAM5 promotes a long-term colonization of the bacteria in the lower genital tract [166]. In addition, it was found that human CEACAM1 facilitates penetration into the tissue [166]. Furthermore, Sintsova *et al.* demonstrated by *in vivo* experiments using the transgenic CEACAM mice that CEACAM-expressing neutrophils migrate faster to the site of infection, to be activated by *N. gonorrhoeae* [167]. Together with the findings of Sarantis *et al.* defining the role of CEACAM3 as a trigger for phagocytosis, CEACAM3 was characterized as a protective as well as pathogenic receptor [113]. For *H. pylori* it is as well known that the bacterium promotes neutrophils recruitment as well as it is engulfed by neutrophils. Thus, in this work neutrophils as well as DCs and M Φ were isolated from the transgenic CEACAM mice to study the role of CEACAMs in their interaction with *H. pylori*.

4.1 *H. pylori* interacts with human CEACAMs to manipulate neutrophils

It was shown that *H. pylori* P12, as well as other *H. pylori* strains, efficiently bind to neutrophils dependent on their expression of human CEACAMs. These results were supported by a reduced binding of the $\Delta hopQ$ mutant strain lacking the adhesin to interact with CEACAMs as well as to wt murine PMNs. The CEACAM specific efficient binding of the bacterium to neutrophils is uniform with the finding of Königer *et al.* on epithelial cells [34]. Moreover, it is consistent with the CEACAM specific binding of *N. gonorrhoeae* via its Opa proteins to neutrophils [163], [97]. In comparison to several Opa proteins of *N. gonorrhoeae*, HopQ is so far the only known counterpart of *H. pylori* for human CEACAMs and in addition, the expression of HopQ is not phase variable. HopQ interacts with CEACAMs via the IgV like N-terminal domain and can inhibit dimerization of human CEACAM1 [38].

CEACAM1 exists in different splice variants. Isoforms of CEACAM1 can form oligomers, which assemble in microdomains. These microdomains are characterized by the presence of constant (IgC2-like) domains. In its dimerized form, the receptor can recruit signaling molecules such as SHP-1 via its ITIMs, which are phosphorylated by Src kinases [107]. Thereby specific signaling pathways such as the PI3K dependent signaling pathways are

activated. They can trigger events like the *de novo* expression of CD105 after interaction of *N. gonorrhoeae* with CEACAMs and promote adhesion followed by the bacterial colonization [165].

Wildtype mice are neither colonized by *N. gonorrhoeae* nor by *H. pylori*. Only a few adapted strains are able to colonize mice. Interestingly, the mouse adapted strain of *H. pylori* called SS1 showed a low CEACAM effect in the interaction with PMNs, whereas the Mongolian gerbil adapted strain demonstrated a strong CEACAM effect. It is known that HopQI is down regulated in the SS1 strain [34]. The finding of a lower CEACAM-dependent binding of the SS1 strain is consistent with the results of Cao *et al.*, describing an enhanced binding and CagA phosphorylation in strains producing HopQI [127]. An explanation for the increased binding of the Mongolian gerbil strain on humanized CEACAM PMNs could be the stronger pathology after a *H. pylori* infection. In Mongolian gerbils the bacterium can induce intestinal metaplasia, gastric ulcer and adenocarcinoma (see section 1.5) [132], [133]. The pathology of Mongolian gerbils is more comparable to humans than the one in mice [135]. But, the stronger CEACAM effect of the Mongolian gerbil adapted B8 strain in comparison to human *H. pylori* strains is still an open question. Thus, it would be interesting to study the role of neutrophils and CEACAMs in the Mongolian gerbil. However, the Mongolian gerbil as a model organisms is not well established so far (see section 1.5) and only little is known about CEACAMs in gerbils.

4.1.1 CEACAMs facilitate survival of phagocytosis

Furthermore, it could be shown that the interaction of *H. pylori* with CEACAMs enable the bacterium to modify neutrophils. Binding of *H. pylori* results in ROS production and neutrophils try to eliminate the bacteria by phagocytosis. However, *H. pylori* resists clearance, because of the active manipulation of immune cells by the bacterium. Notably, *H. pylori* actively recruits neutrophils, which should kill the bacterium, via several factors such as HP-NAP, SabA as well as the T4SS encoded on the Cag-PAI [72], [41]. It is already known that *H. pylori* developed mechanisms to avoid phagocytosis. Allen *et al.* reported that *H. pylori* disrupts the NADPH oxidase and thereby avoids killing by PMNs [60]. Ramarao *et al.* described that the bacterium possesses an active antiphagocytic activity in PMNs and M Φ involving *de novo* protein synthesis by the bacterium and the T4SS [71]. But, it was not known so far whether and how CEACAMs are involved in these processes. In this work it was shown for the first time that *H. pylori* survives phagocytosis via the interaction with CEACAM3 and/or 6 and can not be eliminated by neutrophils. These data are consistent with a higher ROS production in these cells, because disruption of NADPH oxidase results in cell damage and ROS release. Moreover, phagocytosis of neutrophils is a fast process leading to the occurrence of incomplete phagosomal maturation.

tion, which also causes the release of ROS [20].

For other bacteria such as *N. gonorrhoeae*, *H. influenzae*, *M. catarrhalis* it was as well described that after binding to CEACAMs they are engulfed by neutrophils going along with a strong oxidative burst [116], [168]. However, after binding to CEACAM3 these bacteria are rapidly killed by the intracellular oxidative burst [169]. *H. pylori* survives after binding to CEACAM3 and/or 6 on neutrophils, as it could be shown in this work. Notably, it was demonstrated that hCEACAM1 neutrophils act contrary in ROS production and that the bacteria do not survive phagocytosis in hCEACAM1 PMNs. In addition, the survival of the bacterium in PMNs expressing CEACAM1, 3 and 6 was reduced in comparison to neutrophils expressing only CEACAM3 and 6. Human CEACAM1 contains two ITIMs. In B- and T cells CEACAM1 has an inhibitory function because of these ITIMs [101]. Boulton *et al.* demonstrated that binding of *N. gonorrhoeae* to human CEACAM1 leads to inhibition of the CD4+ T-cell response via the ITIM [101]. Boulton *et al.* also showed that CEACAM1 can be phosphorylated in PMNs. In addition, infection of *M. catarrhalis* and *N. meningitidis* by binding to human CEACAM1 inhibit the TLR2 initiated transcription factor NF- κ B and prevent the TLR2 initiated immune response [102]. An inhibitory effect of human CEACAM1 on neutrophils is so far unknown. The results of this work indicate that *H. pylori* may avoid the inhibitory function of CEACAM1 on neutrophils and probably acts on CEACAM3 and 6.

For CEACAM3, which is exclusively expressed on neutrophils, it is known, that it has an influence on ROS production and phagocytosis [116]. Contrary to the survival of *H. pylori* in CEACAM3 and 6 PMNs, it is described that CEACAM3 can direct opsonin independent phagocytosis of *Neisseria*, *Moraxella* and *Haemophilus* species [116]. In addition, Sarantis *et al.* showed that after bacterial binding to CEACAM3, the cytoplasmic tyrosine kinase (spleen tyrosine kinase (Syk)) is recruited and phosphorylates the ITAM of CEACAM3, which is necessary for an efficient killing process [170]. Moreover, in the process of phagocytosis of *N. gonorrhoeae* triggered by CEACAM3 the actin cytoskeleton is completely reorganized regulated by the small GTPases Rac1 and Cdc42, but not Rho, while CEACAM1 and 6 engulfment do not require changes in the actin cytoskeleton [171]. However, *in vitro* experiments show that engulfment of *N. gonorrhoeae* by the human myelomonocytic cell line JOSK-M expressing human CEACAM1, 6 activates a signalling cascade from CEACAMs via Src-like protein tyrosine kinases, Rac1 and PAK to Jun-N-terminal kinase [172]. Moreover, they demonstrated that Inhibition of Src-kinases or Rac1 protects the bacteria from phagocytosis [172].

A possible mechanism to support survival of *H. pylori* after phagocytosis in PMNs expressing CEACAM3 and 6 could be a manipulation of the signaling cascade by interfering with the ITAM motif of CEACAM3 by *H. pylori*, to avoid activating signals. It was shown in this work that human CEACAMs enable CagA phosphorylation, probably by changing signaling cascades. However, in this project it was not possible to distinguish between

CEACAM3 and 6. CEACAM3 is expressed in the transgenic CEABAC mouse [138], but, expression is low and was only detected in very low levels in this work. Thus, also CEACAM6 or a combination of CEACAM3 and 6 can be the reason for the differences. It is known that CEACAM6 promotes formation of tumors [103]. But its role during pathogen interaction is so far unknown. Thus, in future experiments it will be important to use cell lines or mice which allow distinguishing between CEACAM3 and 6.

In addition, it could be shown that a deletion of CagA and especially of VacA decreased the survival of phagocytosis in hCEACAM3, 6 PMNs. Moreover, *H. pylori* strains without VacA show a reduced survival rate in hCEACAM1, 3, 6 PMNs. Survival of the bacterium in PMNs is probably a failure of the killing process of PMNs. A hallmark of phagocytosis of neutrophils is the high speed of the phagocytosis process, which can result in incomplete phagosomal maturations [20]. Already Allen *et al.* reported that VacA is involved in retarding phagocytosis of *H. pylori* by M Φ [60]. They discovered that VacA and urease disrupt membrane trafficking and inhibit phagosome-lysosome fusion in M Φ [173]. Moreover, Zheng *et al.* could show that VacA is important for the disruption of phagosome maturation by recruiting coronin1 in M Φ [174]. However, work by Odenbreit *et al.* and Rittig *et al.* did not notice differences between *H. pylori* strains with or without VacA for phagocytosis by M Φ [152], [175]. Taken together, the data of this project confirm the data of Allen *et al.* and Zheng *et al.* that VacA is involved in survival of phagocytosis. In addition, survival of phagocytosis might be less important for *H. pylori* strains without CagA and VacA, because they induce a weaker response of the immune system resulting in less phagocytosis and inflammation [176].

4.1.2 CEACAMs enable CagA phosphorylation in PMNs

Besides the involvement of CEACAMs in survival of phagocytosis as already mentioned it was shown that human CEACAMs enable CagA phosphorylation in murine PMNs. CagA phosphorylation leads to an activation of the oncoprotein and is associated with an oncogenic progression of the infection.

First, CagA is translocated via the T4SS of *H. pylori* into the host cells. Zhao *et al.* published that CEACAMs, rather than integrin receptors are essential for CagA translocation into human gastric cells [128]. Here, it could be demonstrated that CEACAMs enhance the amount of translocated CagA into neutrophils. Humanized neutrophils showed a higher amount of CagA translocation in comparison to wt mouse neutrophils. Consistent with these findings an infection with the $\Delta hopQ$ mutant strain resulted in a reduced CagA translocation. This results might indicate that the HopQ-CEACAM interaction activates a signaling cascade. However, Bonsor *et al.* analyzed the structure of HopQ-CEACAM and speculated that still the "dwell time" and the high affinity during the HopQ-CEACAM

interaction is responsible for enhanced CagA translocation via CEACAMs [38]. In this project *H. pylori* translocated a higher amount of CagA in hCEACAM1, 3, 6 neutrophils compared to hCEACAM1 and hCEACAM3,6 neutrophils. Comparing hCEACAM1 and hCEACAM3, 6 neutrophils, the amount of translocated CagA was nearly the same. But, other adhesins of *H. pylori* such as BabA and SabA do not result in a higher CagA translocation. Thus, HopQ seems to be special and might activate a signaling cascade.

Moreover, humanized neutrophils showed a higher amount of CagA translocation in comparison to human PMNs. A possible explanation could be the presence of other human receptors on the surface of human PMNs that influence the process. In comparison to human PMNs the humanized mouse PMNs only express the inserted human CEACAM genes and produce human receptors on their surface. This enables an exclusive study of these receptors, however effects of other human receptors that also might have effects are excluded here. Thus, these *in vitro* experiments analyze the interaction of the bacterium with neutrophils in a special situation, which is needed to understand the basic mechanisms of interaction. In future *in vivo* experiments have to be performed to look at other parameters that might influence the processes in an *in vivo* situation as well.

Subsequent to translocation CagA is phosphorylated, which is associated with an oncogenic course of disease. For the first time it was demonstrated in this project that human CEACAMs on humanized neutrophils enable a phosphorylation and activation of the oncoprotein of *H. pylori*, whereas in murine wt neutrophils CagA is not phosphorylated.

These data further support the involvement of a signaling cascade, which is activated by the HopQ-CEACAM interaction.

The mild pathology in mice might be related to the non-phosphorylation of CagA going along with non-activation of phosphorylation dependent signaling cascades in murine PMNs. This indicates that the bacterium infecting normal mice is not able to manipulate murine PMNs. In human PMNs CagA is phosphorylated and is cleaved in 40 kDa fragments for so far unknown reasons. In humanized PMNs CagA is cleaved, too. But, there a full length product of CagA (135 kDa) was detected as well. Thus, it might be that not all CagA is cleaved in humanized PMNs, because of the high amount of CagA. This is consistent with the finding of a higher CagA translocation in humanized PMNs in comparison to human PMNs.

Within the host cell CagA is phosphorylated by Src and c-Abl kinases [45], [49]. Their activity in murine PMNs was proven in an *in vitro* phosphorylation experiment, as well as the translocation of CagA with the β -lactamase dependent reporter assay. However, CagA is not phosphorylated in murine PMNs without human CEACAMs. The exact process of CagA phosphorylation and all involved molecules are unknown so far. Hatakayama *et al.* could show that SHP-1 dephosphorylates CagA in its EPIYA motif resulting in a decrease of its oncogenicity [52]. Thus, experiments with PMNs with an inactivation or deletion of SHP-1 were performed. But, these manipulations did not lead to a CagA phosphorylation

in murine PMNs. Consequently, it is still an ongoing project to solve the mechanism of CagA phosphorylation.

4.1.3 *H. pylori*-CEACAM interactions change the chemokine secretion of neutrophils

For many years it has been claimed that neutrophils only function as phagocytes for invading pathogens. However, these cells are more complex. They can produce cytokines like proinflammatory chemokines resulting in recruitment of further immune cells and intervene in inflammation processes. *H. pylori* translocates via its T4SS CagA in gastric epithelial cells (see section 4.1.2). In this process the T4SS activates the epithelial cells to secrete IL-8 leading to the recruitment of PMNs. Proinflammatory cytokines such as IL-1 β , IL-6, IL-8 and TNF α , which were detected in *in vitro* cultured biopsy samples of infected patients [58], [59], are characteristic of a *H. pylori* infection. Their release recruits immune cells to the site of infection. Neutrophils are the first recruited cells. They phagocytose the bacterium and produce ROS (see section 4.1.1). In addition, they secrete chemokines to attract further immune cells.

In this work it was shown that CEACAM-humanized neutrophils produce significantly more MIP-1 α in comparison to murine neutrophils. Charmoy *et al.* could demonstrate that MIP-1 α is important for the recruitment of DCs. Pharmacological and genetic inhibition of the protein leads to a considerable reduction of the number of recruited DCs [14]. Consequently, humanized PMNs in the *H. pylori* infected mouse should recruit more immune cells, and destroy more tissue leading to a stronger inflammation. These suggestions have to be proven in *in vivo* experiments. So far, Kusugami *et al.* studied the MIP-1 α concentration and the number of M Φ in infected versus uninfected people. They revealed a significant higher concentration of MIP-1 α in persons infected with *H. pylori* and detected an increased number of recruited M Φ in the lamina propria [177]. The results of Kusugami *et al.* are consistent with the findings in this work and confirm the high MIP-1 α concentrations under *in vitro* infection conditions. In further migration experiments it will be tested whether the chemokine MIP-1 α changes the migration behavior of PMNs *in vitro*.

Consistent with the findings of this work Islam *et al.* showed increased levels of MIP-1 α after 6 h of infection of *N. gonorrhoeae* in the upper genital tract of transgenic CEACAM1 as well as CEABAC mice [166]. In addition, Sintsova *et al.* demonstrated a higher concentration of MIP-1 α in neutrophils of CEABAC mice infected with *N. gonorrhoeae* compared to wt mice [167]. This indicates that CEACAMs contribute to an inflammatory response. Moreover, Sintsova *et al.* showed that the CEACAM dependent transcriptional response resulting in the release of MIP-1 α is dependent on p38 MAPK [167].

4.1.4 The role of CEACAM3 in a *H. pylori* infection

CEACAM3 is required for oxidative burst and phagocytosis of *N. gonorrhoeae*. In addition, binding of the bacterium to CEACAM3 results in release of proinflammatory chemokines such as KC, MIP-1 α and MIP-2 [113], [116], [167]. The chemokine release attracts further neutrophils. After their activation by *N. gonorrhoeae* they produce ROS resulting in tissue damage and inflammation. Sintsova *et al.* demonstrated that the release of proinflammatory chemokines depend on TAK-1 activating NF- κ B. Inhibition of TAK-1 stops the chemokine release, the massive infiltration of neutrophils and consequently tissue damage. However, the clearance of *N. gonorrhoeae* by phagocytosis of PMNs is still active [167]. Taken together, CEACAM3 is involved in protection of the host as well as damage of host cells and tissue.

However, in this project it was also demonstrated that CEACAMs enhance the proinflammatory response in an infection of *H. pylori*. Consequently, further neutrophils were attracted and cause tissue damage and inflammation as well as in an infection of *N. gonorrhoeae*. Lamb *et al.* could show that CagA interacts with TAK-1, which is essential for NF- κ B activation in a *H. pylori* infection resulting in chemokine release [57]. Probably, TAK-1 inhibition might stop the massive infiltration of neutrophils in a *H. pylori* infection resulting in limited inflammation as well.

Zimmermann recently described CEACAM3 as a decoy receptor enabling the host to kill invading pathogens, which tried only to bind to CEACAM1 to enter the host and suppress the immune response [178], [101]. Human pathogens such as *N. gonorrhoeae* were phagocytosed after binding to CEACAM3 [116], [113]. However, in this work it was shown that *H. pylori* seems to manage survival of phagocytosis especially in neutrophils expressing CEACAM3 and 6. In comparison to CEACAM1, CEACAM3 emerged evolutionary later and is exclusively expressed in highly developed apes and humans, which represent the only host of *H. pylori*. Strains of the bacterium show a high genetic diversity. It would be interesting to test different *H. pylori* strains and to compare sequence data with *H. pylori* strain databases to see whether the bacterium adapted to the CEACAM3 receptor over time.

4.1.5 CEACAMs play a major role on PMNs rather than on M Φ and DCs

PMNs have only a short lifetime in comparison to DCs and M Φ . These short life time requires immediate activity as well as functionality, whereas DCs and M Φ phagocytose pathogens and develop to a mature cell. Then, as mature cells, M Φ and DCs interact

with B- and T- cells by presenting the antigens of the pathogens. However, *H. pylori* manipulate the maturation of DCs. Interestingly, semimature DCs initiate the development of naive T-cells to regulatory T-cells with suppressed activity [78]. As a result, the adaptive immune response is down-regulated.

In the experiments with immature DCs and M Φ in this project no CEACAM dependent effect was found. This is consistent with the low CEACAM expression in these cells. In the literature there is nearly no evidence for CEACAM6 expression in DCs and M Φ . Only in one paper from 1975 is written: "Antisera directed against the antigen cross-reacting with CEA strongly stain the cytoplasm of polymorphonuclear cells, myelocytes and in mononuclear cells, which probably are macrophages" [179]. But, it is not clear whether they really worked with macrophages.

For human CEACAM1 expression Yu *et al.* demonstrated in immature DCs by the antibody D14HF11, recognizing CEACAM1, 3, 4, 5 and 6, only very low levels of human CEACAM1. In mature human DCs cultivated for three days with CD40LT, Yu *et al.* showed that the CEACAM1 expression doubled as compared to immature DCs. Generally, human CEACAM1 expression was low when compared to CEACAM1 levels in B-cells [180]. Thus, it is questionable whether human CEACAM1 plays a role in mature DCs and whether it plays a role in the manipulation of the adapted immune response, e. g. B- and T- cells. It seems that *H. pylori* uses other receptors for its interaction with DCs and M Φ . This is also supported by the fact that the bacteria are able to manipulate DCs and suppress the adaptive immune response in the mouse model without recognizing CEACAMs [78].

In contrast, CEACAMs play an important role for PMNs (see section 4.1.1-3). Human and humanized PMNs express high amounts of CEACAM6 and moderate amounts of CEACAM1. The expression of human CEACAM3 was detected in low levels, as already reported by Chan [138], who constructed the transgenic CEABAC mouse and detected CEACAM3 only occasionally in tissue neutrophils [138].

Moreover, in further experiments the role of CEACAMs on other cell types and subtypes of immune cells, which could be very different from the M Φ and DCs used in this work, has to be analyzed. Here, immature cells were used to mimic the conditions in a *H. pylori* infection, where the bacterium inhibits the maturation of DCs [78]. The CEACAM expression and secretion of chemokines of stomach epithelial cells as well as tissue M Φ and tissue DCs of humanized CEACAM mice should also be studied in future.

In addition, it would be interesting to study the secretion of IL-1 β in wt and humanized mice, because its production is induced in an *H. pylori* infection [181]. In summary, the data presented in this work suggest that in a *H. pylori* infection CEACAMs are important, especially for PMNs.

All in all, it could be shown that CEACAMs dramatically change the behavior of neutrophils in the interaction with *H. pylori*.

4.1.6 Characterization of PMNs from naive versus *H. pylori*-infected hosts

In addition to the data on the *H. pylori* PMN interaction from *in vitro* experiments also first data with PMNs under *in vivo* conditions were obtained. In these experiments neutrophils were isolated from mice, which were infected for four weeks with a mouse adapted *H. pylori* strain. In addition, PMNs isolated from the blood of individuals chronically infected with the bacterium were also tested. It was demonstrated that *H. pylori* behaves differently in the interaction with neutrophils isolated from naive versus chronically infected mice and humans. The experiments revealed that *H. pylori* translocated a lower amount of CagA in neutrophils of chronically infected mice and humans in comparison to neutrophils of naive mice or humans. Moreover, neutrophils from chronically infected individuals showed a lower CEACAM expression by flow cytometry analysis. It was previously known that co- and preinfections reduce the amount of CagA translocation of a second infecting *H. pylori* strain [159]. Furthermore, Shikotra *et al.* could demonstrate that human CEACAM6 is up regulated in an asthma model [182]. It has been shown that individuals infected with *H. pylori* are protected from the development of asthma. One reason for this might be the initiation of the T helper cell type 1 response by *H. pylori* [79], because in asthma the T helper cell type 2 response is activated. Whether there is a relationship to the down regulation of CEACAM6 in a *H. pylori* infection has to be shown in future.

However, a higher number of volunteers would be necessary to really proof the interesting findings in this work.

4.2 Conclusion and outlook

In conclusion, this is the first study that points out the importance of human CEACAMs on neutrophils for the interaction with *H. pylori*. It could be shown that human CEACAMs enable the phosphorylation of the oncoprotein CagA in murine PMNs, which represents a decisive part of a *H. pylori* infection. Phosphorylation leads to the activation of translocated CagA and is associated with an oncogenic progression of the infection. Moreover, it was demonstrated that humanized PMNs secrete high numbers of MIP-1 α , which might lead to a stronger infiltration of immune cells into the mouse stomach. Recruitment of neutrophils to the gastric submucosa in high numbers might result in a stronger proinflammatory response and a severe outcome of a *H. pylori* infection, because of tissue damage by ROS production. Neutrophils expressing human CEACAM3 and 6 showed an enhanced ROS production and it was demonstrated that the bacterium survives phagocytosis in neutrophils expressing CEACAM3 and 6.

Thus, *H. pylori* uses the interaction with CEACAMs to survive in neutrophils and to induce a stronger inflammatory response. These findings improved the understanding of the *H. pylori* infection.

Many different pathogens interact via CEACAMs of the host cells. Thus, the discoveries of this work also provide starting points for research on other human pathogens. A disadvantage of working with PMNs is their short life time. Thus, for further studies an ER-Hoxb8 neutrophil cell line expressing human CEACAMs was finally generated, however, has not been studied yet. It has to be noted that an immortalized cell line can be useful for many experiments, but never replaces primary cells. Furthermore, future experiments studying the role of CEACAMs in *H. pylori* infections of *Mongolian gerbils* could discover new roles of CEACAMs.

All in all, the findings of this thesis demonstrate the importance of human CEACAMs in the interaction of *H. pylori* with neutrophils. Moreover, these first *in vitro* data indicate that the humanized CEACAM mouse might be a new appropriate model organism for *H. pylori* research.

Abbreviations

| | |
|----------|--|
| °C | degrees Celsius |
| α | anti |
| AP | Alkaline Phosphatase |
| APC | AlloPhycoCyanin |
| ATP | AdenosinTriPhosphate |
| BabA | Blood group antigen binding Adhesin |
| BAC | Bacterial Artical Chromosome |
| BCIP | 5-Bromo-4-Chloro-3-IndolylPhosphate |
| BSA | Bovines Serum Albumin |
| Bgp | Biliary glycoprotein |
| c-Abl | c-Abelson tyrosine kinase |
| CagA | Cytotoxin associated geneA |
| Cag-PAI | Cytotoxin associated Pathogenicity Island |
| CEA | Carcino-Embryonic Antigen |
| CEACAM | CarcinoEmbryonic Antigen-related Cell Adhesion Molecules |
| cfu | colony forming unit |
| ChlampR | Chloramphenicol Resistant |
| CHO | Chinese Hamster Ovaries |
| cm | centimeter |
| CmR | Chloramphenicol Resistant |
| CSF | Colony Stimulating Factor |
| Csk | C-terminal Src kinase |
| Cyt. D | Cytochalasin D |
| Δ | deletion |
| DAPI | 4, 6-DiAmidin-2-PhenylIndol |
| DC | Dendritic Cell |
| DNA | DeoxyriboNucleic Acid |
| DMEM | Dulbeccos Modied Eagle Medium |

| | |
|---------------|--|
| DMSO | Dimethylsulfoxid |
| EDTA | Ethylendiamintetraacetat |
| EPIYA | Glutamate-Proline-Isoleucine-Tyrosine-Alanine |
| ER | Estrogen Receptor |
| ErmR | Erythromycin Resistant |
| <i>et al.</i> | and others |
| FCS | Fetal Calf Serum |
| Fig | Figure |
| FITC | FluoresceInisoThioCyanat |
| GM-CSF | Granulocyte Macrophage - Colony Stimulating Factor |
| GPI | Glykosyl-Phosphatidyl-Inositol |
| Grb | Growth factor receptor-bound protein |
| h | hours |
| HBSS | Hank's Balanced Salt Solution |
| HOP | <i>Helicobacter</i> Outermembrane Protein |
| HP-NAP | <i>Helicobacter</i> Neutrophil Activation Protein |
| HRP | Horseradish Peroxidase |
| IARC | International Agency for Research on Cancer |
| IFN | Interferon |
| IgC | Immunoglobulin Constant domain |
| IgV | Immunoglobulin Variable domain |
| IMDM | Isocovs Modified Dulbeccos Media |
| IL | InterLeukin |
| IP-10 | Interferon-gamma induced Protein 10 kDa |
| ITAM | Immunoreceptor Tyrosine based Activation Motif |
| ITIM | Immunoreceptor Tyrosine based Inhibition Motif |
| ITSM | Immunoreceptor Tyrosine based Switch Motif |
| KanR | Kanamycin Resistant |
| KC | Keratinocyte Chemoattractant |
| kDa | kiloDalton |
| LIX | Lipopolysaccharide (LPS) induced CXC chemokine |
| LPS | LipoPolySaccharide |
| LTB4 | LeukoTriene B4 |
| Ly6G | Lymphocyte antigen 6 complex locus G6D |
| mA | milliampere |
| MALT | Mucosa Associated Lymphoid Tissue |
| MARK2 | Microtubuli Affinity Regulating Kinase2 |

| | |
|----------------|--|
| MCP-1 | Monocyte Chemoattractant Protein 1 |
| M-CSF | Macrophage Colony Stimulating Factor |
| MDC | Macrophage-Derived Chemokine |
| μ l | microliter |
| μ m | micrometer |
| min | minute |
| MIP-1 α | Macrophage Inflammatory Protein-1 alpha |
| MIP-1 β | Macrophage Inflammatory Protein-1 beta |
| MIP-2 | Macrophage Inflammatory Protein-2 |
| ml | milliliter |
| mM | millimolar |
| MOI | Multiplicity Of Infection |
| M Φ | macrophages |
| MPRO | Murine PROmyeolytic cell line |
| NADPH | Nicotinamide Adenine Dinucleotide Phosphate |
| NBT | Nitro Blue Tetrazolium |
| ng | nanogram |
| NO | Nitric Oxid |
| OD | Optical Dense |
| OMP | Outer Membrane Proteins |
| Opa | Opacity protein |
| PAMP | Pathogen Associated Molecular Patterns |
| PBS | Phosphate Buffered Saline |
| PE | Phycoerythrin |
| PI3K | phosphoinositide-3 (PI3)-kinase |
| PMN | PolyMorphoNuclear leukocytes |
| PMSF | PhenylMethylSulFonylfluoride |
| POX | Horseradish PerOxidase |
| PRR | Pattern Recognition Receptors |
| PSG | Pregnancy Specic Glycoproteins |
| PVDF | PolyVinyliDeneFluoride |
| RANTES | Regulated And Normal T cell Expressed and Secreted |
| RAS-GAP | Ras GTPase activating protein |
| rh | recombinant human |
| rm | recombinant mouse |
| ROS | Reactive Oxygen Species |
| RT | Room Temperature |

| | |
|------------|--|
| SabA | Sialyl-Lewis x (sLex) binding Adhesion |
| SCF | StemCell Factor |
| SDS | Sodium Dodecyl Sulfate |
| SDS-PAGE | Sodium Dodecyl Sulfate PolyAcrylamide Gel Electrophoresis |
| SEM | Standard Error of Mean |
| sgRNA | single guide RiboNucleic Acid |
| SH2 domain | Src Homology 2 domain |
| SHP1 | Src Homology region 2 domain-containing Phosphatase-1 |
| s-Lex | sialyl-Lewis x |
| strep | streptomycin |
| Syk | Spleen tyrosine kinase |
| Tab. | Table |
| TAK1 | host protein Transforming growth factor- β -Activated Kinase 1 |
| TARC | Thymus- and Activation-Regulated Chemokine |
| TB | Trypan Blue |
| TBS | Tris Buffered Saline |
| TBS-T | Tris Buffered Saline with Tween |
| T4SS | Type four Secretion System |
| TLR | Toll Like Receptor |
| TNF | Tumor necrosis factor |
| TRIS | Tris-(hydroxymethyl)-Aminomethan |
| U | Unit |
| VacA | Vakuoles forming cytotoxin A |
| v/v | Volumen percentage |
| WGA | Wheat Germ Agglutinin |
| WHO | World Health Organization |
| wt | wildtype |
| w/v | weight volumen percentage |
| x g | x-fold of the acceleration due to gravity |

List of Figures

| | | |
|------|---|----|
| 1.1 | Differentiated neutrophils stained with Giemsa solution | 4 |
| 1.2 | Hematopoiesis of neutrophils, M Φ and DCs | 5 |
| 1.3 | The effect of CagA on host cells | 10 |
| 1.4 | Chemokine secretion after CagA injection | 13 |
| 1.5 | Structure of human CEACAM1, 3 and 6 on neutrophils | 16 |
| 2.1 | CRISPR/Cas9 deletion strategy for SHP-1 and murine CEACAM1 | 42 |
| 3.1 | Characterization of isolated neutrophils | 45 |
| 3.2 | CEACAM expression of human, murine and humanized neutrophils | 46 |
| 3.3 | Analysis of the interaction of <i>H. pylori</i> with PMNs by flow cytometry | 47 |
| 3.4 | Confocal microscopy of CEACAM expression and binding of <i>H. pylori</i> to PMNs | 48 |
| 3.5 | Study of the interaction of different <i>H. pylori</i> strains with PMNs | 49 |
| 3.6 | Analysis of binding versus phagocytosis of <i>H. pylori</i> | 50 |
| 3.7 | Study of survival of <i>H. pylori</i> after phagocytosis by PMNs | 51 |
| 3.8 | Study of survival of <i>H. pylori</i> Δ cagA and Δ vacA after phagocytosis by PMNs | 53 |
| 3.9 | Analysis of ROS production by PMNs | 54 |
| 3.10 | Interaction of <i>H. pylori</i> and PMNs studied by confocal microscopy | 55 |
| 3.11 | Reconstructions of confocal microscopy images of PMNs infected with <i>H. pylori</i> | 56 |
| 3.12 | CagA phosphorylation and quantification of CagA translocation in human, murine and humanized PMNs | 57 |
| 3.13 | Chemical inhibition of SHP-1 in murine PMNs | 59 |
| 3.14 | Immunoblot analysis of different MPRO cells with a deletion in SHP-1 | 60 |
| 3.15 | 2D migration of murine and humanized PMNs | 61 |
| 3.16 | Chemokine secretion of PMNs infected with <i>H. pylori</i> | 62 |
| 3.17 | Chemokine secretion of DCs and M Φ s infected with <i>H. pylori</i> | 64 |
| 3.18 | Characterization and CEACAM expression of DCs and M Φ | 66 |
| 3.19 | Interaction of <i>H. pylori</i> with DCs and M Φ | 67 |
| 3.20 | CagA phosphorylation and quantification of CagA translocation in human, murine and humanized DCs and M Φ | 68 |
| 3.21 | Translocation of CagA into neutrophils isolated from chronically infected mice | 70 |
| 3.22 | Translocation of CagA into neutrophils isolated from naive versus chronically with <i>H. pylori</i> infected humans | 71 |

| | |
|---|----|
| 3.23 CagA phosphorylation in neutrophils from naive versus chronically with <i>H. pylori</i> infected individuals | 72 |
| 3.24 CEACAM expression of neutrophils from naive and chronically infected humans | 73 |

List of Tables

| | | |
|------|--|----|
| 1.1 | Chemokines attracting neutrophils to the site of infection | 6 |
| 1.2 | Chemokines secreted by neutrophils | 7 |
| 2.1 | Overview of all mouse lines used in this work | 23 |
| 2.2 | Medium of murine DCs and M Φ | 25 |
| 2.3 | Cell lines used in this work | 26 |
| 2.4 | Cell culture medium used in this work | 27 |
| 2.5 | <i>H. pylori</i> strains used in this work part I | 29 |
| 2.6 | <i>H. pylori</i> strains used in this work part II | 30 |
| 2.7 | Solutions for lysates | 32 |
| 2.8 | SDS gel mixture | 33 |
| 2.9 | Blotting buffer | 34 |
| 2.10 | Solutions for immunoblots | 35 |
| 2.11 | Primary antibodies - immunoblots | 35 |
| 2.12 | Secondary antibodies - immunoblots | 36 |
| 2.13 | Solutions for the <i>in vitro</i> phosphorylation | 36 |
| 2.14 | Antibodies - flow cytometry | 37 |
| 2.15 | Components of the CCF4-AM loading solution | 40 |
| 2.16 | CRISPR/Cas9 primer list | 43 |
| 2.17 | Components of the Cas9n-GFP vector digestion | 43 |

Literature

- [1] D. W. Sawyer, G. R. Donowitz, and G. L. Mandell. Polymorphonuclear neutrophils: an effective antimicrobial force. *Rev. Infect. Dis.*, 11 Suppl 7:S1532–1544, 1989.
- [2] J. Pillay, I. den Braber, N. Vrisekoop, L. M. Kwast, R. J. de Boer, J. A. Borghans, K. Tesselaar, and L. Koenderman. *In vivo* labeling with $2\text{H}_2\text{O}$ reveals a human neutrophil lifespan of 5.4 days. *Blood*, 116(4):625–627, Jul 2010.
- [3] J. Mestas and C. C. Hughes. Of mice and not men: differences between mouse and human immunology. *J. Immunol.*, 172(5):2731–2738, Mar 2004.
- [4] K. Akashi, D. Traver, T. Miyamoto, and I. L. Weissman. A clonogenic common myeloid progenitor that gives rise to all myeloid lineages. *Nature*, 404(6774):193–197, Mar 2000.
- [5] T. Lammermann, P. V. Afonso, B. R. Angermann, J. M. Wang, W. Kastentmuller, C. A. Parent, and R. N. Germain. Neutrophil swarms require LTB₄ and integrins at sites of cell death *in vivo*. *Nature*, 498(7454):371–375, Jun 2013.
- [6] R. Furuta, J. Yamagishi, H. Kotani, F. Sakamoto, T. Fukui, Y. Matsui, Y. Sohmura, M. Yamada, T. Yoshimura, and C. G. Larsen. Production and characterization of recombinant human neutrophil chemotactic factor. *J. Biochem.*, 106(3):436–441, Sep 1989.
- [7] A. Rot. Chemotactic potency of recombinant human neutrophil attractant/activation protein-1 (interleukin-8) for polymorphonuclear leukocytes of different species. *Cytokine*, 3(1):21–27, Jan 1991.
- [8] Y. Kobayashi. The role of chemokines in neutrophil biology. *Front. Biosci.*, 13:2400–2407, Jan 2008.
- [9] W. S. Modi and T. Yoshimura. Isolation of novel GRO genes and a phylogenetic analysis of the CXC chemokine subfamily in mammals. *Mol. Biol. Evol.*, 16(2):180–193, Feb 1999.
- [10] P. Oquendo, J. Alberta, D. Z. Wen, J. L. Graycar, R. Derynck, and C. D. Stiles. The platelet-derived growth factor-inducible KC gene encodes a secretory protein related to platelet alpha-granule proteins. *J. Biol. Chem.*, 264(7):4133–4137, Mar 1989.
- [11] G. Davatelis, P. Tekamp-Olson, S. D. Wolpe, K. Hermsen, C. Luedke, C. Gallegos, D. Coit, J. Merryweather, and A. Cerami. Cloning and characterization of a cDNA for

- murine macrophage inflammatory protein (MIP), a novel monokine with inflammatory and chemokinetic properties. *J. Exp. Med.*, 167(6):1939–1944, Jun 1988.
- [12] S. D. Wolpe, B. Sherry, D. Juers, G. Davatellis, R. W. Yurt, and A. Cerami. Identification and characterization of macrophage inflammatory protein 2. *Proc. Natl. Acad. Sci. U.S.A.*, 86(2):612–616, Jan 1989.
- [13] T. Kasama, R. M. Strieter, T. J. Standiford, M. D. Burdick, and S. L. Kunkel. Expression and regulation of human neutrophil-derived macrophage inflammatory protein 1 alpha. *J. Exp. Med.*, 178(1):63–72, Jul 1993.
- [14] M. Charmoy, S. Brunner-Agten, D. Aebischer, F. Auderset, P. Launois, G. Milon, A. E. Proudfoot, and F. Tacchini-Cottier. Neutrophil-derived CCL3 is essential for the rapid recruitment of dendritic cells to the site of *Leishmania major* inoculation in resistant mice. *PLoS Pathog.*, 6(2):e1000755, Feb 2010.
- [15] E. von Stebut, M. Metz, G. Milon, J. Knop, and M. Maurer. Early macrophage influx to sites of cutaneous granuloma formation is dependent on MIP-1alpha /beta released from neutrophils recruited by mast cell-derived TNFalpha. *Blood*, 101(1):210–215, Jan 2003.
- [16] S. J. Molesworth-Kenyon, J. E. Oakes, and R. N. Lausch. A novel role for neutrophils as a source of T cell-recruiting chemokines IP-10 and Mig during the DTH response to HSV-1 antigen. *J. Leukoc. Biol.*, 77(4):552–559, Apr 2005.
- [17] S. Gasperini, M. Marchi, F. Calzetti, C. Laudanna, L. Vicentini, H. Olsen, M. Murphy, F. Liao, J. Farber, and M. A. Cassatella. Gene expression and production of the monokine induced by IFN-gamma (MIG), IFN-inducible T cell alpha chemoattractant (I-TAC), and IFN-gamma-inducible protein-10 (IP-10) chemokines by human neutrophils. *J. Immunol.*, 162(8):4928–4937, Apr 1999.
- [18] T. N. Mayadas, X. Cullere, and C. A. Lowell. The multifaceted functions of neutrophils. *Annu Rev Pathol*, 9:181–218, 2014.
- [19] C. Bogdan, M. Rollinghoff, and A. Diefenbach. Reactive oxygen and reactive nitrogen intermediates in innate and specific immunity. *Curr. Opin. Immunol.*, 12(1):64–76, Feb 2000.
- [20] A. W. Segal, J. Dorling, and S. Coade. Kinetics of fusion of the cytoplasmic granules with phagocytic vacuoles in human polymorphonuclear leukocytes. Biochemical and morphological studies. *J. Cell Biol.*, 85(1):42–59, Apr 1980.
- [21] B. Linz, F. Balloux, Y. Moodley, A. Manica, H. Liu, P. Roumagnac, D. Falush, C. Stamer, F. Prugnolle, S. W. van der Merwe, Y. Yamaoka, D. Y. Graham, E. Perez-Trallero, T. Wadstrom, S. Suerbaum, and M. Achtman. An African origin for the intimate association between humans and *Helicobacter pylori*. *Nature*, 445(7130):915–918, Feb 2007.

-
- [22] L. M. Brown. *Helicobacter pylori*: epidemiology and routes of transmission. *Epidemiol Rev*, 22(2):283–297, 2000.
- [23] B. Bjoerkholm, M. Sjolund, P. G. Falk, O. G. Berg, L. Engstrand, and D. I. Andersson. Mutation frequency and biological cost of antibiotic resistance in *Helicobacter pylori*. *Proc. Natl. Acad. Sci. U.S.A.*, 98(25):14607–14612, Dec 2001.
- [24] J. Parsonnet, H. Shmuely, and T. Haggerty. Fecal and oral shedding of *Helicobacter pylori* from healthy infected adults. *JAMA*, 282(23):2240–2245, Dec 1999.
- [25] H. M. Malaty, A. El-Kasabany, D. Y. Graham, C. C. Miller, S. G. Reddy, S. R. Srinivasan, Y. Yamaoka, and G. S. Berenson. Age at acquisition of *Helicobacter pylori* infection: a follow-up study from infancy to adulthood. *Lancet*, 359(9310):931–935, Mar 2002.
- [26] D. Rothenbacher, M. Winkler, T. Gonsler, G. Adler, and H. Brenner. Role of infected parents in transmission of *Helicobacter pylori* to their children. *Pediatr. Infect. Dis. J.*, 21(7):674–679, Jul 2002.
- [27] C. P. Dooley, H. Cohen, P. L. Fitzgibbons, M. Bauer, M. D. Appleman, G. I. Perez-Perez, and M. J. Blaser. Prevalence of *Helicobacter pylori* infection and histologic gastritis in asymptomatic persons. *N. Engl. J. Med.*, 321(23):1562–1566, Dec 1989.
- [28] S. Suerbaum and P. Michetti. *Helicobacter pylori* infection. *N. Engl. J. Med.*, 347(15):1175–1186, Oct 2002.
- [29] IARC Working Group on the Evaluation of Carcinogenic Risks to Humans. Biological agents. volume 100 b. a review of human carcinogens. *IARC monographs on the evaluation of carcinogenic risks to humans*, 100:1–441, 2012.
- [30] B. E. Dunn, G. P. Campbell, G. I. Perez-Perez, and M. J. Blaser. Purification and characterization of urease from *Helicobacter pylori*. *J. Biol. Chem.*, 265(16):9464–9469, Jun 1990.
- [31] S. Schreiber, M. Konradt, C. Groll, P. Scheid, G. Hanauer, H. O. Werling, C. Josenhans, and S. Suerbaum. The spatial orientation of *Helicobacter pylori* in the gastric mucus. *Proc. Natl. Acad. Sci. U.S.A.*, 101(14):5024–5029, Apr 2004.
- [32] K. Terry, S. M. Williams, L. Connolly, and K. M. Ottemann. Chemotaxis plays multiple roles during *Helicobacter pylori* animal infection. *Infect. Immun.*, 73(2):803–811, Feb 2005.
- [33] K. A. Eaton, S. Suerbaum, C. Josenhans, and S. Krakowka. Colonization of gnotobiotic piglets by *Helicobacter pylori* deficient in two flagellin genes. *Infect. Immun.*, 64(7):2445–2448, Jul 1996.
- [34] V. Königer, L. Holsten, U. Harrison, B. Busch, E. Loell, Q. Zhao, D. A. Bonsor, A. Roth, A. Kengmo-Tchoupa, S. I. Smith, S. Mueller, E. J. Sundberg, W. Zimmermann, W. Fischer, C. R. Hauck, and R. Haas. *Helicobacter pylori* exploits human ceacams via HopQ for adherence and translocation of CagA. *Nat Microbiol*, 2:16188, Oct 2016.

- [35] A. Javaheri, T. Kruse, K. Moonens, R. Mejias-Luque, A. Debraekeleer, C. I. Asche, N. Tegtmeyer, B. Kalali, N. C. Bach, S. A. Sieber, D. J. Hill, V. Koniger, C. R. Hauck, R. Moskalenko, R. Haas, D. H. Busch, E. Klaile, H. Slevogt, A. Schmidt, S. Backert, H. Remaut, B. B. Singer, and M. Gerhard. *Helicobacter pylori* adhesin HopQ engages in a virulence-enhancing interaction with human CEACAMs. *Nat Microbiol*, 2:16189, Oct 2016.
- [36] D. Ilver, A. Arnqvist, J. Ogren, I. M. Frick, D. Kersulyte, E. T. Incecik, D. E. Berg, A. Covacci, L. Engstrand, and T. Boren. *Helicobacter pylori* adhesin binding fucosylated histo-blood group antigens revealed by retagging. *Science*, 279(5349):373–377, Jan 1998.
- [37] J. Mahdavi, B. Sonden, M. Hurtig, F. O. Olfat, L. Forsberg, N. Roche, J. Angstrom, T. Larsson, S. Teneberg, K. A. Karlsson, S. Altraja, T. Wadstrom, D. Kersulyte, D. E. Berg, A. Dubois, C. Petersson, K. E. Magnusson, T. Norberg, F. Lindh, B. B. Lundskog, A. Arnqvist, L. Hammarstrom, and T. Boren. *Helicobacter pylori* SabA adhesin in persistent infection and chronic inflammation. *Science*, 297(5581):573–578, Jul 2002.
- [38] D. A. Bonsor, Q. Zhao, B. Schmidinger, E. Weiss, J. Wang, D. Deredge, R. Beadenkopf, B. Dow, W. Fischer, D. Beckett, P. L. Wintrode, R. Haas, and E. J. Sundberg. The *Helicobacter pylori* adhesin protein HopQ exploits the dimer interface of human CEACAMs to facilitate translocation of the oncoprotein CagA. *EMBO J.*, 37(13), Jul 2018.
- [39] S. Linden, H. Nordman, J. Hedenbro, M. Hurtig, T. Boren, and I. Carlstedt. Strain- and blood group-dependent binding of *Helicobacter pylori* to human gastric MUC5AC glycoforms. *Gastroenterology*, 123(6):1923–1930, Dec 2002.
- [40] A. C. Goodwin, D. M. Weinberger, C. B. Ford, J. C. Nelson, J. D. Snider, J. D. Hall, C. I. Paules, R. M. Peek, and M. H. Forsyth. Expression of the *Helicobacter pylori* adhesin SabA is controlled via phase variation and the ArsRS signal transduction system. *Microbiology (Reading, Engl.)*, 154(Pt 8):2231–2240, Aug 2008.
- [41] M. Unemo, M. Aspholm-Hurtig, D. Ilver, J. Bergstrom, T. Boren, D. Danielsson, and S. Teneberg. The sialic acid binding SabA adhesin of *Helicobacter pylori* is essential for nonopsonic activation of human neutrophils. *J. Biol. Chem.*, 280(15):15390–15397, Apr 2005.
- [42] S. Censini, C. Lange, Z. Xiang, J. E. Crabtree, P. Ghiara, M. Borodovsky, R. Rappuoli, and A. Covacci. *cag*, a pathogenicity island of *Helicobacter pylori*, encodes type I-specific and disease-associated virulence factors. *Proc. Natl. Acad. Sci. U.S.A.*, 93(25):14648–14653, Dec 1996.
- [43] S. Backert, N. Tegtmeyer, and W. Fischer. Composition, structure and function of the *Helicobacter pylori* *cag* pathogenicity island encoded type IV secretion system. *Future Microbiol*, 10(6):955–965, 2015.

- [44] S. Odenbreit, J. Puls, B. Sedlmaier, E. Gerland, W. Fischer, and R. Haas. Translocation of *Helicobacter pylori* CagA into gastric epithelial cells by type IV secretion. *Science*, 287(5457):1497–1500, Feb 2000.
- [45] M. Selbach, S. Moese, C. R. Hauck, T. F. Meyer, and S. Backert. Src is the kinase of the *Helicobacter pylori* CagA protein *in vitro* and *in vivo*. *J. Biol. Chem.*, 277(9):6775–6778, Mar 2002.
- [46] M. Stein, F. Bagnoli, R. Halenbeck, R. Rappuoli, W. J. Fantl, and A. Covacci. c-Src/Lyn kinases activate *Helicobacter pylori* CagA through tyrosine phosphorylation of the EPIYA motifs. *Mol. Microbiol.*, 43(4):971–980, Feb 2002.
- [47] N. Ohnishi, H. Yuasa, S. Tanaka, H. Sawa, M. Miura, A. Matsui, H. Higashi, M. Musashi, K. Iwabuchi, M. Suzuki, G. Yamada, T. Azuma, and M. Hatakeyama. Transgenic expression of *Helicobacter pylori* CagA induces gastrointestinal and hematopoietic neoplasms in mouse. *Proc. Natl. Acad. Sci. U.S.A.*, 105(3):1003–1008, Jan 2008.
- [48] S. Backert, N. Tegtmeyer, and M. Selbach. The versatility of *Helicobacter pylori* CagA effector protein functions: The master key hypothesis. *Helicobacter*, 15(3):163–176, Jun 2010.
- [49] M. Stein, P. Ruggiero, R. Rappuoli, and F. Bagnoli. *Helicobacter pylori* CagA: From Pathogenic Mechanisms to Its Use as an Anti-Cancer Vaccine. *Front Immunol*, 4:328, Oct 2013.
- [50] H. Higashi, R. Tsutsumi, S. Muto, T. Sugiyama, T. Azuma, M. Asaka, and M. Hatakeyama. SHP-2 tyrosine phosphatase as an intracellular target of *Helicobacter pylori* CagA protein. *Science*, 295(5555):683–686, Jan 2002.
- [51] R. Tsutsumi, A. Takahashi, T. Azuma, H. Higashi, and M. Hatakeyama. Focal adhesion kinase is a substrate and downstream effector of SHP-2 complexed with *Helicobacter pylori* CagA. *Mol. Cell. Biol.*, 26(1):261–276, Jan 2006.
- [52] P. Saju, N. Murata-Kamiya, T. Hayashi, Y. Senda, L. Nagase, S. Noda, K. Matsusaka, S. Funata, A. Kunita, M. Urabe, Y. Seto, M. Fukayama, A. Kaneda, and M. Hatakeyama. Host SHP1 phosphatase antagonizes *Helicobacter pylori* CagA and can be downregulated by Epstein-Barr virus. *Nat Microbiol*, 1:16026, Mar 2016.
- [53] J. Zhang, A. K. Somani, and K. A. Siminovitch. Roles of the SHP-1 tyrosine phosphatase in the negative regulation of cell signalling. *Semin. Immunol.*, 12(4):361–378, Aug 2000.
- [54] H. Mimuro, T. Suzuki, J. Tanaka, M. Asahi, R. Haas, and C. Sasakawa. Grb2 is a key mediator of *Helicobacter pylori* CagA protein activities. *Mol. Cell*, 10(4):745–755, Oct 2002.
- [55] Y. Churin, L. Al-Ghoul, O. Kepp, T. F. Meyer, W. Birchmeier, and M. Naumann. *Helicobacter pylori* CagA protein targets the c-Met receptor and enhances the motogenic response. *J. Cell Biol.*, 161(2):249–255, Apr 2003.

- [56] I. Saadat, H. Higashi, C. Obuse, M. Umeda, N. Murata-Kamiya, Y. Saito, H. Lu, N. Ohnishi, T. Azuma, A. Suzuki, S. Ohno, and M. Hatakeyama. *Helicobacter pylori* CagA targets PAR1/MARK kinase to disrupt epithelial cell polarity. *Nature*, 447(7142):330–333, May 2007.
- [57] A. Lamb, X. D. Yang, Y. H. Tsang, J. D. Li, H. Higashi, M. Hatakeyama, R. M. Peek, S. R. Blanke, and L. F. Chen. *Helicobacter pylori* CagA activates NF-kappaB by targeting TAK1 for TRAF6-mediated Lys 63 ubiquitination. *EMBO Rep.*, 10(11):1242–1249, Nov 2009.
- [58] J. E. Crabtree, T. M. Shallcross, R. V. Heatley, and J. I. Wyatt. Mucosal tumour necrosis factor alpha and interleukin-6 in patients with *Helicobacter pylori* associated gastritis. *Gut*, 32(12):1473–1477, Dec 1991.
- [59] J. E. Crabtree, P. Peichl, J. I. Wyatt, U. Stachl, and I. J. Lindley. Gastric interleukin-8 and IgA IL-8 autoantibodies in *Helicobacter pylori* infection. *Scand. J. Immunol.*, 37(1):65–70, Jan 1993.
- [60] L. A. Allen, B. R. Beecher, J. T. Lynch, O. V. Rohner, and L. M. Wittine. *Helicobacter pylori* disrupts NADPH oxidase targeting in human neutrophils to induce extracellular superoxide release. *J. Immunol.*, 174(6):3658–3667, Mar 2005.
- [61] L. A. Allen, L. S. Schlesinger, and B. Kang. Virulent strains of *Helicobacter pylori* demonstrate delayed phagocytosis and stimulate homotypic phagosome fusion in macrophages. *J. Exp. Med.*, 191(1):115–128, Jan 2000.
- [62] M. Boncristiano, S. R. Paccani, S. Barone, C. Ulivieri, L. Patrussi, D. Ilver, A. Amedei, M. M. D’Elios, J. L. Telford, and C. T. Baldari. The *Helicobacter pylori* vacuolating toxin inhibits T cell activation by two independent mechanisms. *J. Exp. Med.*, 198(12):1887–1897, Dec 2003.
- [63] N. Hida, T. Shimoyama, P. Neville, M. F. Dixon, A. T. Axon, T. Shimoyama, and J. E. Crabtree. Increased expression of IL-10 and IL-12 (p40) mRNA in *Helicobacter pylori* infected gastric mucosa: relation to bacterial cag status and peptic ulceration. *J. Clin. Pathol.*, 52(9):658–664, Sep 1999.
- [64] A. P. Moran, B. Lindner, and E. J. Walsh. Structural characterization of the lipid A component of *Helicobacter pylori* rough- and smooth-form lipopolysaccharides. *J. Bacteriol.*, 179(20):6453–6463, Oct 1997.
- [65] T. W. Cullen, D. K. Giles, L. N. Wolf, C. Ecobichon, I. G. Boneca, and M. S. Trent. *Helicobacter pylori* versus the host: remodeling of the bacterial outer membrane is required for survival in the gastric mucosa. *PLoS Pathog.*, 7(12):e1002454, Dec 2011.
- [66] E. Andersen-Nissen, K. D. Smith, K. L. Strobe, S. L. Barrett, B. T. Cookson, S. M. Logan, and A. Aderem. Evasion of Toll-like receptor 5 by flagellated bacteria. *Proc. Natl. Acad. Sci. U.S.A.*, 102(26):9247–9252, Jun 2005.

- [67] A. T. Gewirtz, Y. Yu, U. S. Krishna, D. A. Israel, S. L. Lyons, and R. M. Peek. *Helicobacter pylori* flagellin evades toll-like receptor 5-mediated innate immunity. *J. Infect. Dis.*, 189(10):1914–1920, May 2004.
- [68] W. Fischer, J. Puls, R. Buhrdorf, B. Gebert, S. Odenbreit, and R. Haas. Systematic mutagenesis of the *Helicobacter pylori* cag pathogenicity island: essential genes for CagA translocation in host cells and induction of interleukin-8. *Mol. Microbiol.*, 42(5):1337–1348, Dec 2001.
- [69] W. Fischer, S. Prassl, and R. Haas. Virulence mechanisms and persistence strategies of the human gastric pathogen *Helicobacter pylori*. *Curr. Top. Microbiol. Immunol.*, 337:129–171, 2009.
- [70] V. Necchi, M. E. Candusso, F. Tava, O. Luinetti, U. Ventura, R. Fiocca, V. Ricci, and E. Solcia. Intracellular, intercellular, and stromal invasion of gastric mucosa, preneoplastic lesions, and cancer by *Helicobacter pylori*. *Gastroenterology*, 132(3):1009–1023, Mar 2007.
- [71] N. Ramarao, S. D. Gray-Owen, S. Backert, and T. F. Meyer. *Helicobacter pylori* inhibits phagocytosis by professional phagocytes involving type IV secretion components. *Mol. Microbiol.*, 37(6):1389–1404, Sep 2000.
- [72] B. Satin, G. Del Giudice, V. Della Bianca, S. Dusi, C. Laudanna, F. Tonello, D. Kelleher, R. Rappuoli, C. Montecucco, and F. Rossi. The neutrophil-activating protein (HP-NAP) of *Helicobacter pylori* is a protective antigen and a major virulence factor. *J. Exp. Med.*, 191(9):1467–1476, May 2000.
- [73] I. C. Arnold, X. Zhang, S. Urban, M. Artola-Boran, M. G. Manz, K. M. Ottemann, and A. Muller. NLRP3 Controls the Development of Gastrointestinal CD11b+ Dendritic Cells in the Steady State and during Chronic Bacterial Infection. *Cell Rep*, 21(13):3860–3872, Dec 2017.
- [74] A. P. Gobert, D. J. McGee, M. Akhtar, G. L. Mendz, J. C. Newton, Y. Cheng, H. L. Mobley, and K. T. Wilson. *Helicobacter pylori* arginase inhibits nitric oxide production by eukaryotic cells: a strategy for bacterial survival. *Proc. Natl. Acad. Sci. U.S.A.*, 98(24):13844–13849, Nov 2001.
- [75] A. P. Gobert, Y. Cheng, J. Y. Wang, J. L. Boucher, R. K. Iyer, S. D. Cederbaum, R. A. Casero, J. C. Newton, and K. T. Wilson. *Helicobacter pylori* induces macrophage apoptosis by activation of arginase II. *J. Immunol.*, 168(9):4692–4700, May 2002.
- [76] C. Alfaro, N. Suarez, C. Onate, J. L. Perez-Gracia, I. Martinez-Forero, S. Hervas-Stubbs, I. Rodriguez, G. Perez, E. Bolanos, A. Palazon, M. F. Sanmamed, A. Morales-Kastresana, A. Gonzalez, and I. Melero. Dendritic cells take up and present antigens from viable and apoptotic polymorphonuclear leukocytes. *PLoS ONE*, 6(12):e29300, 2011.
- [77] S. Boudaly. Activation of dendritic cells by polymorphonuclear neutrophils. *Front Biosci (Landmark Ed)*, 14:1589–1595, Jan 2009.

- [78] M. Oertli, M. Sundquist, I. Hitzler, D. B. Engler, I. C. Arnold, S. Reuter, J. Maxeiner, M. Hansson, C. Taube, M. Quiding-Jarbrink, and A. Muller. DC-derived IL-18 drives Treg differentiation, murine *Helicobacter pylori*-specific immune tolerance, and asthma protection. *J. Clin. Invest.*, 122(3):1082–1096, Mar 2012.
- [79] K. B. Bamford, X. Fan, S. E. Crowe, J. F. Leary, W. K. Gourley, G. K. Luthra, E. G. Brooks, D. Y. Graham, V. E. Reyes, and P. B. Ernst. Lymphocytes in the human gastric mucosa during *Helicobacter pylori* have a T helper cell 1 phenotype. *Gastroenterology*, 114(3):482–492, Mar 1998.
- [80] H. A. Haeberle, M. Kubin, K. B. Bamford, R. Garofalo, D. Y. Graham, F. El-Zaatari, R. Karttunen, S. E. Crowe, V. E. Reyes, and P. B. Ernst. Differential stimulation of interleukin-12 (IL-12) and IL-10 by live and killed *Helicobacter pylori* in vitro and association of IL-12 production with gamma interferon-producing T cells in the human gastric mucosa. *Infect. Immun.*, 65(10):4229–4235, Oct 1997.
- [81] A. Amedei, A. Cappon, G. Codolo, A. Cabrelle, A. Polenghi, M. Benagiano, E. Tasca, A. Azzurri, M. M. D’Elios, G. Del Prete, and M. de Bernard. The neutrophil-activating protein of *Helicobacter pylori* promotes Th1 immune responses. *J. Clin. Invest.*, 116(4):1092–1101, Apr 2006.
- [82] A. Galmiche, J. Rasso, A. Doye, S. Cagnol, J. C. Chambard, S. Contamin, V. de Thillot, I. Just, V. Ricci, E. Solcia, E. Van Obberghen, and P. Boquet. The N-terminal 34 kDa fragment of *Helicobacter pylori* vacuolating cytotoxin targets mitochondria and induces cytochrome c release. *EMBO J.*, 19(23):6361–6370, Dec 2000.
- [83] I. Szabo, S. Brutsche, F. Tombola, M. Moschioni, B. Satin, J. L. Telford, R. Rappuoli, C. Montecucco, E. Papini, and M. Zoratti. Formation of anion-selective channels in the cell plasma membrane by the toxin VacA of *Helicobacter pylori* is required for its biological activity. *EMBO J.*, 18(20):5517–5527, Oct 1999.
- [84] P. Gold and S. O. Freedman. Specific carcinoembryonic antigens of the human digestive system. *J. Exp. Med.*, 122(3):467–481, Sep 1965.
- [85] P. Gold and S. O. Freedman. Demonstration of tumor specific antigens in human colonic carcinomata by immunological tolerance and absorption techniques. *J. Exp. Med.*, 121:439–462, Mar 1965.
- [86] S. von Kleist and P. Burtin. [Cellular localization of an embryonic antigen in human colonic tumors]. *Int. J. Cancer*, 4(6):874–879, Nov 1969.
- [87] D. Boucher, D. Cournoyer, C. P. Stanners, and A. Fuks. Studies on the control of gene expression of the carcinoembryonic antigen family in human tissue. *Cancer Res.*, 49(4):847–852, Feb 1989.

- [88] J. A. Thompson, F. Grunert, and W. Zimmermann. Carcinoembryonic antigen gene family: molecular biology and clinical perspectives. *J. Clin. Lab. Anal.*, 5(5):344–366, 1991.
- [89] R. J. Paxton, G. Mooser, H. Pande, T. D. Lee, and J. E. Shively. Sequence analysis of carcinoembryonic antigen: identification of glycosylation sites and homology with the immunoglobulin supergene family. *Proc. Natl. Acad. Sci. U.S.A.*, 84(4):920–924, Feb 1987.
- [90] N. Beauchemin, P. Draber, G. Dveksler, P. Gold, S. Gray-Owen, F. Grunert, S. Hammarstrom, K. V. Holmes, A. Karlsson, M. Kuroki, S. H. Lin, L. Lucka, S. M. Najjar, M. Neumaier, B. Obrink, J. E. Shively, K. M. Skubitz, C. P. Stanners, P. Thomas, J. A. Thompson, M. Virji, S. von Kleist, C. Wagener, S. Watt, and W. Zimmermann. Redefined nomenclature for members of the carcinoembryonic antigen family. *Exp. Cell Res.*, 252(2):243–249, Nov 1999.
- [91] A. K. Tchoupa, T. Schuhmacher, and C. R. Hauck. Signaling by epithelial members of the CEACAM family - mucosal docking sites for pathogenic bacteria. *Cell Commun. Signal*, 12:27, Apr 2014.
- [92] R. Zebhauser, R. Kammerer, A. Eisenried, A. McLellan, T. Moore, and W. Zimmermann. Identification of a novel group of evolutionarily conserved members within the rapidly diverging murine Cea family. *Genomics*, 86(5):566–580, Nov 2005.
- [93] R. Kammerer and W. Zimmermann. Coevolution of activating and inhibitory receptors within mammalian carcinoembryonic antigen families. *BMC Biol.*, 8:12, Feb 2010.
- [94] J. A. Thompson. Molecular cloning and expression of carcinoembryonic antigen gene family members. *Tumour Biol.*, 16(1):10–16, 1995.
- [95] S. Schoelzel, W. Zimmermann, G. Schwarzkopf, F. Grunert, B. Rogaczewski, and J. Thompson. Carcinoembryonic antigen family members CEACAM6 and CEACAM7 are differentially expressed in normal tissues and oppositely deregulated in hyperplastic colorectal polyps and early adenomas. *Am. J. Pathol.*, 156(2):595–605, Feb 2000.
- [96] H. G. Leusch, Z. Drzeniek, Z. Markos-Pusztai, and C. Wagener. Binding of *Escherichia coli* and Salmonella strains to members of the carcinoembryonic antigen family: differential binding inhibition by aromatic alpha-glycosides of mannose. *Infect. Immun.*, 59(6):2051–2057, Jun 1991.
- [97] M. Virji, D. Evans, J. Griffith, D. Hill, L. Serino, A. Hadfield, and S. M. Watt. Carcinoembryonic antigens are targeted by diverse strains of typable and non-typable *Haemophilus influenzae*. *Mol. Microbiol.*, 36(4):784–795, May 2000.
- [98] M. Virji, K. Makepeace, D. J. Ferguson, and S. M. Watt. Carcinoembryonic antigens (CD66) on epithelial cells and neutrophils are receptors for Opa proteins of pathogenic neisseriae. *Mol. Microbiol.*, 22(5):941–950, Dec 1996.

- [99] D. J. Hill and M. Virji. A novel cell-binding mechanism of *Moraxella catarrhalis* ubiquitous surface protein UspA: specific targeting of the N-domain of carcinoembryonic antigen-related cell adhesion molecules by UspA1. *Mol. Microbiol.*, 48(1):117–129, Apr 2003.
- [100] E. Klaile, M. M. Muller, M. R. Schafer, A. K. Clauder, S. Feer, K. A. Heyl, M. Stock, T. E. Klassert, P. F. Zipfel, B. B. Singer, and H. Slevogt. Binding of *Candida albicans* to Human CEACAM1 and CEACAM6 Modulates the Inflammatory Response of Intestinal Epithelial Cells. *mBio*, 8(2), Mar 2017.
- [101] I. C. Boulton and S. D. Gray-Owen. Neisserial binding to CEACAM1 arrests the activation and proliferation of CD4+ T lymphocytes. *Nat. Immunol.*, 3(3):229–236, Mar 2002.
- [102] H. Slevogt, S. Zabel, B. Opitz, A. Hocke, J. Eitel, P. D. N’guessan, L. Lucka, K. Riesbeck, W. Zimmermann, J. Zweigner, B. Temmesfeld-Wollbrueck, N. Suttorp, and B. B. Singer. CEACAM1 inhibits Toll-like receptor 2-triggered antibacterial responses of human pulmonary epithelial cells. *Nat. Immunol.*, 9(11):1270–1278, Nov 2008.
- [103] C. Ilantzis, L. DeMarte, R. A. Screaton, and C. P. Stanners. Deregulated expression of the human tumor marker CEA and CEA family member CEACAM6 disrupts tissue architecture and blocks colonocyte differentiation. *Neoplasia*, 4(2):151–163, 2002.
- [104] M. N. Poy, Y. Yang, K. Rezaei, M. A. Fernstrom, A. D. Lee, Y. Kido, S. K. Erickson, and S. M. Najjar. CEACAM1 regulates insulin clearance in liver. *Nat. Genet.*, 30(3):270–276, Mar 2002.
- [105] A. K. Horst, W. D. Ito, J. Dabelstein, U. Schumacher, H. Sander, C. Turbide, J. Brummer, T. Meinertz, N. Beauchemin, and C. Wagener. Carcinoembryonic antigen-related cell adhesion molecule 1 modulates vascular remodeling *in vitro* and *in vivo*. *J. Clin. Invest.*, 116(6):1596–1605, Jun 2006.
- [106] F. Prall, P. Nollau, M. Neumaier, H. D. Haubeck, Z. Drzeniek, U. Helmchen, T. Loning, and C. Wagener. CD66a (BGP), an adhesion molecule of the carcinoembryonic antigen family, is expressed in epithelium, endothelium, and myeloid cells in a wide range of normal human tissues. *J. Histochem. Cytochem.*, 44(1):35–41, Jan 1996.
- [107] T. Chen, W. Zimmermann, J. Parker, I. Chen, A. Maeda, and S. Bolland. Biliary glycoprotein (BGP, CD66a, CEACAM1) mediates inhibitory signals. *J. Leukoc. Biol.*, 70(2):335–340, Aug 2001.
- [108] D. A. Bonsor, S. Gunther, R. Beadenkopf, D. Beckett, and E. J. Sundberg. Diverse oligomeric states of CEACAM IgV domains. *Proc. Natl. Acad. Sci. U.S.A.*, 112(44):13561–13566, Nov 2015.
- [109] Z. Chen, L. Chen, S. W. Qiao, T. Nagaishi, and R. S. Blumberg. Carcinoembryonic antigen-related cell adhesion molecule 1 inhibits proximal TCR signaling by targeting ZAP-70. *J. Immunol.*, 180(9):6085–6093, May 2008.

- [110] B. B. Singer, E. Klaile, I. Scheffrahn, M. M. Muller, R. Kammerer, W. Reutter, B. Obrink, and L. Lucka. CEACAM1 (CD66a) mediates delay of spontaneous and Fas ligand-induced apoptosis in granulocytes. *Eur. J. Immunol.*, 35(6):1949–1959, Jun 2005.
- [111] M. Voges, V. Bachmann, J. Naujoks, K. Kopp, and C. R. Hauck. Extracellular IgC2 constant domains of CEACAMs mediate PI3K sensitivity during uptake of pathogens. *PLoS ONE*, 7(6):e39908, 2012.
- [112] H. Pan and J. E. Shively. Carcinoembryonic antigen-related cell adhesion molecule-1 regulates granulopoiesis by inhibition of granulocyte colony-stimulating factor receptor. *Immunity*, 33(4):620–631, Oct 2010.
- [113] H. Sarantis and S. D. Gray-Owen. Defining the roles of human carcinoembryonic antigen-related cellular adhesion molecules during neutrophil responses to *Neisseria gonorrhoeae*. *Infect. Immun.*, 80(1):345–358, Jan 2012.
- [114] T. Chen and E. C. Gotschlich. CGM1a antigen of neutrophils, a receptor of gonococcal opacity proteins. *Proc. Natl. Acad. Sci. U.S.A.*, 93(25):14851–14856, Dec 1996.
- [115] G. Nagel, F. Grunert, T. W. Kuijpers, S. M. Watt, J. Thompson, and W. Zimmermann. Genomic organization, splice variants and expression of CGM1, a CD66-related member of the carcinoembryonic antigen gene family. *Eur. J. Biochem.*, 214(1):27–35, May 1993.
- [116] T. Schmitter, F. Agerer, L. Peterson, P. Munzner, and C. R. Hauck. Granulocyte CEACAM3 is a phagocytic receptor of the innate immune system that mediates recognition and elimination of human-specific pathogens. *J. Exp. Med.*, 199(1):35–46, Jan 2004.
- [117] A. Buntru, K. Kopp, M. Voges, R. Frank, V. Bachmann, and C. R. Hauck. Phosphatidylinositol 3'-kinase activity is critical for initiating the oxidative burst and bacterial destruction during CEACAM3-mediated phagocytosis. *J. Biol. Chem.*, 286(11):9555–9566, Mar 2011.
- [118] R. A. Sreaton, L. DeMarte, P. Draber, and C. P. Stanners. The specificity for the differentiation blocking activity of carcinoembryonic antigen resides in its glycoposphatidylinositol anchor. *J. Cell Biol.*, 150(3):613–626, Aug 2000.
- [119] F. Naghibalhossaini and C. P. Stanners. Minimal mutations are required to effect a radical change in function in CEA family members of the Ig superfamily. *J. Cell. Sci.*, 117(Pt 5):761–769, Feb 2004.
- [120] P. Nedellec, G. S. Dveksler, E. Daniels, C. Turbide, B. Chow, A. A. Basile, K. V. Holmes, and N. Beauchemin. Bgp2, a new member of the carcinoembryonic antigen-related gene family, encodes an alternative receptor for mouse hepatitis viruses. *J. Virol.*, 68(7):4525–4537, Jul 1994.
- [121] P. Nedellec, C. Turbide, and N. Beauchemin. Characterization and transcriptional activity of the mouse biliary glycoprotein 1 gene, a carcinoembryonic antigen-related gene. *Eur. J. Biochem.*, 231(1):104–114, Jul 1995.

- [122] E. Han, D. Phan, P. Lo, M. N. Poy, R. Behringer, S. M. Najjar, and S. H. Lin. Differences in tissue-specific and embryonic expression of mouse Ceacam1 and Ceacam2 genes. *Biochem. J.*, 355(Pt 2):417–423, Apr 2001.
- [123] J. Robitaille, L. Izzi, E. Daniels, B. Zelus, K. V. Holmes, and N. Beauchemin. Comparison of expression patterns and cell adhesion properties of the mouse biliary glycoproteins Bbgs1 and Bbgs2. *Eur. J. Biochem.*, 264(2):534–544, Sep 1999.
- [124] M. M. Alshahrani, E. Yang, J. Yip, S. S. Ghanem, S. L. Abdallah, A. M. deAngelis, C. J. O’Malley, F. Moheimani, S. M. Najjar, and D. E. Jackson. CEACAM2 negatively regulates hemi (ITAM-bearing) GPVI and CLEC-2 pathways and thrombus growth *in vitro* and *in vivo*. *Blood*, 124(15):2431–2441, Oct 2014.
- [125] M. Voges, V. Bachmann, R. Kammerer, U. Gophna, and C. R. Hauck. CEACAM1 recognition by bacterial pathogens is species-specific. *BMC Microbiol.*, 10:117, Apr 2010.
- [126] A. Gu, Z. Zhang, N. Zhang, W. Tsark, and J. E. Shively. Generation of human CEACAM1 transgenic mice and binding of Neisseria Opa protein to their neutrophils. *PLoS ONE*, 5(4):e10067, Apr 2010.
- [127] P. Cao and T. L. Cover. Two different families of hopQ alleles in *Helicobacter pylori*. *J. Clin. Microbiol.*, 40(12):4504–4511, Dec 2002.
- [128] Q. Zhao, B. Busch, L. F. Jimenez-Soto, H. Ishikawa-Ankerhold, S. Massberg, L. Terradot, W. Fischer, and R. Haas. Integrin but not CEACAM receptors are dispensable for *Helicobacter pylori* CagA translocation. *PLoS Pathog.*, 14(10):e1007359, Oct 2018.
- [129] M. T. Cantorna and E. Balish. Inability of human clinical strains of *Helicobacter pylori* to colonize the alimentary tract of germfree rodents. *Can. J. Microbiol.*, 36(4):237–241, Apr 1990.
- [130] A. Lee, J. O’Rourke, M. C. De Ungria, B. Robertson, G. Daskalopoulos, and M. F. Dixon. A standardized mouse model of *Helicobacter pylori* infection: introducing the Sydney strain. *Gastroenterology*, 112(4):1386–1397, Apr 1997.
- [131] F. Hirayama, S. Takagi, Y. Yokoyama, E. Iwao, and Y. Ikeda. Establishment of gastric *Helicobacter pylori* infection in Mongolian gerbils. *J. Gastroenterol.*, 31 Suppl 9:24–28, Nov 1996.
- [132] T. Ikeno, H. Ota, A. Sugiyama, K. Ishida, T. Katsuyama, R. M. Genta, and S. Kawasaki. *Helicobacter pylori*-induced chronic active gastritis, intestinal metaplasia, and gastric ulcer in Mongolian gerbils. *Am. J. Pathol.*, 154(3):951–960, Mar 1999.
- [133] S. Honda, T. Fujioka, M. Tokieda, R. Satoh, A. Nishizono, and M. Nasu. Development of *Helicobacter pylori*-induced gastric carcinoma in Mongolian gerbils. *Cancer Res.*, 58(19):4255–4259, Oct 1998.

- [134] S. Matsumoto, Y. Washizuka, Y. Matsumoto, S. Tawara, F. Ikeda, Y. Yokota, and M. Karita. Induction of ulceration and severe gastritis in Mongolian gerbil by *Helicobacter pylori* infection. *J. Med. Microbiol.*, 46(5):391–397, May 1997.
- [135] T. Watanabe, M. Tada, H. Nagai, S. Sasaki, and M. Nakao. *Helicobacter pylori* infection induces gastric cancer in mongolian gerbils. *Gastroenterology*, 115(3):642–648, Sep 1998.
- [136] D. A. R. Zorio, S. Monsma, D. H. Sanes, N. L. Golding, E. W. Rubel, and Y. Wang. De novo sequencing and initial annotation of the Mongolian gerbil (*Meriones unguiculatus*) genome. *Genomics*, 111(3):441–449, May 2019.
- [137] A. M. Eades-Perner, H. van der Putten, A. Hirth, J. Thompson, M. Neumaier, S. von Kleist, and W. Zimmermann. Mice transgenic for the human carcinoembryonic antigen gene maintain its spatiotemporal expression pattern. *Cancer Res.*, 54(15):4169–4176, Aug 1994.
- [138] C. H. Chan and C. P. Stanners. Novel mouse model for carcinoembryonic antigen-based therapy. *Mol. Ther.*, 9(6):775–785, Jun 2004.
- [139] J. Schymeinsky, C. Then, A. Sindrilaru, R. Gerstl, Z. Jakus, V. L. Tybulewicz, K. Scharffetter-Kochanek, and B. Walzog. Syk-mediated translocation of PI3Kdelta to the leading edge controls lamellipodium formation and migration of leukocytes. *PLoS ONE*, 2(11):e1132, Nov 2007.
- [140] J. Schymeinsky, A. Sindrilaru, D. Frommhold, M. Sperandio, R. Gerstl, C. Then, A. Mocsai, K. Scharffetter-Kochanek, and B. Walzog. The Vav binding site of the non-receptor tyrosine kinase Syk at Tyr 348 is critical for beta2 integrin (CD11/CD18)-mediated neutrophil migration. *Blood*, 108(12):3919–3927, Dec 2006.
- [141] D. Ruf, V. Brantl, and J. Wagener. Mitochondrial Fragmentation in *Aspergillus fumigatus* as Early Marker of Granulocyte Killing Activity. *Front Cell Infect Microbiol*, 8:128, 2018.
- [142] M. B. Lutz, N. Kukutsch, A. L. Ogilvie, S. Rossner, F. Koch, N. Romani, and G. Schuler. An advanced culture method for generating large quantities of highly pure dendritic cells from mouse bone marrow. *J. Immunol. Methods*, 223(1):77–92, Feb 1999.
- [143] G. G. Wang, K. R. Calvo, M. P. Pasillas, D. B. Sykes, H. Hacker, and M. P. Kamps. Quantitative production of macrophages or neutrophils ex vivo using conditional Hoxb8. *Nat. Methods*, 3(4):287–293, Apr 2006.
- [144] J. F. Tomb, O. White, A. R. Kerlavage, R. A. Clayton, G. G. Sutton, R. D. Fleischmann, K. A. Ketchum, H. P. Klenk, S. Gill, B. A. Dougherty, K. Nelson, J. Quackenbush, L. Zhou, E. F. Kirkness, S. Peterson, B. Loftus, D. Richardson, R. Dodson, H. G. Khalak, A. Glodek, K. McKenney, L. M. Fitzgerald, N. Lee, M. D. Adams, E. K. Hickey, D. E. Berg, J. D. Gocayne, T. R. Utterback, J. D. Peterson, J. M. Kelley, M. D. Cotton, J. M. Weidman, C. Fujii, C. Bowman, L. Wathley, E. Wallin, W. S. Hayes, M. Borodovsky,

- P. D. Karp, H. O. Smith, C. M. Fraser, and J. C. Venter. The complete genome sequence of the gastric pathogen *Helicobacter pylori*. *Nature*, 388(6642):539–547, Aug 1997.
- [145] A. Covacci, S. Censini, M. Bugnoli, R. Petracca, D. Burroni, G. Macchia, A. Massone, E. Papini, Z. Xiang, and N. Figura. Molecular characterization of the 128-kDa immunodominant antigen of *Helicobacter pylori* associated with cytotoxicity and duodenal ulcer. *Proc. Natl. Acad. Sci. U.S.A.*, 90(12):5791–5795, Jun 1993.
- [146] M. Farnbacher, T. Jahns, D. Willrodt, R. Daniel, R. Haas, A. Goesmann, S. Kurtz, and G. Rieder. Sequencing, annotation, and comparative genome analysis of the gerbil-adapted *Helicobacter pylori* strain B8. *BMC Genomics*, 11:335, May 2010.
- [147] H. Kleanthous, T. J. Tibbitts, H. L. Gray, G. A. Myers, C. K. Lee, T. H. Ermak, and T. P. Monath. Sterilizing immunity against experimental *Helicobacter pylori* infection is challenge-strain dependent. *Vaccine*, 19(32):4883–4895, Sep 2001.
- [148] I. C. Arnold, J. Y. Lee, M. R. Amieva, A. Roers, R. A. Flavell, T. Sparwasser, and A. Muller. Tolerance rather than immunity protects from *Helicobacter pylori*-induced gastric preneoplasia. *Gastroenterology*, 140(1):199–209, Jan 2011.
- [149] W. Schmitt and R. Haas. Genetic analysis of the *Helicobacter pylori* vacuolating cytotoxin: structural similarities with the IgA protease type of exported protein. *Mol. Microbiol.*, 12(2):307–319, Apr 1994.
- [150] K. T. Pham, E. Weiss, L. F. Jimenez Soto, U. Breithaupt, R. Haas, and W. Fischer. CagI is an essential component of the *Helicobacter pylori* Cag type IV secretion system and forms a complex with CagL. *PLoS ONE*, 7(4):e35341, 2012.
- [151] F. Schindele, E. Weiss, R. Haas, and W. Fischer. Quantitative analysis of CagA type IV secretion by *Helicobacter pylori* reveals substrate recognition and translocation requirements. *Mol. Microbiol.*, 100(1):188–203, Apr 2016.
- [152] S. Odenbreit, B. Gebert, J. Puls, W. Fischer, and R. Haas. Interaction of *Helicobacter pylori* with professional phagocytes: role of the cag pathogenicity island and translocation, phosphorylation and processing of CagA. *Cell. Microbiol.*, 3(1):21–31, Jan 2001.
- [153] M. K. Pathak and T. Yi. Sodium stibogluconate is a potent inhibitor of protein tyrosine phosphatases and augments cytokine responses in hemopoietic cell lines. *J. Immunol.*, 167(6):3391–3397, Sep 2001.
- [154] Y. S. Cho, S. Y. Oh, and Z. Zhu. Tyrosine phosphatase SHP-1 in oxidative stress and development of allergic airway inflammation. *Am. J. Respir. Cell Mol. Biol.*, 39(4):412–419, Oct 2008.
- [155] S. Pils, T. Schmitter, F. Neske, and C. R. Hauck. Quantification of bacterial invasion into adherent cells by flow cytometry. *J. Microbiol. Methods*, 65(2):301–310, May 2006.

- [156] Y. Chen and W. G. Junger. Measurement of oxidative burst in neutrophils. *Methods Mol. Biol.*, 844:115–124, 2012.
- [157] L. Cong, F. A. Ran, D. Cox, S. Lin, R. Barretto, N. Habib, P. D. Hsu, X. Wu, W. Jiang, L. A. Marraffini, and F. Zhang. Multiplex genome engineering using CRISPR/Cas systems. *Science*, 339(6121):819–823, Feb 2013.
- [158] X. Cullere, M. Lauterbach, N. Tsuboi, and T. N. Mayadas. Neutrophil-selective CD18 silencing using RNA interference *in vivo*. *Blood*, 111(7):3591–3598, Apr 2008.
- [159] L. F. Jimenez-Soto, S. Clausen, A. Sprenger, C. Ertl, and R. Haas. Dynamics of the Cag-type IV secretion system of *Helicobacter pylori* as studied by bacterial co-infections. *Cell. Microbiol.*, 15(11):1924–1937, Nov 2013.
- [160] B. B. Finlay and S. Falkow. Common themes in microbial pathogenicity revisited. *Microbiol. Mol. Biol. Rev.*, 61(2):136–169, Jun 1997.
- [161] S. N. Abraham, A. B. Jonsson, and S. Normark. Fimbriae-mediated host-pathogen cross-talk. *Curr. Opin. Microbiol.*, 1(1):75–81, Feb 1998.
- [162] M. Virji, S. M. Watt, S. Barker, K. Makepeace, and R. Doyonnas. The N-domain of the human CD66a adhesion molecule is a target for Opa proteins of *Neisseria meningitidis* and *Neisseria gonorrhoeae*. *Mol. Microbiol.*, 22(5):929–939, Dec 1996.
- [163] S. D. Gray-Owen, C. Dehio, A. Haude, F. Grunert, and T. F. Meyer. CD66 carcinoembryonic antigens mediate interactions between Opa-expressing *Neisseria gonorrhoeae* and human polymorphonuclear phagocytes. *EMBO J.*, 16(12):3435–3445, Jun 1997.
- [164] P. Muenzner, M. Rohde, S. Kneitz, and C. R. Hauck. CEACAM engagement by human pathogens enhances cell adhesion and counteracts bacteria-induced detachment of epithelial cells. *J. Cell Biol.*, 170(5):825–836, Aug 2005.
- [165] P. Muenzner, V. Bachmann, W. Zimmermann, J. Hentschel, and C. R. Hauck. Human-restricted bacterial pathogens block shedding of epithelial cells by stimulating integrin activation. *Science*, 329(5996):1197–1201, Sep 2010.
- [166] E. A. Islam, V. C. Anipindi, I. Francis, Y. Shaik-Dasthagirisahab, S. Xu, N. Leung, A. Sintsova, M. Amin, C. Kaushic, L. M. Wetzler, and S. D. Gray-Owen. Specific Binding to Differentially Expressed Human Carcinoembryonic Antigen-Related Cell Adhesion Molecules Determines the Outcome of *Neisseria gonorrhoeae* Infections along the Female Reproductive Tract. *Infect. Immun.*, 86(8), Aug 2018.
- [167] A. Sintsova, H. Sarantis, E. A. Islam, C. X. Sun, M. Amin, C. H. Chan, C. P. Stanners, M. Glogauer, and S. D. Gray-Owen. Global analysis of neutrophil responses to *Neisseria gonorrhoeae* reveals a self-propagating inflammatory program. *PLoS Pathog.*, 10(9):e1004341, Sep 2014.

- [168] S. E. McCaw, J. Schneider, E. H. Liao, W. Zimmermann, and S. D. Gray-Owen. Immunoreceptor tyrosine-based activation motif phosphorylation during engulfment of *Neisseria gonorrhoeae* by the neutrophil-restricted CEACAM3 (CD66d) receptor. *Mol. Microbiol.*, 49(3):623–637, Aug 2003.
- [169] F. L. Naidu and R. F. Rest. Stimulation of human neutrophil oxidative metabolism by nonopsonized *Neisseria gonorrhoeae*. *Infect. Immun.*, 59(12):4383–4390, Dec 1991.
- [170] H. Sarantis and S. D. Gray-Owen. The specific innate immune receptor CEACAM3 triggers neutrophil bactericidal activities via a Syk kinase-dependent pathway. *Cell. Microbiol.*, 9(9):2167–2180, Sep 2007.
- [171] O. Billker, A. Popp, V. Brinkmann, G. Wenig, J. Schneider, E. Caron, and T. F. Meyer. Distinct mechanisms of internalization of *Neisseria gonorrhoeae* by members of the CEACAM receptor family involving Rac1- and Cdc42-dependent and -independent pathways. *EMBO J.*, 21(4):560–571, Feb 2002.
- [172] C. R. Hauck, T. F. Meyer, F. Lang, and E. Gulbins. CD66-mediated phagocytosis of Opa52 *Neisseria gonorrhoeae* requires a Src-like tyrosine kinase- and Rac1-dependent signalling pathway. *EMBO J.*, 17(2):443–454, Jan 1998.
- [173] L. A. Allen. Phagocytosis and persistence of *Helicobacter pylori*. *Cell. Microbiol.*, 9(4):817–828, Apr 2007.
- [174] P. Y. Zheng and N. L. Jones. *Helicobacter pylori* strains expressing the vacuolating cytotoxin interrupt phagosome maturation in macrophages by recruiting and retaining TACO (coronin 1) protein. *Cell. Microbiol.*, 5(1):25–40, Jan 2003.
- [175] M. G. Rittig, B. Shaw, D. P. Letley, R. J. Thomas, R. H. Argent, and J. C. Atherton. *Helicobacter pylori*-induced homotypic phagosome fusion in human monocytes is independent of the bacterial *vacA* and *cag* status. *Cell. Microbiol.*, 5(12):887–899, Dec 2003.
- [176] M. J. Blaser and J. Parsonnet. Parasitism by the "slow" bacterium *Helicobacter pylori* leads to altered gastric homeostasis and neoplasia. *J. Clin. Invest.*, 94(1):4–8, Jul 1994.
- [177] K. Kusugami, T. Ando, A. Imada, K. Ina, M. Ohsuga, T. Shimizu, T. Sakai, T. Konagaya, and H. Kaneko. Mucosal macrophage inflammatory protein-1 α activity in *Helicobacter pylori* infection. *J. Gastroenterol. Hepatol.*, 14(1):20–26, Jan 1999.
- [178] W. Zimmermann. Evolution: Decoy Receptors as Unique Weapons to Fight Pathogens. *Curr. Biol.*, 29(4):R128–R130, Feb 2019.
- [179] M. Bordes, S. Knobel, and F. Martin. Carcinoembryonic antigen (CEA) and related antigens in blood cells and hematopoietic tissues. *Eur J Cancer*, 11(11):783–786, Nov 1975.

- [180] Q. Yu, E. M. Chow, S. E. McCaw, N. Hu, D. Byrd, T. Amet, S. Hu, M. A. Ostrowski, and S. D. Gray-Owen. Association of *Neisseria gonorrhoeae* Opa(CEA) with dendritic cells suppresses their ability to elicit an HIV-1-specific T cell memory response. *PLoS ONE*, 8(2):e56705, 2013.
- [181] E. M. El-Omar, M. Carrington, W. H. Chow, K. E. McColl, J. H. Bream, H. A. Young, J. Herrera, J. Lissowska, C. C. Yuan, N. Rothman, G. Lanyon, M. Martin, J. F. Fraumeni, and C. S. Rabkin. Interleukin-1 polymorphisms associated with increased risk of gastric cancer. *Nature*, 404(6776):398–402, Mar 2000.
- [182] A. Shikotra, D. F. Choy, S. Siddiqui, G. Arthur, D. R. Nagarkar, G. Jia, A. K. Wright, C. M. Ohri, E. Doran, C. A. Butler, B. Hargadon, A. R. Abbas, J. Jackman, L. C. Wu, L. G. Heaney, J. R. Arron, and P. Bradding. A CEACAM6-High Airway Neutrophil Phenotype and CEACAM6-High Epithelial Cells Are Features of Severe Asthma. *J. Immunol.*, 198(8):3307–3317, Apr 2017.

Acknowledgement

Zuallererst möchte ich meinem Doktorvater Prof. Dr. Rainer Haas für die Möglichkeit dieses spannende Thema im Rahmen des SFB914 in der AG Haas bearbeiten zu dürfen bedanken. Weiter danke ich ihm für sein mir entgegengebrachtes Vertrauen, meine Freiheiten in der Forschung und die hervorragende wissenschaftliche Betreuung.

Dem SFB914 und der integrierten IRTG914 bin ich für die professionellen Workshops, die Finanzierung, die vielen Vorträge und Diskussionsrunden, die mein Wissen erweitert haben, dankbar. Besonders möchte ich mich bei meinem "Thesis Advisory Committee", bestehend aus Prof. Dr. Rainer Haas, Prof. Dr. Markus Sperandio, Prof. Dr. Wolfgang Zimmermann und PD Dr. Wolfgang Fischer, für die konstruktiven Diskussionen bedanken.

PD Dr. Wolfgang Fischer möchte ich zudem für seine Anregungen, das Korrekturlesen meiner Arbeit, sowie seine Tätigkeit als Studienleiter für die *Helicobacter*-Studie danken. In diesem Zusammenhang gilt mein Dank auch den Diagnostikärzten, besonders Karl, für die Blutentnahmen und natürlich den Probanden für ihre Teilnahme an unserer Studie.

Unseren Kooperationspartnern Prof. Dr. Scott Gray Owen, Prof. Dr. John E. Shively und Prof. Dr. Clifford Stanners danke ich für die Zurverfügungstellung der CEACAM Mäuse. Weiter danke ich Hellen für die Unterstützung bei der Mikroskopie und den Rekonstruktionen.

Ein besonderes Dankeschön möchte ich Ben für seine Unterstützung aussprechen. Danke, für die wissenschaftlichen Diskussionen, die Hilfsbereitschaft und natürlich den Spaß, den wir im Laboralltag zusammen hatten. Weiter gilt mein Dank meinen beiden längsten gemeinsamen Kolleginnen Barbara und Clara für die gegenseitige Hilfe, das Korrekturlesen meiner Arbeit und all den Spaß.

Zudem danke ich den beiden Tierärztinnen Pia und Ute für ihre Hilfe, und ihnen und meinen weiteren Kolleginnen Ciara, Evelyn, Franziska, Friederike, Katrin und Qing für die schöne gemeinsame Zeit, die wir zusammen hatten; sowie allen Mitarbeitern des Max von Pettenkofer Instituts für die angenehme Arbeitsatmosphäre.

Zum Schluss möchte ich mich bei meiner Familie und meinen Freunden für ihre emotionale Unterstützung und ihr Verständnis bedanken.